

Study and correction of defects in tyrosine hydroxylase, the rate-limiting enzyme in the synthesis of dopamine

Master Thesis in Pharmacy

Maria Phuong Anh Tran



Center for Pharmacy and
Department of Biomedicine

University of Bergen

May 2019

Acknowledgement

The work presented in this master thesis was performed in the Biorecognition group at the Martinez & Teigen lab, Department of Biomedicine at the University of Bergen from August 2018 to May 2019.

First and foremost, I would like to express my deepest gratitude to my lovely supervisor Marte Innselset Flydal for her support and engagement throughout this project. Her willingness to provide her time so generously has been very much appreciated. I have to give her credit for being so patient with me during this research. My time as a Master student would not have been the same without her encouragement and constant feedback, and I could not have imagined having a better supervisor for my master study.

My sincerest thanks also go to my co-supervisor, Professor Aurora Martinez, for her guidance and constructive suggestions during my thesis, and for giving me the opportunity of attending the Røros winter meeting. My research would have been impossible without her advice and immense knowledge. My special thanks are extended to Professor Knut Teigen for his valuable help in doing the molecular docking.

I would also like to thank the Lab E members, especially to my fellow pharmacist Åge Aleksander Skjevik and others for taking interests in my project and for creating such an including and joyful environment. I will miss being part of your team.

Last but not least, a heartfelt thank you goes to my family and friends for cheering and supporting me during my master thesis.

Maria Phuong Anh Tran

May 2019

Table of contents

Summary.....	1
Abbreviations.....	2
1 Introduction.....	3
1.1 <i>Tyrosine hydroxylase.....</i>	3
1.1.1 Structure of tyrosine hydroxylase	4
1.1.1.1 The regulatory domain	5
1.1.1.2 The catalytic domain.....	5
1.1.1.3 The oligomerization domain	6
1.1.2 The catalytic mechanism	7
1.1.3 Regulation of tyrosine hydroxylase activity	8
1.1.3.1 Feedback inhibition by catecholamines.....	8
1.1.3.2 Activation by phosphorylation.....	9
1.1.3.3 Negative cooperativity of BH ₄ binding and substrate inhibition	9
1.1.4 Dysfunctions of tyrosine hydroxylase and disease.....	10
1.1.4.1 Mutant R202H-hTH1.....	11
1.2 <i>Protein stability.....</i>	13
1.2.1 Pharmacological chaperones	14
1.3 <i>From gene to pharmacological chaperone – a methodological overview</i>	16
1.3.1 Recombinant protein expression and purification.....	16
1.3.1.1 Affinity chromatography.....	16
1.3.1.2 Size-Exclusion Chromatography	17
1.3.2 Differential Scanning Fluorimetry	18
1.3.3 TH activity assay	19
1.3.3.1 EC ₅₀ and IC ₅₀	20
1.3.4 Limited proteolysis by trypsin	20
1.3.5 Isothermal Titration Calorimetry.....	21
1.3.6 Molecular docking.....	22
2 Aims of the project.....	23
3 Materials and Methods.....	24
3.1 <i>Materials.....</i>	24
3.2 <i>Preparation of pure and stable TH enzymes.....</i>	25
3.2.1 Expression of His-MBP-TH proteins.....	26
3.2.2 Purification of His-MBP-TH by affinity chromatography.....	26
3.2.3 Removal of tag and isolation of TH	27
3.2.3.1 Testing the quality of fusion protein by SEC.....	27
3.2.3.2 Optimizing TEV-protease cutting.....	28
3.2.3.3 Isolation of TH from His-MBP-TH.....	28
3.2.4 Finding an appropriate buffer for TH by DSF	28
3.2.4.1 RUBIC Buffer Screen	29
3.2.4.2 NaCl concentrations.....	29
3.3 <i>Finding potential pharmacological chaperones for TH.....</i>	29
3.3.1 Screening of the NOCE library by high throughput screening using DSF	30
3.3.2 Validation of primary hits on TH	30
3.3.2.1 First validation	30
3.3.2.2 Second validation.....	30
3.3.2.3 Testing the stabilizing effect of DA on TH.....	31

3.4	<i>Evaluating the effect of hit compounds on TH activity</i>	31
3.4.1	Testing inhibitory effect on TH.....	31
3.5	<i>Protection of TH towards limited proteolysis by trypsin</i>	32
3.5.1	Limited proteolysis with DA.....	32
3.5.2	Limited proteolysis with hit compounds.....	33
3.6	<i>Determination of binding affinities</i>	33
3.7	<i>Molecular docking of hit compounds to TH</i>	33
3.8	<i>Statistical analysis</i>	35
4	Results	36
4.1	<i>Preparation of pure and stable TH enzymes</i>	36
4.1.1	Expression and Purification of His-MBP-TH.....	36
4.1.2	Removal of tag and isolation of TH.....	36
4.1.2.1	Assessing the quality of purified His-MBP-TH proteins by SEC.....	36
4.1.2.2	Cutting tests with TEV-protease.....	37
4.1.2.3	Isolation of TH.....	39
4.1.3	Finding an appropriate buffer for TH by DSF.....	40
4.1.3.1	RUBIC Buffer Screen.....	40
4.1.3.2	NaCl concentrations.....	41
4.2	<i>Finding potential pharmacological chaperones for TH</i>	41
4.2.1	Screening of the NOCE library.....	41
4.2.2	Validation of primary hits.....	42
4.2.2.1	First validation.....	42
4.2.2.2	Second validation.....	44
4.3	<i>Evaluating the effect of hit compounds on TH activity</i>	46
4.3.1	Testing inhibitory effect on TH.....	46
4.4	<i>Protection of TH towards limited proteolysis by trypsin</i>	47
4.4.1	Limited proteolysis with hit compounds.....	47
4.5	<i>Determination of binding affinities</i>	48
4.5.1	Determination of K_d by ITC.....	48
4.6	<i>Molecular docking</i>	50
4.7	<i>The mutant TH-R202H</i>	54
4.7.1	Testing the effect of DA on TH-R202H mutant.....	54
4.7.1.1	Stabilizing effect of DA on TH-R202H.....	54
4.7.1.2	Protective effect of DA on TH-wt and TH-R202H mutant.....	56
4.7.2	Testing effect of hit compounds on R202H mutant.....	57
4.7.2.1	Determination of EC_{50} with hit compounds using DSF.....	57
4.7.2.2	Limited proteolysis with hit compounds.....	58
5	Discussion	59
6	Conclusion	65
7	Future work	66
8	References	67
9	Appendix	73
	<i>Layout of the RUBIC Buffer Screen</i>	73

Summary

Tyrosine hydroxylase (TH; tyrosine 3-monooxygenase) is an enzyme that catalyzes the first and rate-limiting step in the biosynthesis of neurotransmitters and hormones dopamine (DA), noradrenaline and adrenaline. The iron-containing enzyme uses (6*R*)-L-erythro-5,6,7,8-tetrahydrobiopterin (BH₄) as cofactor and molecular oxygen (O₂) to hydroxylate the substrate L-tyrosine (L-Tyr) to L-3,4-dihydroxyphenylalanine (L-DOPA), which is the precursor of DA. Tyrosine hydroxylase deficiency (THD), also known as Segawa syndrome, is caused by a mutation in the *TH*-gene resulting in misfolding of TH. A novel approach to treat misfolding diseases is the use of small molecules called pharmacological chaperones that correct the folding of mutant proteins, thus recovering the protein activity.

The search for pharmacological chaperones that stabilize TH and its disease-associated mutant, involved experimental screening of compound libraries containing a total of 1624 compounds (Prestwick[®]) using differential scanning fluorimetry (DSF), followed by concentration-dependent binding assay and activity assay with hit compounds as validation of stabilizing efficacy and functionality on TH. The hit compounds were further tested using limited proteolysis and isothermal titration calorimetry (ITC) for further characterization regarding binding and conformational changes of TH. Finally, a docking program was used to analyze possible binding pockets on TH with the hit compounds.

By combining experimental and virtual methods in this work, we identified four primary hit compounds and one compound shows potential as a pharmacological chaperone. The THD-associated mutant bind to the hit compounds to a lesser extent than wild-type TH as it appears that this common mutation cause a discrete conformational change of the tetrameric structure. The identified compounds might have a potential in pharmacological chaperone therapy for THD but should be further investigated.

Abbreviations

CD	Catalytic domain
CNS	Central nervous system
DA	Dopamine
DMSO	Dimethyl sulfoxide
DSF	Differential scanning fluorimetry
HPLC	High performance liquid chromatography
IPTG	Isopropyl- β -D-1-thiogalactopyranoside
ITC	Isothermal Titration Calorimetry
kDa	Kilodaltons
K_m	The Michaelis constant
L-DOPA	L-3,4-dihydroxyphenylalanine
MBP	Maltose binding protein
OD	Optical density or oligomerization domain
OMIM	Online Mendelian Inheritance in Man [®]
RD	Regulatory domain
SDS-PAGE	Sodium dodecyl polyacrylamide gel electrophoresis
SEC	Size-exclusion chromatography
SO	SYPRO Orange
TH	Tyrosine hydroxylase
T_m	Midpoint temperature
Wt	wild-type
Å	Ångström

1 Introduction

1.1 Tyrosine hydroxylase

Tyrosine hydroxylase (TH; tyrosine 3-monooxygenase) is an enzyme that catalyzes the first and rate-limiting step in the biosynthesis of the catecholamine neurotransmitters and hormones dopamine (DA), adrenaline and noradrenaline (Molinoff et al., 1971). In the central nervous system (CNS), TH is found in the brain and is otherwise localized in the sympathetic nervous system, gut, retina and the adrenal medulla (Nagatsu et al., 1964). DA serves both as a neurotransmitter released by nerve cells to send signal to other neurons and as a hormone outside the CNS, its most important function however is in the brain (Axelrod et al., 1972; Molinoff & Axelrod, 1971). Adrenaline and noradrenaline mainly function as hormones produced by the adrenal medulla and certain neurons primarily to stimulate the fight-or-flight response. TH, an iron-containing monooxygenase, uses (6*R*)-L-erythro-5,6,7,8-tetrahydrobiopterin (BH₄) as cofactor and molecular oxygen (O₂) to hydroxylate the substrate L-tyrosine (L-Tyr) to L-3,4-dihydroxyphenylalanine (L-DOPA). BH₄ is often referred to as a cofactor, when in fact is a co-substrate that is also hydroxylated in the reaction and dissociates from the active site in each cycle (Fitzpatrick, 1999; Nagatsu et al., 2018). L-DOPA is the precursor for DA, and adrenaline and noradrenaline are in turn synthesized from DA. An overview of the catecholamine synthesis pathway is shown in Figure 1.1.

TH belongs to the family of aromatic amino acid hydroxylases (AAAHs) which also includes phenylalanine 4-hydroxylase (PAH) and the tryptophan 5-hydroxylases (TPH1 and TPH2). The AAAHs have evolved from a common ancestral PAH (Siltberg-Liberles et al., 2008) and are structurally and functionally similar. They catalyze the rate-limiting step of their respective metabolic pathways through hydroxylation of their aromatic amino acid substrates. PAH is located mainly in the liver and catalyzes the hydroxylation of L-phenylalanine (L-Phe) to L-Tyr, the first step in the degradation pathway of L-Phe, while TPH1 and 2, which are present mainly in the brain, catalyze the hydroxylation of L-tryptophan to 5-hydroxytryptophan, the first step in the biosynthesis of serotonin and melatonin (Roberts et al., 2013).

Humans have four isoforms of TH (hTH1-hTH4), which differ only in the length of their N-terminal regulatory domain (RD). The differences originate from pre-mRNA splicing, resulting in insertion of additional amino acids after methionine in position 30 (Daubner et al., 2011). In this thesis, we are working with TH1, the isoform that is most abundant in the brain (Lewis et al., 1993) and the shortest among the four TH isoforms, presenting no insertions

(Kaneda et al., 1987). Also, TH1 is the isoform that corresponds to only TH enzyme in rats and most other mammals and is often used in *in vitro* investigations and studies (Haycock, 2002). Thus, TH1 will in this thesis be referred to as TH.

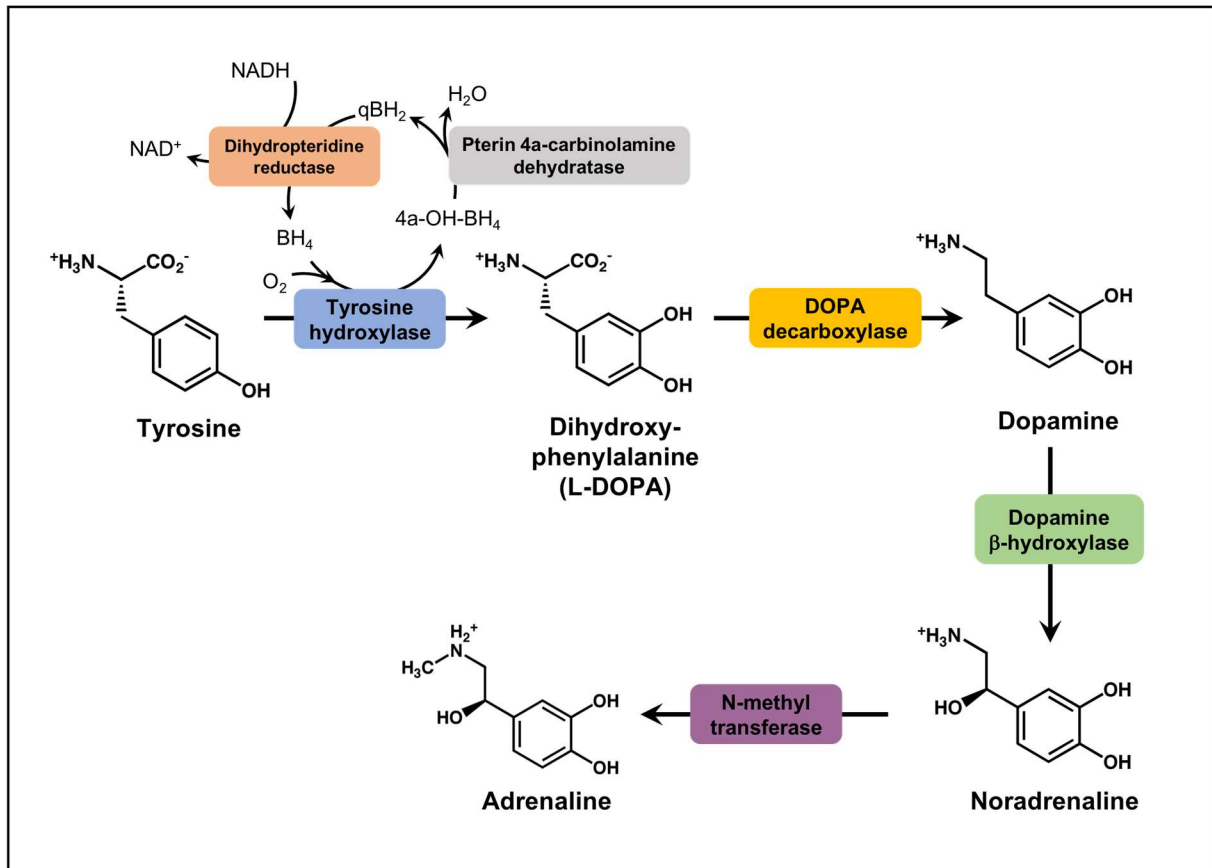


Figure 1.1: The catecholamine synthesis pathway. The pathway is initiated by hydroxylation of L-Tyr to L-DOPA by TH, which is the rate-limiting step. This reaction is dependent on BH₄ and thus on the required regeneration of this co-substrate.

1.1.1 Structure of tyrosine hydroxylase

TH is a complex tetrameric enzyme where each of the four identical subunits is composed of three domains with hinges that facilitate movements and flexibility. Each subunit consists of an N-terminal RD with an extended N-terminus with regulatory phosphorylation sites, a central catalytic domain (CD) containing the active site iron and a C-terminal oligomerization domain (OD) that facilitates dimerization and subsequent tetramerization (Figure 1.2) (reviewed in (Daubner et al., 2011)). The exact domain borders in TH are not defined, but the approximate transitions are at residues ~160 (RD to CD) and ~456 (CD to OD) (Figure 1.2A). To date, crystal structure determination of the 3D structure of full-length TH has not been successful, although the crystal structure of truncated forms containing only the CD and OD were published

more than 20 years ago (Figure 1.2B) (Goodwill et al., 1997; Goodwill et al., 1998). More recently, the structure of the isolated RD has been visualized by NMR (Figure 1.2C) (Zhang et al., 2014) and two low-resolution small-angle X-ray scattering (SAXS) structures of full-length TH have recently been published, although suggesting a somewhat contradictory shape of TH (Figure 1.2D) (Bezem et al., 2016; Szigetvari et al., 2019).

1.1.1.1 *The regulatory domain*

It is known that the AAAH enzymes have very similar structures. One exception is the RD in TH which is substantially longer than in PAH and TPH1. The 70 amino acids long N-terminal tail in TH has four phosphorylation sites (Ser/Thr-8, Ser-19, Ser-31 and Ser-40) that are important for regulation of TH-activity (Campbell et al., 1986).

The solution structure of the isolated RD of rat TH has been solved using NMR spectroscopy establishing that the RD (residues 65-159) is an ACT domain (Zhang et al., 2014) (Figure 1.2C). Two RD monomers are joined to form an ACT domain dimer and if this applies to the RDs in the full-length TH as suggested by Bezem *et al.*, the dimer is creating a tetramer both via the RDs and the OD (Bezem et al., 2016). This is however still a debated issue (Szigetvari et al., 2019). An ACT domain is characterized by a ferredoxin-like $\beta\alpha\beta\beta\alpha\beta$ -fold which consists of an antiparallel sheet of eight strands and four α -helices located on one side of the sheet (Chipman et al., 2001). ACT domains (named after the first letters of aspartate kinase, chorismate mutase and tyrA) are involved in the binding of regulatory ligands (small molecules) and are also found in other metabolic enzymes, e.g. phosphoglycerate dehydrogenase, aspartate kinase and PAH (Grant, 2006).

1.1.1.2 *The catalytic domain*

The CD is in the region from residues 160-456 (Daubner et al., 2011; Goodwill et al., 1997). This region is made up of approximately 50% α -helices, 10% β -sheet and 40% random coil (Tekin et al., 2014). This domain contains the active site that lies in a 17 Å deep cleft at the centre and is lined primarily by four α -helices (α 6- α 9) (Goodwill et al., 1997). There are two loops (residues 423-428 and 290-296) guarding the opening into the active site. Within the active site cleft, there are three coordinating residues required for iron binding: His 331, His 336 and Glu 376. They are ligands to the iron atom that must be in the ferrous state (Fe^{2+}) to carry out the catalysis. The iron atom is 10 Å below the enzyme surface. This arrangement of

metal binding formed by His 331, His 336 and Glu 376 residues is referred to as the 2-his-carboxylate facial triad (Daubner et al., 2011).

The iron atom in the active site is essential for the role that the catecholamines play in regulation of TH-activity. All the catecholamines bind to TH via the iron atom when it is in its ferric form (Gordon et al., 2008; Tekin et al., 2014). DA has also shown to competitively bind in the cofactor binding pocket. There are crystal structures of PAH CD bound to catecholamines, BH₄ and a substrate analog (Andersen et al., 2002; Erlandsen et al., 1998). Although there is no crystal structure of TH with catecholamines bound, it is likely that the binding arrangement of DA in the active site of TH is similar (Daubner et al., 2011).

1.1.1.3 The oligomerization domain

The OD consists of two main elements; a dimerization motif composed of two β -strands (β 7 and β 8) and a tetramerization α -helix (Goodwill et al., 1997). For each subunit the OD begins with the dimerization motif which is then followed by the α 14-helix. There are twenty-four amino acids forming the α 14-helix in the OD, which forms an anti-parallel coiled coil cylinder located in the middle of the four subunits, connecting the dimers to a tetramer. In the SAXS model of TH where the RDs are separate, these helices are the only interaction points between the dimers (Szigetvari et al., 2019). This is the arrangement seen in rat PAH (Arturo et al., 2016; Meisburger et al., 2016). The α -helices interact with each other through hydrophobic residues. The contact between the hydrophobic leucine (Leu) residues mediate a 3D-structural motif called a leucine zipper, which makes the interaction between the α -helices especially stable (O'Shea et al., 1989). This enables two dimers to interact with each other, making TH a dimer of dimers (Goodwill et al., 1997; Gordon et al., 2008).

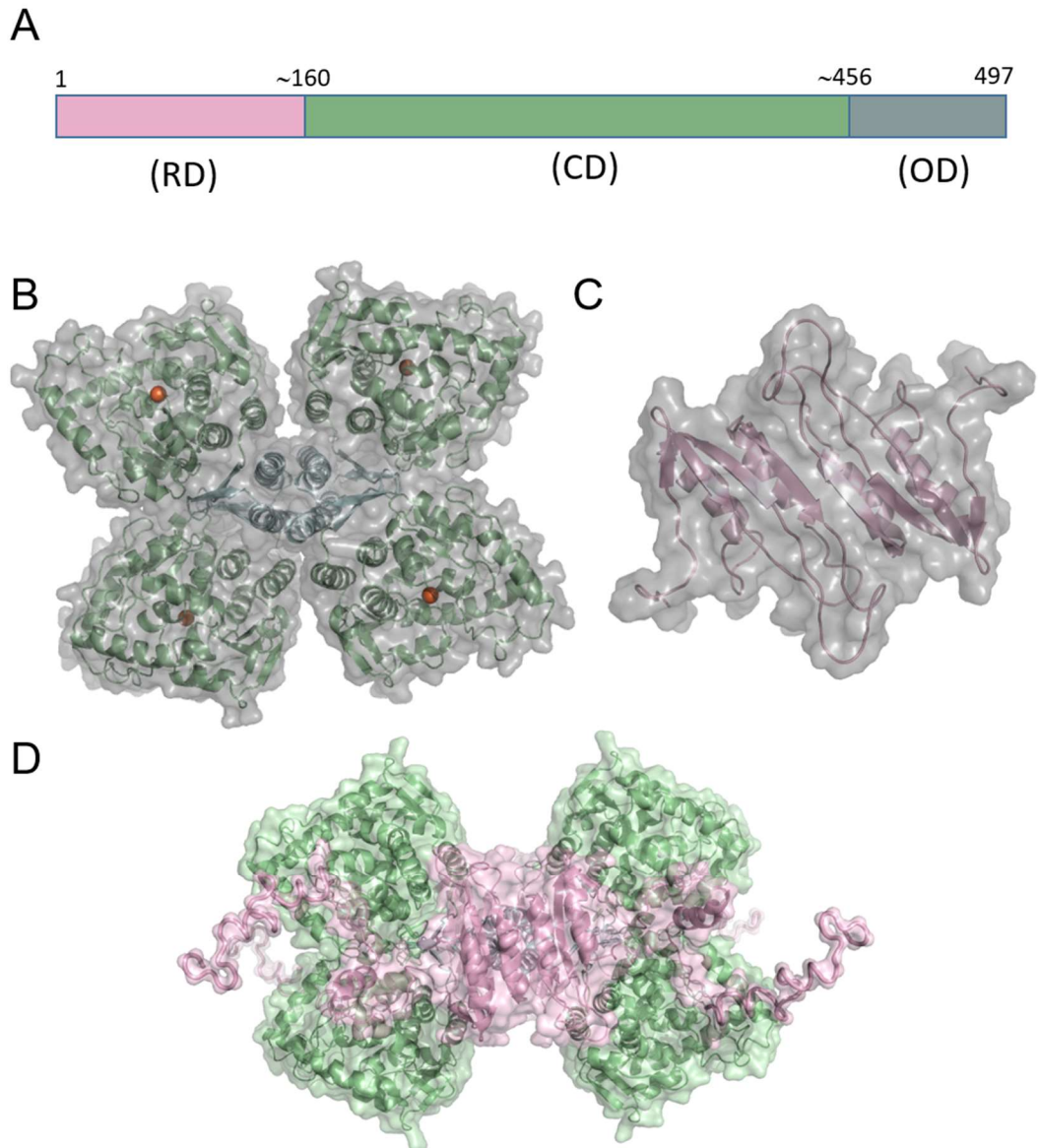


Figure 1.2: The published structures of TH. (A) shows the domain boundaries in different colors, corresponding to (B) the CD and OD (crystal structure lacking the RD, PDB ID: 1TOH), (C) the RD (NMR structure, PDB ID: 2MDA). In (D) the low-resolution solution structure of full-length TH is shown (Bezern et al., 2016).

1.1.2 The catalytic mechanism

The cofactor BH_4 , O_2 and iron are required for TH to carry out the hydroxylation of L-Tyr to form L-DOPA. Studies suggest that BH_4 must bind before the amino acid substrate so that an opening site for oxygen occurs in the presence of both substrate and cofactor (Roberts & Fitzpatrick, 2013). The binding pocket for BH_4 is made up of Glu332, Phe300, Tyr371 and Ser368 and Arg316, Ser395, Pro327 and Trp371 form the binding site for the substrate (Teigen et al., 2007). During the hydroxylation reaction, BH_4 serves as an electron donor producing

water by giving two hydrogens to one atom from molecular oxygen (Fitzpatrick, 1999; Nagatsu et al., 2018). The mechanism of oxygen activation is not fully understood but it is thought that the activation of the enzyme is initiated when oxygen reacts with ferric iron (Fe^{3+}) forming an Fe^{3+} -superoxide intermediate that further reacts with BH_4 to form an Fe^{2+} -peroxypterin species. This Fe^{2+} -peroxypterin intermediate is the precursor of the reactive Fe(IV)=O intermediate which is believed to hydroxylate the amino acid (reviewed in (Roberts & Fitzpatrick, 2013)). It has been shown that ferrous iron is required and that no other metal is catalytically active. In fact, divalent metals such as Ni^{2+} , Zn^{2+} and Co^{2+} appear to inhibit TH activity (Bezem et al., 2016; Haavik et al., 1991).

1.1.3 Regulation of tyrosine hydroxylase activity

Catecholamines are important neurotransmitters in the CNS and hormones in the endocrine system. Owing to their physiological and behavioral role in movement, cognition, emotion, pain, memory processing and endocrine modulation the TH activity is strictly regulated (Kobayashi, 2001; Tekin et al., 2014). Catecholamines must be synthesized in appropriate amounts depending on the situation as an excess is neurotoxic; the monoamines undergo oxidation reactions generating toxic catechol quinones, which can be accelerated by high amounts of metal ions such as iron, that lead to cellular macromolecular damage and eventually cell death (Hastings et al., 1994; Stokes et al., 1999). A strict regulation of TH activity is therefore important as it minimizes the toxic quinone formation and maintains the optimal level of catecholamines. TH activity is mainly controlled by three mechanisms; feedback inhibition by catecholamines (negative feedback), phosphorylation and dephosphorylation of serine residues, and by the concentration of cofactor and substrate (L-Tyr) (Nagatsu et al., 2018; Tekin et al., 2014). These regulatory mechanisms are short-term regulations and will be introduced in the following sections.

1.1.3.1 Feedback inhibition by catecholamines

Feedback inhibition by catecholamines, combined with phosphorylation, is one of the main short-term regulation mechanisms for TH activity. This negative feedback can be divided in two parts (Tekin et al., 2014). The first is when DA competes with BH_4 for active-site binding as both molecules have overlapping binding sites (Kumer et al., 1996). This makes DA a competitive inhibitor of TH. DA also inhibits TH in a non-competitive manner towards L-Tyr. The second inhibition mechanism is when DA binds directly to the active site, via the ferric

iron (Fe^{3+}) atom, generating a tight enzyme-iron-catecholamine complex which prevents further activation of the enzyme (Andersson et al., 1988). The conformation of the RD is altered when DA binds to TH, prohibiting entry of substrates into the active site (reviewed in (Daubner et al., 2011)). It is suggested that the effect of DA binding also converts TH to its stable resting state (Fujisawa et al., 2005).

1.1.3.2 Activation by phosphorylation

The second short-term regulation of TH activity is reversible phosphorylation of threonine (Thr) or serine (Ser) residues in position 8, 19, 31 and 40 in the RD (Campbell et al., 1986; Daubner et al., 2011; Ramsey et al., 1998). Tekin *et al.* have reviewed a range of protein kinases that are involved in the phosphorylation reaction, showing that each phosphorylation site has a main kinase responsible for their phosphorylation (Tekin et al., 2014). Ser19 is phosphorylated by calcium-calmodulin-dependent protein kinase II (CaMPKII), Ser31 by extracellular signal-regulated kinase 1 and 2 (ERK_{1/2}) and Ser40 by cAMP-dependent protein kinase A (PKA) (Haycock, 1993; Ramsey & Fitzpatrick, 1998). However, there is lack of evidence that phosphorylation of Ser/Thr8 has any regulatory effect on TH activity (Dunkley et al., 2004). Moreover, phosphorylation of Ser19 does not increase the TH activity directly but does in fact increase the phosphorylation rate of Ser40 (Gordon et al., 2008) and induces the interaction with the stabilizing 14-3-3 proteins, which is a family of conserved regulatory molecules (Kleppe et al., 2001). Data has been reported that phosphorylation of Ser19 can potentiate phosphorylation of Ser40 in intact cells (Bobrovskaya et al., 2004). Phosphorylation of Ser40 will decrease the affinity for DA 300-fold and relieve it from catecholamine inhibition, thus increasing the enzyme activity (Daubner et al., 2011). The phosphorylation of Ser31, that causes a decrease in the Michaelis constant (K_m) for BH₄, will also increase enzyme activity but to a much lesser extent (Dunkley et al., 2004). Recently, phosphorylation of TH at Ser31 has been associated with the interaction of the enzyme with the vesicular monoamine transporter (VMAT2), targeting TH for transport to the terminals (Jorge-Finnigan et al., 2017).

1.1.3.3 Negative cooperativity of BH₄ binding and substrate inhibition

There has been reported a potential third regulation mechanism of TH activity *in vitro* where BH₄ shows negative cooperative behavior towards TH (Flatmark et al., 1999). The underlying principle of negative cooperativity is that when BH₄ binds to the active site of TH, a conformational change occurs which results in decreased ligand affinity, both in equilibrium

binding and in kinetic studies (Flatmark et al., 1999). Thus, the ligand affinity decreases with increasing amount of bound ligand. Therefore, TH activity also depends on the concentration of BH₄. At last, the enzyme activity is also dependent on the concentration of L-Tyr. At very high levels of the L-Tyr (>50 μM), TH is subjected to very strong inhibition (Quinsey et al., 1998). Indeed, substrate inhibition plays a role in TH-regulation and hence in the biosynthesis of catecholamines.

1.1.4 Dysfunctions of tyrosine hydroxylase and disease

Catecholamines are produced in the brainstem, nerve tissue and adrenal glands and play roles in many brain functions such as memory, cognition, movements, emotion and attention (reviewed in (Daubner et al., 2011)). The importance of DA is evident in the neurodegenerative Parkinson's disease (PD) which is characterized by selective and severe loss of dopaminergic neurons in substantia nigra causing lack of DA in these brain areas (Haavik et al., 1998; Zhu et al., 2012). Since adrenaline and noradrenaline are involved in maintaining blood pressure and blood sugar, dysfunction and subsequent reduction in DA synthesis will affect these cardiovascular and endocrine systems as well.

Most often dysfunction of TH is caused by mutations in the *TH*-gene which affect the folding of TH and lead to a disease called tyrosine hydroxylase deficiency (THD), also known as Segawa syndrome (OMIM #605407). THD is an autosomal recessive disorder manifesting as a progressive movement retardation and include clinical features such as tremor, rigidity, chorea, bradykinesia, hypokinesia and dystonia. The diagnosis is based on clinical symptoms and measurements of normal concentration of 5-hydroxyindolacetic acid (5-HIAA), low homovanillic acid (HVA), low 3-methoxy-4-hydroxyphenylethylene glycol (MHPG) and low HVA:5-HIAA ratio in cerebrospinal fluid. The homovanillic acid is the catabolic product of DA in CNS whereas MHPG is from noradrenaline.

As is the case in PD, most THD patients are mainly treated with L-DOPA – the precursor of DA – which is used therapeutically because of its ability to cross the blood-brain barrier (BBB) by an amino acid transporter called system L (Kageyama et al., 2000). In the brain, dopaminergic neurons will convert L-DOPA into DA, catalyzed by aromatic amino acid decarboxylase, increasing the dopamine level. L-DOPA is usually co-administrated with a decarboxylase inhibitor to block the conversion of L-DOPA to DA within peripheral tissues,

thus preventing possible adverse side effects and also for avoiding loss of L-DOPA in the circulation (Bartholini et al., 1967; Willemsen et al., 2010). The decarboxylase inhibitors, e.g. carbidopa, selectively inhibit peripheral but not the neuronal decarboxylase, as the decarboxylase inhibitors are unable to cross the BBB (Hoffmann et al., 2003). L-DOPA is therefore known as a dopamine replacement agent that is also used in treatment of THD.

Patients diagnosed with THD are categorized into two subgroups: type A is a mild progressive neurological condition with onset in infancy that is responsive to L-DOPA treatment, and type B is a more severe complex encephalopathy with neonatal onset that is L-DOPA-nonresponsive (reviewed in (Willemsen et al., 2010)). However, long-term L-DOPA treatment is associated with side effects, for type B patients especially, and is not considered as being sufficient for efficient treatment (Pons et al., 2013). Thus, an alternative therapeutic treatment is highly needed for these severe THD patients.

1.1.4.1 Mutant R202H-hTH1

The most common missense mutation in THD is Arg233His (*TH*-p.R233H) in exon 6 in isoform 4 of human TH (hTH4) (Fossbakk et al., 2014; Hoffmann et al., 2003). *TH*-p.R233H is caused by a mutation of the arginine (R) in position 233 to a histidine (H) resulting in decreased enzyme stability and activity. The R233 is equivalent to R202 in hTH1. From now on, this mutation will therefore be referred to as R202H.

The R202H mutation accounts for about 30% of all alleles in the THD cases studied (Willemsen et al., 2010). The mutant is associated with autosomal recessive L-DOPA-responsive infantile parkinsonism (Hoffmann et al., 2003) and also both type A or type B THD, although there is an abundance of type B patients when in homozygosity (Willemsen et al., 2010). Patients diagnosed with L-DOPA-responsive dystonia caused by the R202H mutation have been reported in The Netherlands (van den Heuvel et al., 1998).

There are several studies that have been conducted to investigate different therapeutic strategies and increase our understanding on the R202H mutant (Calvo et al., 2010; Hole et al., 2016; Korner et al., 2015). Korner *et al.* discovered that mice with the R202H mutation (R203H in mice) lacks TH in the brain striatum, which has also been shown to be associated with PD. TH is expressed in the substantia nigra and the lack of TH in the striatum was explained by Korner *et al.* to be caused by the inability of the mutant TH to bind and be stabilized by DA. As it is believed that TH is transported in the dopaminergic pathway from the substantia nigra to the

striatum as a TH-DA complex, a functional transport of the TH-R202H will not be possible, since DA does not bind and stabilize this mutant properly (Korner et al., 2015). R202 is positioned in an α -helix that lies close to the active site and its ability to form strong bonds to E223 and E228 is likely important for keeping the structure of the CD in the correct shape and possibly also for keeping DA stably bound (Figure 1.3). In this respect, developing strategies to stabilize TH-R202H and other TH mutants will be a potential target for THD, and also other genetic dopaminergic deficiencies.

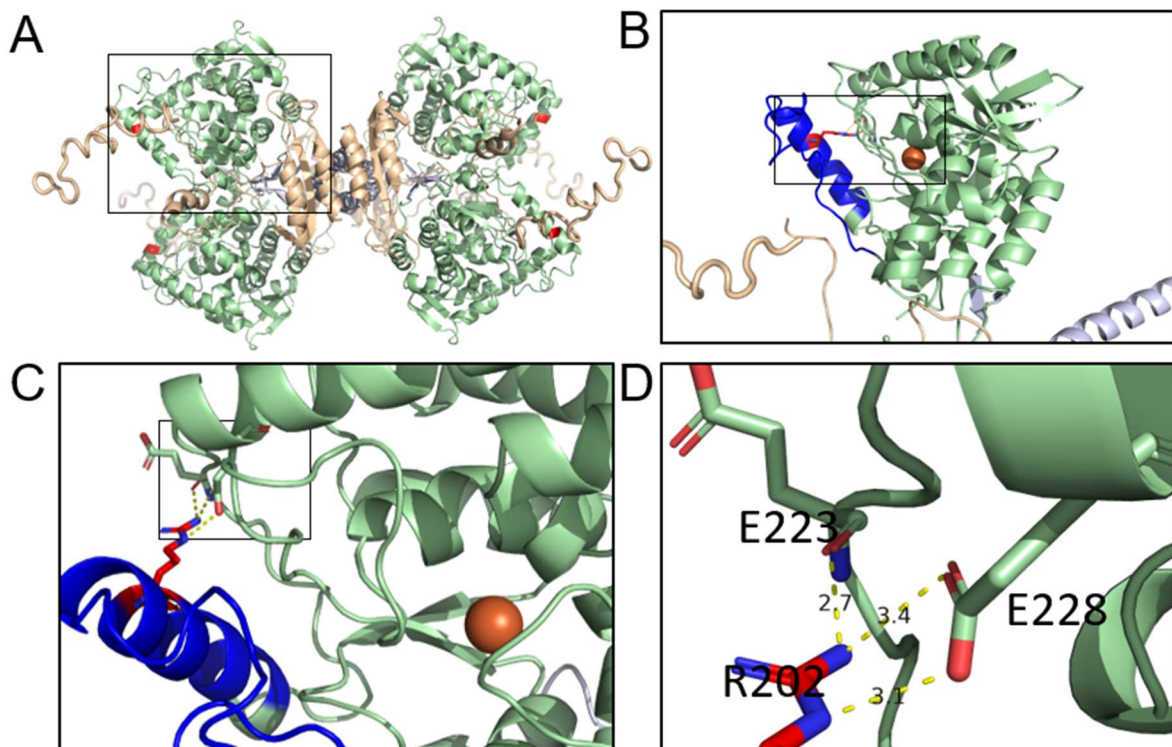


Figure 1.3: Position of R202 in TH. (A) The tetrameric SAXS structure of TH showing the position of R202 (red) in each subunit. In the close-up in (B), the α -helix where R202 is located is shown in blue and the FE from PDB ID: 1TOH is placed to show its proximity to the active site. (C,D) the interaction between the positively charged R202 with the negatively charged E223 and E228 appears important for holding the α -helix in place close to the active site.

1.2 Protein stability

Protein folding is the physicochemical process by which a polypeptide chain spontaneously folds into its native characteristic three-dimensional (3D) structure. The amino acid sequence determines the 3D structure of proteins that must be correct for the protein to perform its biological function (Dobson, 2003). The transition from the unfolded to the native state involves the search for the conformation of correct free energy (ΔG) (Figure 1.4). Failure to fold into the native confirmation causes an incorrect protein structure, normally associated with defective protein function and stability.

Inside cells, large protein complexes called molecular *chaperones* prevent unfolded proteins to be tangled up with one another and form unwanted aggregates (Ellis, 1990). These protein complexes are part of the cellular protein quality control system that controls the protein production status, localization, folding and degradation, which is necessary to avoid misfolding and aggregation of proteins (Figure 1.4). Some of these chaperones have also been proved to rescue an already misfolded or partially folded protein, enabling them to fold correctly (Dobson, 2003; Hartl et al., 2011). A certain level of misfolded non-functional forms of proteins can still occur which will lead to gradually build up in cells. The ubiquitin-proteasome system (UPS) prevents accumulation of misfolded, damaged and mutant proteins by cellular proteolysis. The misfolded proteins are first tagged by a protein known as ubiquitin and then recognized, proteolyzed and eliminated by proteasomes (Nandi et al., 2006). This is contrary to autophagy, a nonselective degradation system, that disassembles dysfunctional or unnecessary components without the requirement of specific tag recognition (Mizushima, 2007). The UPS and the autophagy lysosomal systems are the two main protein degradation systems in the cell (reviewed in (Lilienbaum, 2013)). However, excess of misfolded protein molecules can overload the capacity of the UPS and the autophagy systems, allowing soluble aggregates to undergo further assembly into amyloid fibrils or plaques which can harm and injure cells (Gregersen et al., 2006; Hartl et al., 2002). Deposition of such protein aggregates and amyloid fibrils are reported in neurological disorders such as Alzheimer and Parkinson's diseases (Muchowski, 2002).

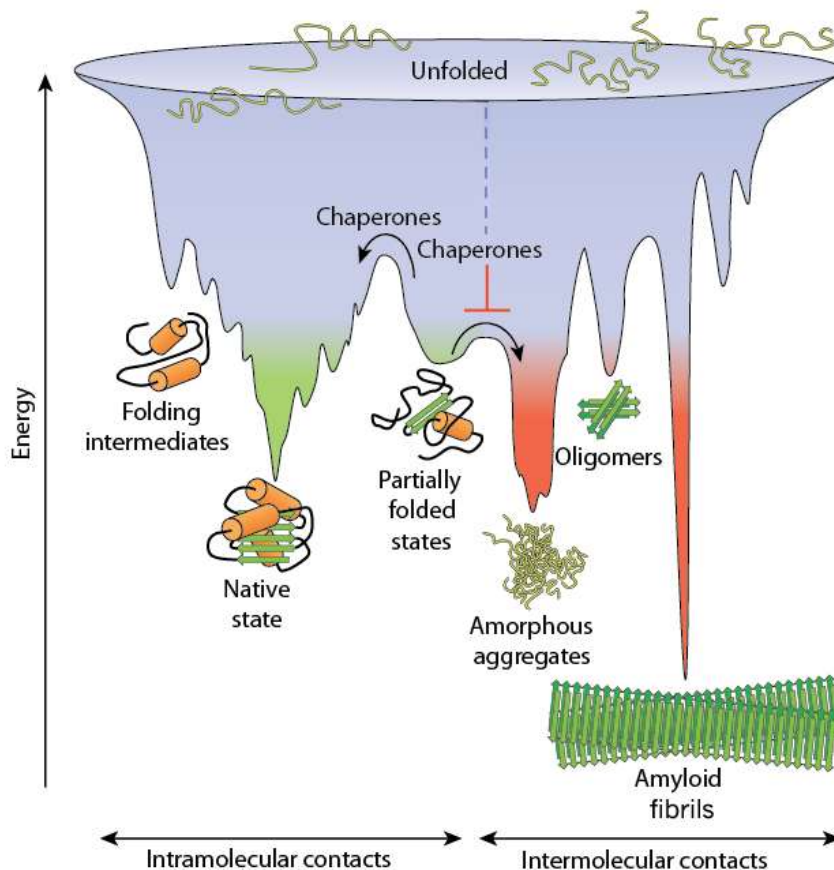


Figure 1.4: Schematic energy funnel illustrating the folding process of proteins. Unfolded conformers are seeking the correctly folded conformation via intermediate states. Protein complexes, known as molecular chaperones in cells, help partially folded proteins to fold to into a native state. (Figure taken from (Hartl et al., 2011)).

1.2.1 Pharmacological chaperones

A wide range of illnesses often occur because of protein misfolding that causes premature degradation and/or loss of protein function. However, the protein activity can be recovered by small molecules that bind, stabilize and accelerate folding of the native conformation. Such low molecular weight molecules are called pharmacological chaperones (PC) as they have similar roles as protein chaperones in cells. Instead of assisting in folding, they mainly stabilize an already folded but unstable protein by protecting it from proteolytic degradation and aggregate formation (Ringe et al., 2009). PCs with high affinity binding to a specific protein is an important property for achieving stabilization through molecular interactions including van der Waals, electrostatic – and hydrogen binding with residues in the binding site, holding parts of the protein structure together thus contributing to a correct protein function (Figure 1.5) (Hole et al., 2016).

PCs have the potential to be used as a therapeutic strategy for correction of misfolded mutant proteins and have already been implemented in treatment of some protein-misfolding diseases, in particular lysosomal storage disorders such as Fabry – and Gaucher disease (Markham, 2016). The concept of PC therapy is relatively new but has been growing in the research field the last years.

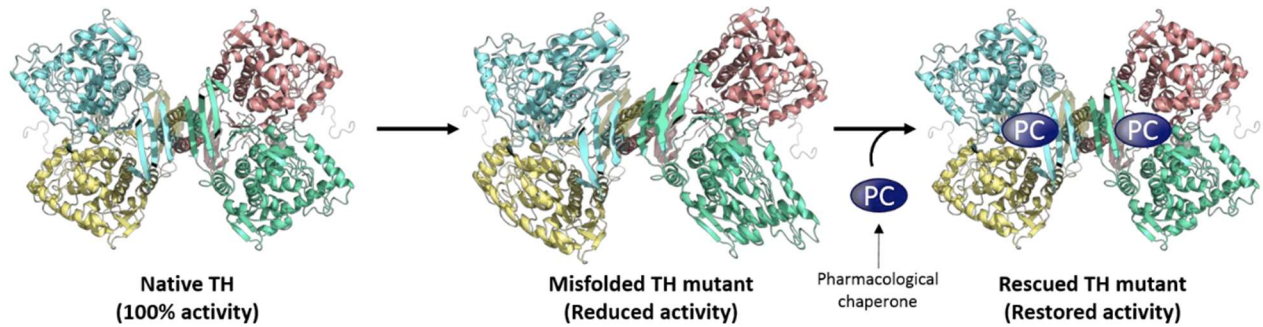


Figure 1.5: Pharmacological chaperones bind and stabilize TH mutants without inhibiting activity.

1.3 From gene to pharmacological chaperone – a methodological overview

The work presented in this thesis presents the workflow from expression of TH protein to the identification of potential PCs using the following methods:

1.3.1 Recombinant protein expression and purification

Overexpression of recombinant protein is a known and widely used methodological approach in science for making specific proteins that can be used in studies of their function, in drug discovery or as biotherapeutics to treat diseases. Recombinant proteins are expressed by using various expression systems or hosts including yeast, bacteria, insect- and mammalian cells or without the use of living cells. The best protein production system is dependent on the protein, e.g. membrane proteins often fail in bacterial systems. However, the most used and well-established expression system is the bacteria, *E.coli* in particular, where the cDNA of the gene of interest is introduced on a plasmid expression vector (Rosano et al., 2014). Overexpression in *E.coli* is carried out by cloning the cDNA for the protein of interest into a high-copy plasmid, often containing the lac or T7 promoter which is induced by lactose or its analog.

After overexpression, the recombinant proteins in *E.coli* are purified using an appropriate method and used for further studies. The main benefits of bacterial expression are the fast exponential growth of the organism and the ease of genetic manipulation. Besides, it only requires simple and relatively cheap equipment and materials.

1.3.1.1 Affinity chromatography

Affinity chromatography is a method used for separating specific molecules from a complex mixture as a step in the purification process of proteins (Urh et al., 2009). Separation is achieved by loading the mobile phase, which contains a variety of biomolecules, onto a column containing a specific ligand – the stationary phase – that can interact with the biomolecule of interest (Figure 1.6A). In order to facilitate the purification of proteins by affinity chromatography, different affinity fusion tags are often utilized. Some commonly used affinity tags for purification of recombinant proteins are the hexahistidine tag (6xHis-tag), glutathione S-transferase (GST), calmodulin-binding peptide (CBP) and maltose-binding protein (MBP) (Zhao et al., 2013).

Target proteins that are fused to the maltose binding protein (MBP) specifically – a widely used protein expression tag – permits its purification using amylose resin as the stationary phase

(Terpe, 2003). During the chromatography, the target protein binds to the immobilized ligand (amylose resin) via the highly specific interactions between the MBP-partner and the resin. All other (non-target) biomolecules will be removed by a washing buffer due to their weaker interactions with the stationary phase and eventually only the fusion protein will remain on the column. When changing the composition of the mobile phase by adding maltose, it will outcompete the resin for binding to MBP as its affinity is higher, effectively releasing the fusion protein.

1.3.1.2 Size-Exclusion Chromatography

Size-exclusion chromatography (SEC), also known as gel filtration, is a chromatographic method which separates proteins in solution according to their size as they are filtrated through a column containing a porous matrix of specific size distribution (Figure 1.6B). Molecules larger than the pores elute first as they are unable to diffuse into the porous matrix, while smaller molecules that are able to enter the pores will spend more time in the packed matrix and flow through the column more slowly, thus eluting later. Analytical SEC is often used to test the quality of a protein sample. This technique will reveal if it contains e.g. aggregates or other oligomers and is therefore an important step in monitoring the purification process of proteins. Chromatographic conditions such as column length, pore size, flow rate, and volume load are important factors that can have a big impact on the resolution, sensitivity and analysis time when performing SEC and must be considered (Hong et al., 2012).

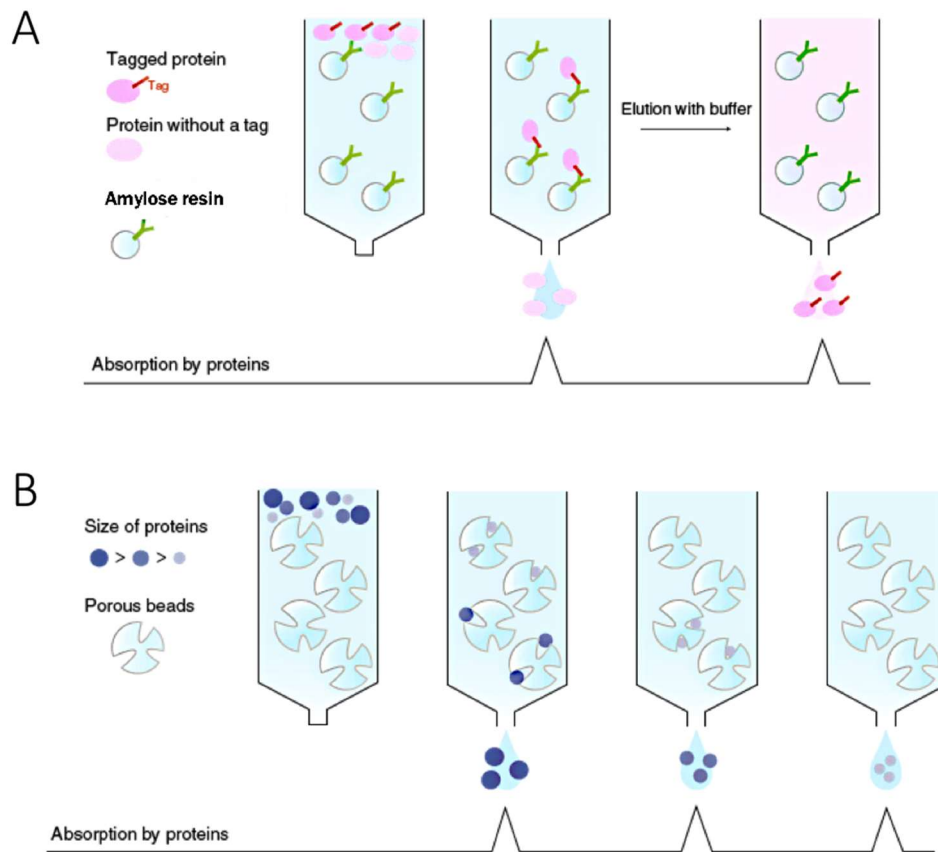


Figure 1.6: Principle of (A) affinity chromatography and (B) size-exclusion chromatography. Figure modified from MBL Life Science home page.

1.3.2 Differential Scanning Fluorimetry

Differential scanning fluorimetry (DSF) is a high throughput method used to determine conditions that affect protein stability (Brennecke et al., 2019; Niesen et al., 2007). The method relies on the fact that proteins denature when subjected to sufficient heat and when the temperature reaches the midpoint temperature (T_m) of the particular protein – defined as the temperature where 50% of protein is unfolded - it exposes its internal hydrophobic protein core. SYPRO Orange (SO) can be used as a probe as it fluoresces upon binding to hydrophobic patches. In DSF the temperature is steadily increased, and the fluorescence intensity is plotted as a function of temperature to show the fraction of unfolded protein (Figure 1.7). By comparing the T_m -values obtained in different conditions one can identify those that have an impact on protein stability. DSF is typically performed by using a real-time PCR instrument such as LightCycler® that allows high-throughput performance. DSF is an inexpensive method that allows rapid analysis of multiple samples simultaneously, thus being an important tool in screening and validation assays.

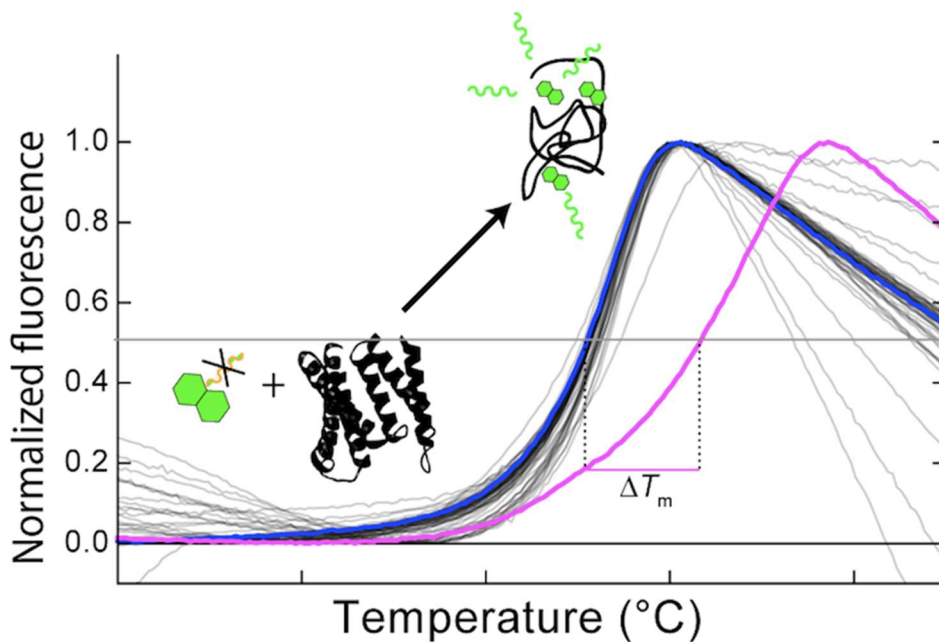


Figure 1.7: The principle of DSF. The fluorescence intensity is plotted as a function of temperature to show the fraction of unfolded protein and the midpoint of the curve defines the T_m . Figure taken from Brennecke et al.

1.3.3 TH activity assay

An assay of TH activity is based on quantification of L-DOPA by high-performance liquid chromatography (HPLC) (Haavik et al., 1980). As mentioned previously, TH catalyzes the hydroxylation of L-Tyr to L-DOPA in the biosynthesis of catecholamines neurotransmitters with an absolute requirement of BH_4 . Addition of the cofactor is therefore crucial to start the catalytic reaction. HPLC with fluorescence detection enables separation of L-Tyr and L-DOPA in the solution and since the enzyme activity is directly correlated to the L-DOPA production from L-Tyr, L-DOPA is quantified. The chromatographic separation is based on different degrees of interaction between the components of the sample and the adsorbent material in the column. The separation occurs under significantly higher pressure forcing the molecules to flow through very fast. In normal-phase chromatography, the stationary phase is polar while the solvent is non-polar. Non-polar molecules in the sample mixture will move with the solvent and elute first relative to the polar molecules (such as L-DOPA). The fluorescence emission spectra of both components will be detected revealing the L-DOPA production. L-Tyr is excited at wavelength 274 nm and emits at 304 nm, while L-DOPA is excited and fluorescence at 281 nm and 314 nm, respectively (Haavik & Flatmark, 1980). Finally, molecules that bind and

stabilize TH can have an impact on the enzyme activity and these are thus added to the enzyme solution before starting the assay.

1.3.3.1 EC_{50} and IC_{50}

The concepts of EC_{50} and IC_{50} are well known in pharmacology and are terms widely used to measure the efficacy of a drug. The definition of EC_{50} is the concentration of a drug, toxicant or compound which induces a response halfway between the baseline and maximum after a specified exposure time. The half maximal inhibitory concentration (IC_{50}) however, is the concentration of a compound that is required to inhibit a given maximal biological function by half (Sebaugh, 2011). The IC_{50} terminology is used when the maximal effect of a response is related to inhibition. This concept is important in drug discovery and was applied in our search for pharmacological chaperones for TH. Measurements of EC_{50}/IC_{50} for compounds allow those with pharmacological chaperone potential and those with inhibitory potential to be discovered and recognized. In this work, the EC_{50} and IC_{50} values were determined using the four-parameter logistic nonlinear regression equation in SigmaPlot:

$$(1) \quad y = \mathit{min} + \frac{(\mathit{max} - \mathit{min})}{1 + \left(\frac{x}{EC_{50}}\right)^{-\mathit{Hillslope}}}$$

1.3.4 Limited proteolysis by trypsin

Limited proteolysis is a simple biochemical method based on a short exposure of a protein to low concentration of a proteolytic enzyme (e.g. trypsin). Trypsin is an enzyme that cleaves other proteins in flexible areas. For TH, treatment with trypsin has been reported to cleave the N-terminal region (70-80 residues), shortening the 60 kDa (full-length) to 57 kDa and 52-54 kDa (Hole et al., 2015). By N-terminal sequencing of the products, four cleavage sites have been identified after arginines in position 33, 37, 38 and 49 making the N-terminal the most sensitive region upon proteolysis (McCulloch et al., 1999). It has however been demonstrated that the binding of DA decreases the rate of trypsinization, protecting the protein from further cleavage (Hole et al., 2015; McCulloch & Fitzpatrick, 1999). The susceptibility of TH to limited tryptic proteolysis can thus be tested with different compounds which can support information regarding binding, thermal stabilization and conformational changes of TH.

1.3.5 Isothermal Titration Calorimetry

Isothermal titration calorimetry (ITC) is a technique used to directly measure the heat that is absorbed or released during a binding event. This method provides important thermodynamic information such as enthalpy (ΔH), entropy (ΔS), reaction stoichiometry (N) and binding affinity (K_d). Moreover, ITC gives insight into understanding of the nature of the molecular interaction occurring (Leavitt et al., 2001). The calorimeter consists of a sample cell, that contains one of the binding partners (e.g. a protein), and a reference cell that contains only water. The two cells are kept at exactly the same temperature. As the other binding-partner (e.g. a compound) is gradually injected into the sample cell, a binding occurs releasing (or absorbing) heat that will be measured. A heat sensing device will detect the temperature differences between the cells and therefore compensate for the small heat changes by returning both cells to equal temperature. At one point, the protein will get saturated thus limiting binding of compound, and the heat transferring will decrease as followed. The system and example results are shown in Figure 1.8.

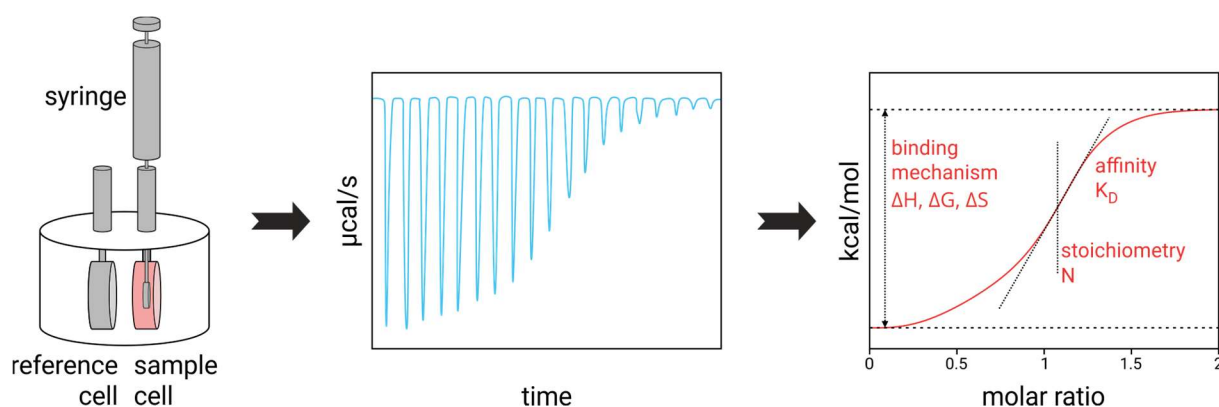


Figure 1.8: Illustration of the Isothermal titration calorimetry (ITC) system. The area under each peak correlates to fractional heat of binding (in microcalories). The quantity of heat measured, and the amount of binding is directly proportional to each other. As the protein is saturated, the peaks have lower intensity. The data is normalized and plotted against the molar ratio of binding partners. Figure from 2bind molecular interactions home page.

1.3.6 Molecular docking

Molecular docking, also known as target-based virtual screening, is frequently used in drug design and analysis. It is a computational method that involves positioning the ligands of interest in the binding site of a target protein of known three-dimensional structure generating a protein-ligand complex (Meng et al., 2011). The stability of a protein-ligand complex is related to its binding free energy, so that the ligand molecule is placed at what is considered to be the most energetically favorable position in the site. The binding affinity of the ligand for the protein is determined by a scoring function (e.g. Glide score) pointing to whether these orientations are the most optimal (Friesner et al., 2004). Molecular docking is an important tool not only used in computational chemistry, but also recently in the field of modern drug discovery and development. The main aim of the docking process is to predict the predominant binding mode of a ligand with a target protein which might give a deeper understanding of the structure-function relationship (Morris et al., 2008).

2 Aims of the project

The main objective of the project is to screen and validate compounds with pharmacological chaperone potential that stabilize tyrosine hydroxylase (TH) and its disease associated mutants, notably TH1-p.R202H. Compounds that correct the conformation of the mutant are also expected to correct its localization and function in the brain. An important objective of the thesis is thus to get expertise in a series of methods of relevance in early stage drug development.

3 Materials and Methods

3.1 Materials

Chemical	Supplier
Luria Bertani Broth (Lennox)	Sigma Aldrich
Kanamycin sulfate	Sigma Aldrich
Chloramphenicol	Sigma Aldrich
Isopropyl-β-D-1-thiogalactopyranoside	Apollo Scientific
Ammonium iron (II) sulfate hexahydrate	Sigma Aldrich
Benzamidine hydrochloride hydrate	Sigma Aldrich
Phenylmethanesulfonyl fluoride	Sigma Aldrich
cOmplete EDTA-free tablets	Roche
Amylose resin	BioLabs
Tobacco Etch Virus protease	Purified in lab E
D-(+)-Maltose monohydrate	Sigma Aldrich
Loading buffer/Laemmlis Sample Buffer	Bio-Rad
Dithiothreitol	Sigma Aldrich
Coomassie G-250	Bio-Rad
Urea	MERCK
SYPRO™ Orange 5000X, Invitrogen S6650	Fisher Scientific
Bovine serum albumin	Sigma Aldrich
Catalase	Sigma Aldrich
L-Tyrosine	Sigma Aldrich
L-3,4-dihydroxyphenylalanine	Sigma Aldrich
Dopamine hydrochloride	Sigma Aldrich
Ethanol	VWR Chemicals
Acetic acid >99,8%	Sigma Aldrich
Propanol	VWR Chemicals
Glycerol (solution) 86-89% (T)	Sigma Aldrich
Peptone	Sigma Aldrich
Yeast extract	Merck
TPCK treated trypsin	Sigma Aldrich
Trypsin soybean inhibitor	Sigma Aldrich
DMSO	Sigma Aldrich

Common chemicals not mentioned in the table are supplied by Sigma Aldrich.

3.2 Preparation of pure and stable TH enzymes

In this work, we will focus on expressing His-MBP-TH and the His-MBP-TH-R202H. Tyrosine hydroxylase (TH) is expressed with an N-terminal His-tagged Maltose binding protein (MBP) fusion partner in bacterial cultures of *BL21-CodonPlus* by the gene encoding His-MBP-TH in the plasmid vector pET-MBP-1a (Figure 3.1). We will do a first attempt to express His-MBP-TH from a modified and thus novel version of the previously published pET-MBP-1a/TH (Bezem et al., 2016). This new construct has been optimized (by deletion mutagenesis) to not contain extra residues (GAM) at the N-terminus after cutting with Tobacco Etch Virus (TEV) protease. This new fusion protein will be referred to as *optimized* His-MBP-TH. The previously published pET-MBP-1a/TH vector was also used as template to make the hTH1-p.R202H mutant (Korner et al., 2015).

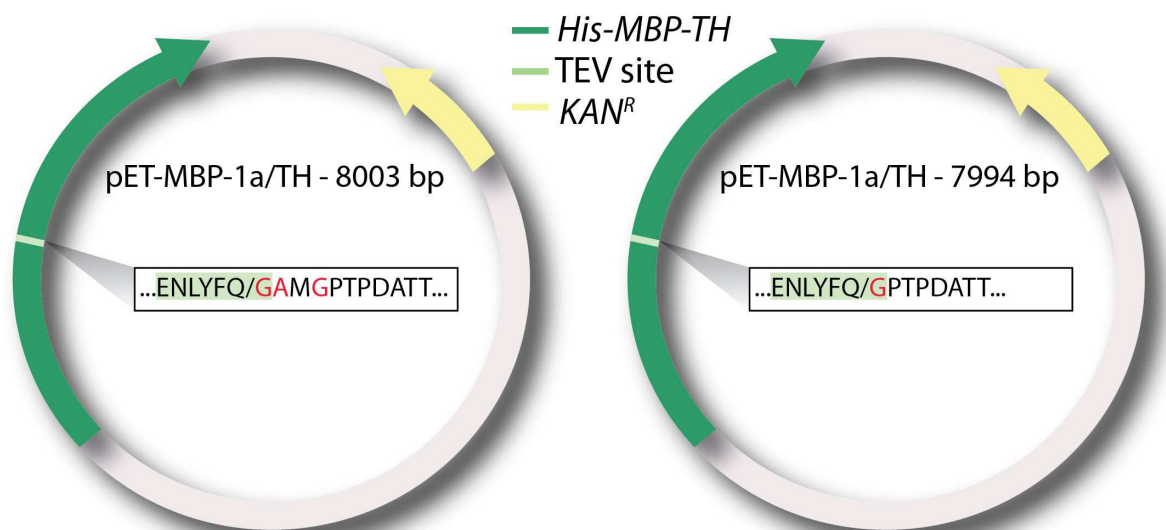


Figure 3.1: Schematic view of the plasmid vector pET-MBP-1a encoding published (left) and optimized (right) His-MBP-TH. Extra amino acids compared to the native amino acid sequence are denoted in red for both plasmids.

As BL21 CodonPlus is resistant to chloramphenicol (cam) and the pET-MBP-1a plasmid confers kanamycin (kan) resistance, both antibiotics are used during growth and expression (Figure 3.1). MBP facilitates affinity purification of His-MBP-TH as the MBP binds to amylose resin and stays bound during wash-out of other proteins (Terpe, 2003). The high affinity of MBP for maltose enables elution with maltose-supplemented buffer. MBP is also used to reduce aggregation of recombinant proteins (Waugh, 2016). A modified TEV protease (van den Berg

et al., 2006) is used to release TH from the fusion partner as it recognizes and cuts the sequence ENLYFQ/(G/S) encoded by the plasmid (Bezem et al., 2016).

3.2.1 Expression of His-MBP-TH proteins

Luria-Bertani (LB) medium (50 ml) containing 34 µg/ml cam and 50 µg/ml kan were inoculated with *E. coli* BL21-CodonPlus and incubated overnight at 28°C, before diluted in 1 L LB-medium with the same concentration of antibiotics. The bacterial cultures were shaken (200 rpm) at 37°C and the growth was monitored with Biowave C08000 Cell Density Meter. At $OD_{600nm} \approx 0.7$, 0.5 mM isopropyl-β-D-1-thiogalactopyranoside (IPTG) was added to induce expression of His-MBP-TH and ~100 mg of ammonium iron (II) sulfate hexahydrate (FAS) was added simultaneously to saturate the TH active site. The cultures were incubated for 22 hours at 28°C. The cultures were harvested by centrifugation at 4000 x g (4°C, 20 min) and resuspended in a smaller volume and centrifuged for another 20 minutes at 3000 x g (4°C) in 50 ml Falcon-tubes. As a preparation for sonication the pellets were stored at – 80°C for about 2 hours to make the bacteria more fragile.

The mutant TH-R202H was also expressed in *E. coli* BL21-CodonPlus, but grown in Terrific Broth medium (4 ml/L glycerol, 20 g/L peptone, 24 g/L yeast extract with 0.017 M KH_2PO_4 and 0.072 M K_2HPO_4) and induced for 24 h at 20°C.

3.2.2 Purification of His-MBP-TH by affinity chromatography

The bacterial pellets were resuspended in 5 ml/g Lysis buffer (20 mM Hepes pH 7, 200 mM NaCl, 10 mM Benzamidine hydrochloride hydrate, 1 mM Phenylmethanesulfonyl fluoride (PSMF) and 1 tablet of cOmplete™ EDTA-free/70 ml buffer) and sonicated on ice in three rounds of 45 s using a Sonics Vibra cell™ (pulser 9 sec, output 20 Watts). The sonicate was centrifuged for 30 min at 23500 x g (4°C), and the crude extract containing soluble proteins was collected. For the wild-type proteins, amylose resin (5 ml/L original culture volume) was equilibrated with Binding buffer (Lysis buffer without protease inhibitors) and incubated with the crude extract for 3 hours in the cold room on a rotary wheel before most of the unbound proteins were removed by centrifugation (2844 x g, 10 min at 4°C) and the amylose resin was transferred to an empty XK-column connected to an ÄKTAprime Plus Liquid Chromatography system (GE Healthcare) at 4°C. For the mutant fusion protein, the crude extract obtained was

loaded into empty PD-10 columns (GE Healthcare) containing buffer-equilibrated amylose resin (2.5 ml/original culture volume) in the cold room until all the extract had run through by gravity flow and subsequently washed with Binding buffer. In both methods, the resin was washed with Binding buffer until the OD_{280nm} was below 0.01.

The His-MBP-TH proteins were eluted with Elution buffer (Binding buffer with 10 mM maltose) using a flow rate of 2 ml/min (for the normal, wild-type (wt) TH) or gravity (for the TH-R202H mutant). Eluted fusion protein were concentrated in 15 ml Amicon® Ultra-15 50 MWCO Centrifugal Filter Devices and the protein concentration was measured spectrophotometrically at 280 nm using ϵ_{280} (1 mg/ml) = 1.63. The fusion proteins were stored in liquid nitrogen for later use.

Sodium dodecyl polyacrylamide gel electrophoresis (SDS-PAGE) was used to evaluate the purification process and check the purity of the His-MBP-TH proteins. Samples were diluted 1:1 in 2x loading buffer (LB) with fresh dithiothreitol (DTT) and heated at 95°C for 5 min before applied to a *Mini-PROTEAN® TGX™ Precast Gel* (Bio-Rad) in a Bio-Rad Mini-PROTEAN® Tetra Cell system with Tris-glycine-SDS (TGS) running buffer. Low molecular weight marker (LMW) (Bio-Rad SDS-PAGE Molecular Weight Standards, Low range) was used to determine the size of the proteins. The gel ran at 300 V for 15 minutes. After the electrophoresis the gel was immersed in Coomassie Blue G-250, heated in the microwave and gently agitated at room temperature until bands appeared. After destaining with water, the gel was photographed using a Bio-Rad ChemiDoc™ XRS+.

3.2.3 Removal of tag and isolation of TH

3.2.3.1 *Testing the quality of fusion protein by SEC*

The quality and oligomeric distribution of the original and *optimized* wild-type and of the R202H mutant fusion proteins were analyzed by size-exclusion chromatography (SEC) at a flowrate of 0.5 ml/min. SEC separates proteins in solution by size and thus, the analysis reveals if our purified fusion protein samples contain aggregates, the expected tetramer of His-MBP-TH or other oligomers. The column used was a Superdex™ 200 Increase 10/300 connected to an Äkta Pure (GE Healthcare), at 4°C.

3.2.3.2 Optimizing TEV-protease cutting

As the amino acid sequence around the TEV-protease cleavage site (ENLYFQ/G) in the *optimized* His-MBP-TH is reduced by 3 amino acids (GAM) as shown in Figure 3.1, the linker between the MBP and TH is shorter than in the fusion protein previously published (Bezem 2016). As this change can potentially influence the access to the TEV protease cutting site and thus the efficiency of the cutting, cutting tests with TEV-protease were performed under different conditions. The cutting of the His-MBP-TH-R202H-mutant was also tested.

The first test was performed with the *optimized* His-MBP-TH. To test different protein:protease ratios and incubation-time, 10 µg samples were mixed with either 0.2 µg TEV-protease (1/50 w/w ratio) or 1 µg TEV-protease (1/10 w/w ratio) and incubated at 4°C. Samples from both ratios were taken out after 1, 2 and 3 hours. To stop the reaction the samples were immediately mixed with loading buffer containing DTT and heated at 95°C for 5 minutes before loading onto the gel at the end of the experiment. The gel electrophoresis and staining were performed as in section 3.2.2. In the second test, the cutting of the *optimized* His-MBP-TH was compared to the cutting of the original His-MBP-TH at the same ratios, and the effect of adding 0.5 M urea to the reaction was also tested on both for 1 h. The third test was performed on the His-MBP-R202H protein using the same conditions as in the first test, but at protease/protein ratios of 1/10, 1/50 and 1/100 for 1 h at 4°C.

3.2.3.3 Isolation of TH from His-MBP-TH

To obtain pure TH, His-MBP-TH was mixed with 1/50 TEV-protease (w/w ratio) for 1.5 h at 4°C and separated from the fusion partner and aggregates by SEC as performed in section 3.2.3.1. Fractions containing tetrameric TH were concentrated in 15 ml Amicon® Ultra-15 50 MWCO Centrifugal Filter Device for 30 min at 4°C and the concentration was measured at 280 nm using ϵ_{280} (1 mg/ml) = 1. The purity of TH was examined by running SDS-PAGE at the end of the experiment. The TH-R202H mutant was isolated from the fusion partner in the same way, except that a 1/10 ratio of protease/protein was used.

3.2.4 Finding an appropriate buffer for TH by DSF

In this work we tested the stability of TH-wt in the commercial RUBIC Buffer Screen MD1-96 (Molecular Dimensions Ltd), a set of 96 different conditions chosen according to pH, salt

concentrations, buffer type and concentrations designed at the EMBL Hamburg (Appendix), and a more limited home-made buffer screen with different concentrations of NaCl.

3.2.4.1 RUBIC Buffer Screen

The RUBIC Buffer Screen MD1-96, reviewed in (Senisterra et al., 2009), was tested according to the RUBIC Buffer Screen protocol (Appendix) with 0.075 mg/ml TH-wt and 5x SO. Multichannel pipetting of protein and SO into the 96 wells, each containing different buffer conditions, was performed by the TTP labtech mosquito® High Volume (HV) and the plate was sealed using the Axygen™ PlateMax™ Semi-Automated Plate Sealers (Axygen Scientific) and heated from 20-99 °C using the LightCycler® 480 Instrument II plate-based real-time PCR System (Roche Life Science) at 4.5°C/min.

3.2.4.2 NaCl concentrations

To further determine optimal buffer conditions for TH-wt, we prepared a buffer screen with 20 mM Hepes pH 7 and five different concentrations of NaCl; 100 mM, 200 mM, 300 mM, 400 mM and 500 mM NaCl. Triplicate samples were prepared and analyzed with 0.075 mg/ml TH-wt and 5x SO as described but with manual pipetting.

3.3 Finding potential pharmacological chaperones for TH

The search for compounds that increase TH stability is based on a high-throughput screening of different chemical libraries using DSF (Niesen et al., 2007). For TH, screening of the MyriaScreen diversity collection with 10 000 compounds (Sigma Aldrich/TimTec) and validation of obtained hits has already been performed and published (Hole et al., 2016; Hole et al., 2015). In addition, a library of FDA-approved drugs (1280 compounds) (<http://www.prestwickchemical.com/libraries-screening-lib-pcl.html>), here referred to as FDA, has been screened, but the hits are not yet validated. In this work we set out to validate these hits and in addition we screened a library of Innovative Compounds amenable to modification (344 compounds) (<http://www.prestwickchemical.com/libraries-screening-lib-pom.html>). This library, here referred to as NOCE, has been selected for their favorable drug-like and ADME-Tox pharmacological properties; absorption, distribution, metabolism, excretion and toxicity (Di et al., 2009).

3.3.1 Screening of the NOCE library by high throughput screening using DSF

In order to identify potential high-quality hits from the NOCE library, 0.075 mg/ml of protein in 20 mM Hepes pH 7, 200 mM NaCl and 5X SO was pipetted into a 384-well plate using the Thermo Scientific Multidrop® Combi instrument. The prepared protein solution and compounds (dissolved in 100% DMSO) were mixed in each well and DSF was run as previously described with wells containing 5% DMSO instead of compound as reference. Compounds that stabilized TH $\geq 1.8^{\circ}\text{C}$ were considered primary hits and selected for further validation.

3.3.2 Validation of primary hits on TH

The primary hits obtained from the NOCE library and hits previously obtained from the library of FDA-approved drugs (Prestwick Ltd) were further validated by concentration-dependent binding assays.

3.3.2.1 First validation

For the first validation, the compounds were diluted by a factor of 2 for each concentration with 20 mM Hepes pH 7, 200 mM NaCl and 5X SO using the Serial Dilution program on the TTP labtech mosquito® HV, making a concentration range from 250 μM to 0.12 μM . TH-wt (final concentration of 0.075 mg/ml) was then added to each well using Thermo Scientific Multidrop® Combi. The unfolding was monitored by DSF as described. Compounds that showed a tendency towards binding that was concentration-dependent were selected for further validation.

3.3.2.2 Second validation

Hits obtained after the first concentration-dependent assay were selected for a second validation diluted by a factor of 1.33 to make 24 concentrations ranging from 500 μM to 0.7 μM as described. The EC_{50} -values was determined by using equation (1) in SigmaPlot. The primary hits were also tested on the mutant with a 24 concentrations range as for TH-wt and the EC_{50} -values for each compound were also determined.

3.3.2.3 Testing the stabilizing effect of DA on TH

TH-wt and TH-R202H (final concentration of 0.075 mg/ml) were tested with increasing concentration of DA using DSF. The standard mix contained the TH which was incubated with 5 μ M FAS for 2 min at room temperature (RT) before added to solution containing buffer and 5X SO. DA was added to the standard mix and allowed to bind 5-10 minutes at RT before starting DSF.

3.4 Evaluating the effect of hit compounds on TH activity

3.4.1 Testing inhibitory effect on TH

The effect of hit compounds on the enzymatic activity of TH was determined by a well established enzymatic activity assay (Haavik & Flatmark, 1980) at 37°C. TH was diluted with 0.005% bovine serum albumin in 20 mM Hepes pH 7, 200 mM NaCl and added to a final concentration of 0.01 mg/ml in 40 mM Hepes pH 7, 0.1 mg/ml catalase, 10 μ M ferrous ammonium sulphate, 50 μ M L-Tyr and \sim 100 μ M compound. After preincubation at 37°C for 1 min, the reaction was started by adding 200 μ M BH₄ and 5 mM DTT and stopped after 5 min with cold 2% (v/v) acetic acid (Hac) in ethanol. After 90 min at -20°C, the samples were centrifuged at 20000 x g for 14 min at 4°C to remove precipitated protein. The reference activity assay was performed without compound, but with 2% DMSO.

The samples were analyzed by high performance liquid chromatography (HPLC) using a polar bonded-phase Agilent Zorbax 300-SCX column (4.6 x 150 mm) connected to Agilent Technologies 1290 Infinity II LC System at 4°C. A pump forced a liquid mobile phase of 1 mM Hac buffer (pH 3.5) with 0.2% (v/v) propanol through the column at a flowrate of 3 ml/min. Standards of L-DOPA at 39.6 μ M and 20 μ M was dissolved in 1.25 mM L-Tyr and 2% (v/v) Hac in ethanol, respectively. In order to detect L-DOPA the excitation wavelength (λ_{ex}) of 280 nm was used with emission wavelength (λ_{em}) set to 314 nm. L-DOPA was quantified from the HPLC chromatogram. The Student's *t*-test was performed (section 3.8) to determine whether the difference was significant compared to the control without compound (*p-value <0.05).

For compounds that inhibit TH activity, the half maximal inhibitory concentration (IC₅₀) was determined. The determination of IC₅₀ value for the compounds was performed by the described

activity assay in the presence of 0-100 μM compounds. The DMSO concentration was kept constant at 2%. The samples were analyzed using HPLC as described. The fitting and determination of IC_{50} value was obtained using the four-parameter logistic nonlinear regression equation in SigmaPlot.

3.5 Protection of TH towards limited proteolysis by trypsin

Before testing the ability of the hit compounds to confer structural protection against proteolysis of the TH protein, we optimized conditions for length and TH:trypsin ratio (50:1, 100:1, 150:1 and 200:1) using DA.

3.5.1 Limited proteolysis with DA

The following ratios of 50:1, 100:1, 150:1 and 200:1 were tested with 2.5 μM per subunit TH-wt before testing with TH-R202H. The protein (TH-wt) was added to buffer and then incubated at 25°C for 5 min. After 60 s with trypsin the reaction was stopped with TI (1.5 $\mu\text{g}/\text{ml}$) and analyzed by SDS-PAGE at 300V for 15 min. 20 and 10 μl of the samples were loaded to obtain the correct visualization. Different dopamine (DA) concentrations of 5 μM , 50 μM and 200 μM with 2.5 μM per subunit TH-wt were also tested at 100:1 ratio (TH:trypsin). The proteolysis was performed at 25°C with pre-incubation of buffer (20 mM Hepes pH 7, 200 mM NaCl) and TH for 5 min, Fe^{2+} for 2 min and DA for 3 min. The reaction was started, stopped and analyzed as described. The determined conditions provided from the optimization were applied to the final experiment testing the protection of DA and compounds towards proteolysis by trypsin.

We then performed limited proteolysis by trypsin at a TH:trypsin ratio of 200:1 with 2.5 μM per subunit of TH (wt and R202H). The proteolysis was performed at 25°C where the protein was incubated with buffer and 5 μM Fe^{2+} for 2 min before adding 5 μM DA for another 3 min. The reaction was started by adding trypsin and after 60 s, 1.5 $\mu\text{g}/\text{ml}$ trypsin soybean inhibitor (TI) was added to stop the proteolysis. SDS-PAGE was used to analyze the protection DA confers against proteolysis of the N-terminal of TH, at 180V for 45 min. The SDS-PAGE and staining of gels were performed as described and subsequently scanned by ChemiDoc XRS + from Bio-Rad, and the intensities of the 60 kDa (full-length TH), 57 kDa, 54 kDa bands (section

1.3.4) were measured using Image Lab 6.0.1 software. This experiment was performed once and thus SD and statistics does not apply.

3.5.2 Limited proteolysis with hit compounds

Next, we tested the susceptibility of the protein (2.5 μ M subunit) to proteolysis by trypsin at 200:1 ratio (TH:trypsin) with compounds. After some further optimizations, the temperature in this assay was 37°C. The protein was incubated with buffer and 5 μ M FAS for 2 min and with DA for 3 min afterwards. The reaction lasted for 60 s after adding trypsin and was stopped with TI (1.5 μ g/ml). The bands in lanes with compounds were compared to corresponding band in lane without compound by quantification as described in the previous section. The Student's *t*-test was performed (section 3.8) to determine whether the difference was significant compared to the control without compound (**p*-value <0.05).

3.6 Determination of binding affinities

Determination of the binding affinity between TH and the compounds was performed using Isothermal titration calorimetry (ITC) using the MicroCal ITC-200 instrument (Malvern Panalytical). An initial test of 30 μ M TH in the cell and 300 μ M compound in the syringe was carried out at 25°C for each of the hit compounds. Powdered compounds were dissolved in 100% DMSO and diluted in 20 mm Hepes pH 7, 200 mM NaCl until 5% DMSO (300 μ M compound). TH was diluted in the same buffer supplemented with 5% DMSO. The titration was carried out with 1 0.5 μ l injection followed by 12 3 μ l injections with a stirring speed of 1000 rpm. Concentrations were adjusted in the next experiments with 90 μ M TH instead. The data was analyzed by Peter Gimeson (Malvern Panalytical) using PEAQ-ITC software. The single set of sites binding model (Wiseman et al., 1989) was applied to obtain affinity constants.

3.7 Molecular docking of hit compounds to TH

Molecular docking was performed using Schrödinger Release 2018-1: Maestro, Schrödinger, LLC, New York, NY, 2018. The hit compounds were docked to the active site of a crystal structure of human TH, retrieved from the protein data bank (PDB ID: 2XSN), which contains the catalytic domain and tetramerization domain. In addition, the hit compounds were docked to the allosteric binding site of the tetrameric TH (PDB ID: 1TOH) by Professor Knut Teigen (not described in this section).

Firstly, the compounds were prepared by LigPrep for producing low-energy 3D structures from 2D structures and generating stereochemistry, tautomers and different protonation states. Possible protonation states of the ligands were generated in water at pH 7 ± 2 (Schrödinger Release 2018-1: LigPrep, Schrödinger, LLC, New York, NY, 2018).

Secondly, the protein was optimized using the Protein Preparation Wizard which are filling in missing partial charges, hydrogens, side chains or whole loop regions, depending on the needs of the protein structure (**Schrödinger Release 2018-1**: Schrödinger Suite 2018-1 Protein Preparation Wizard; Epik, Schrödinger, LLC, New York, NY, 2016; Impact, Schrödinger, LLC, New York, NY, 2016; Prime, Schrödinger, LLC, New York, NY, 2018). Water molecules were removed from the protein to more extensively explore the binding pocket for possible orientations of the docked ligands. Hydrogen atoms were added to optimize the hydrogen bonding networks and distances were also minimized. Protonation state of the protein was generated at pH 7, taking into account the local environment of each titratable group as well as optimization of hydrogen bonding networks.

The active site iron of TH was defined as center of the pocket to dock molecules into. A receptor grid was generated in which the bounding boxes defined the region that the docked molecule(s) and the centroid of the docked molecule(s) must occupy to satisfy or pass the initial stages of docking.

Finally, the prepared ligands were docked to the protein using the standard precision (SP) protocol ensuring that the ligand sampling were set to be flexible to adapt to the defined active site of the protein, with all other options set to default (Schrödinger Release 2018-1: Glide, Schrödinger, LLC, New York, NY, 2018). The docking results were analyzed using the Ligand Interaction diagram, and the Glide score (gscore) were also used as guidance. BH₄ and the substrate analogue thienylalanine (THA) from PAH (PDB ID: 1MMK) were used for comparison purposes.

3.8 Statistical analysis

As otherwise indicated, experiments were performed in various number of parallels and data are represented as the mean and standard deviation (mean \pm SD) to quantify the amount of variations between the parallels. A *p*-value was calculated for each compound compared to the control in the activity assay (section 3.4.1) and limited proteolysis by trypsin (section 3.5.2). For figures with gels, representative results are shown by measuring the intensity of bands as described. The *p*-values were calculated using a two-tailed *t*-test analysis in Excel, and $p < 0.05$ indicated significant differences which is marked with asterisk (*).

4 Results

4.1 Preparation of pure and stable TH enzymes

The gene encoding His-MBP-TH was previously cloned into the pET-MBP-1a vector (Bezem et al., 2016) and was used as template to make the R202H mutation (Korner et al., 2015). The original His-MBP-TH and p.R202H mutant were overexpressed in this work, and a modified version of the vector encoding the wild-type fusion protein His-MBP-TH was also attempted to be expressed and purified.

4.1.1 Expression and Purification of His-MBP-TH

The His-MBP-TH proteins were successfully expressed, and fusion proteins of expected size were obtained. The purification of the *optimized* His-MBP-TH by affinity chromatography is shown in Figure 4.1A as absorbance at 280 nm versus elution volume. The first very large and broad peak in the chromatogram represents the unbound proteins that flows through upon washing with Binding buffer. After addition of maltose, the peak representing the fusion protein that has bound to the resin appears. An identical chromatogram was obtained for the original His-MBP-TH. The mutant His-MBP-TH-R202H was purified by gravity flow without the use of a recorder, but the principle is the same. As shown by SDS-PAGE, the elution peak contained pure His-MBP-TH for all three fusion proteins (Figure 4.1B). The yield was similar for both wt and mutant fusion proteins.

4.1.2 Removal of tag and isolation of TH

4.1.2.1 Assessing the quality of purified His-MBP-TH proteins by SEC

After observing the purity of the denatured subunits in SDS-PAGE, the quality of the His-MBP-TH proteins was evaluated using SEC to ensure that the oligomeric distribution is dominated by the functional unit which is a tetramer. As shown in Figure 4.1C-E the main proportion of all three fusion proteins elute in the volume corresponding to that of the tetrameric His-MBP-TH (Bezem et al., 2016). There are negligible amounts of aggregation in all samples, but the *optimized* His-MBP-TH (Figure 4.1D) contains a slight proportion of a band that is believed to be aggregated and/or octameric proteins (Szigetvari et al., 2019).

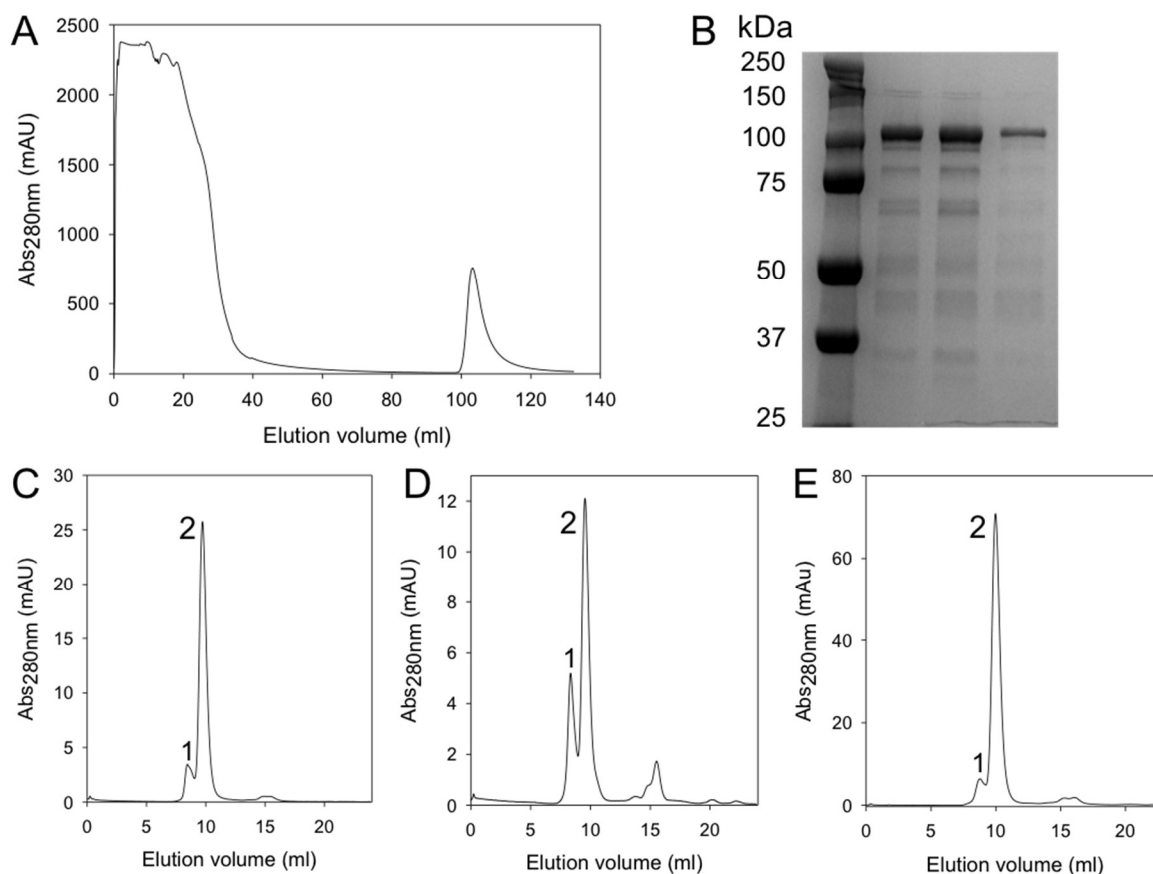


Figure 4.1: The expression and purification of fusion proteins. (A) Example of chromatographic profile from affinity purification of the optimized fusion protein (FP) performed at a flow rate of 2 ml/min showing elution of FP after addition of 10 mM maltose at ~90 ml. (B) SDS-PAGE of three fusion proteins (FP) in pure form with a precision marker (lane 1), optimized FP (lane 2), original FP (lane 3) and His-MBP-TH-R202H (lane 4). Bands at 98 kDa correspond to fusion proteins. SEC profiles of purified fusion proteins on a Superdex™ 200 Increase 10/300 column performed at a flow rate of 0.5 ml/min are shown for the original His-MBP-TH (C), the optimized His-MBP-TH (D) and the His-MBP-TH-R202H mutant (E). Peak 1 represents aggregated and/or octameric proteins and peak 2 is the tetrameric fusion protein.

4.1.2.2 Cutting tests with TEV-protease

To examine the efficiency of TEV-protease to separate TH from the fusion partner, cutting tests were performed on the purified fusion proteins and the result was analyzed by SDS-PAGE. As shown in Figure 4.2A, increasing the incubation time to 3 hours or decreasing the TEV:MBP-TH ratio to 1:10 did not have any effect on the cutting efficiency for the *optimized* His-MBP-TH. As a control we compared the cutting of the *optimized* His-MBP-TH to the original fusion protein (Figure 4.2B) and TEV-protease cuts the original protein as expected (complete cutting at 1:10 TEV:MBP-TH ratio at 3 hours). In an attempt to facilitate access to the cleavage site, we added 0.5 M urea (Hung et al., 2014). However, this had no effect on cutting of the *optimized* His-MBP-TH (Figure 4.2B). The original His-MBP-TH was cut equally well with and without

urea (Figure 4.2B). The TEV cutting test, performed at three different ratios, showed that 1/10 (TEV:TH) was the most efficient ratio for 1 hour cutting of His-MBP-R202H (Figure 4.2C).

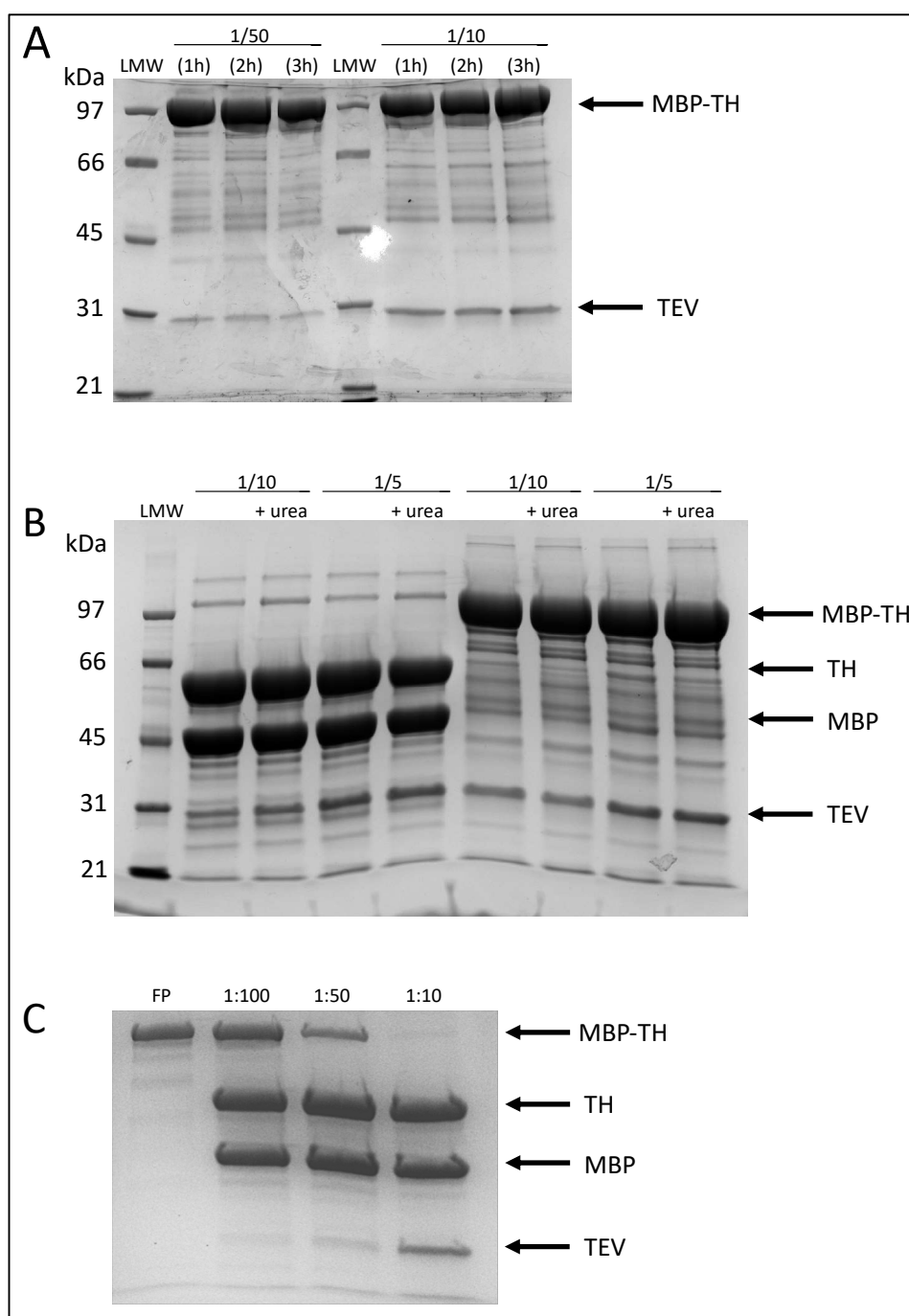


Figure 4.2: SDS-PAGE of cutting tests. (A) Optimized His-MBP-TH tested at 1:50 and 1:10 ratio (TEV:TH) after 1, 2 and 3 hours, respectively. (B) Original (left) and optimized His-MBP-TH (right) with addition of urea at ratios of 1:10 and 1:5 (TEV:TH). (C) Isolated fusion protein (FP) of His-MBP-R202H-mutant cut in ratios of 1:100, 1:50 and 1:10. The gel lacks the LMW marker but corresponds in size as in (A) and (B). Bands at 98, 60, 43 and 27 kDa corresponds to fusion protein, TH, MBP and TEV, respectively.

4.1.2.3 Isolation of TH

As the *optimized* His-MBP-TH is not cut with TEV protease under standard or additionally tested conditions, this novel construct was abandoned, and all the following work was performed using the original His-MBP-TH and the His-MBP-TH-R202H mutant. Both fusion proteins were successfully cut with TEV-protease and analyzed by SEC. The elution profiles for separation of fusion partner and aggregates from the TH proteins are shown in Figure 4.3A and C for TH-wt and TH-R202H, respectively. Fractions containing tetrameric TH were pooled and concentrated. The yield of TH-wt was 34% of the fusion protein and the yield of TH-R202H was 24%. Both TH proteins were obtained in a pure form (4th lanes in Figure 4.3B and D).

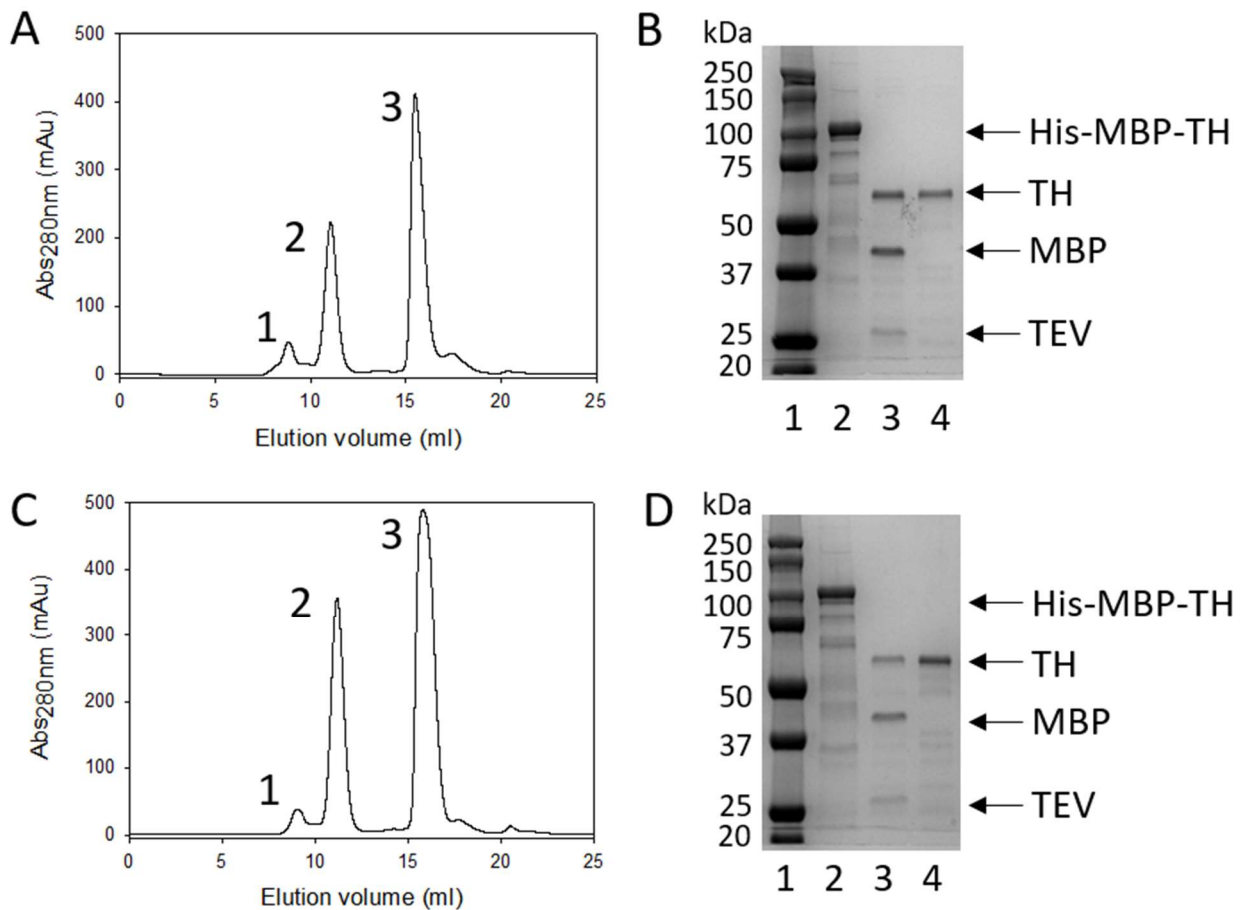


Figure 4.3: Removal of fusion partner. (A) Separation of TH-wt (peak #2) and fusion partner His-MBP (peak #3) on a Superdex™ 200 Increase 10/300 column. (B) SDS-PAGE profile of TH-wt representing fusion protein (lane 2), TEV cutting with TEV:MBP-TH ratio at 1:10 (lane 3) and 1 µg isolated TH-wt (lane 4) (C) Separation of TH-R202H (peak 2) and His-MBP (peak 3) on a Superdex™ 200 Increase 10/300 column. Peak 1 elutes at the position corresponding to aggregated proteins. (D) SDS-PAGE profile of TH-R202H. Lanes 1-4 correspond to the SDS-PAGE gel for TH-wt in (B).

4.1.3 Finding an appropriate buffer for TH by DSF

4.1.3.1 RUBIC Buffer Screen

To test for optimal buffer conditions for TH, we tested the commercial RUBIC Buffer Screen MD1-96 with 96 different buffer conditions using DSF. Following the protocol for this screen, the T_m of the assayed protein in pure water is defined as $T_{m,ref}$, and for TH this was 50.9°C (shown in blue in Figure 4.4A). Buffers that provided 2-5°C thermal stability of TH, compared to $T_{m,ref}$, were in the range of 0.03 – 0.15 M Tris-HCl at pH 7.5-8.0 with addition of 0.15 M NaCl (see Appendix). As shown in Figure 4.4B, the highest stabilization was obtained in 0.12 M Tris-HCl and 0.15 M Tris-HCl, indicating that Tris-HCl is the preferred buffer type for enhanced TH thermal stability within pH 7-8. However, as the pH of Tris-buffers are affected by temperature they are not optimal for these experiments. We thus decided to continue using the purification buffer from SEC (20 mM Hepes pH 7, 200 mM NaCl) and rather optimize this buffer for future compound screening.

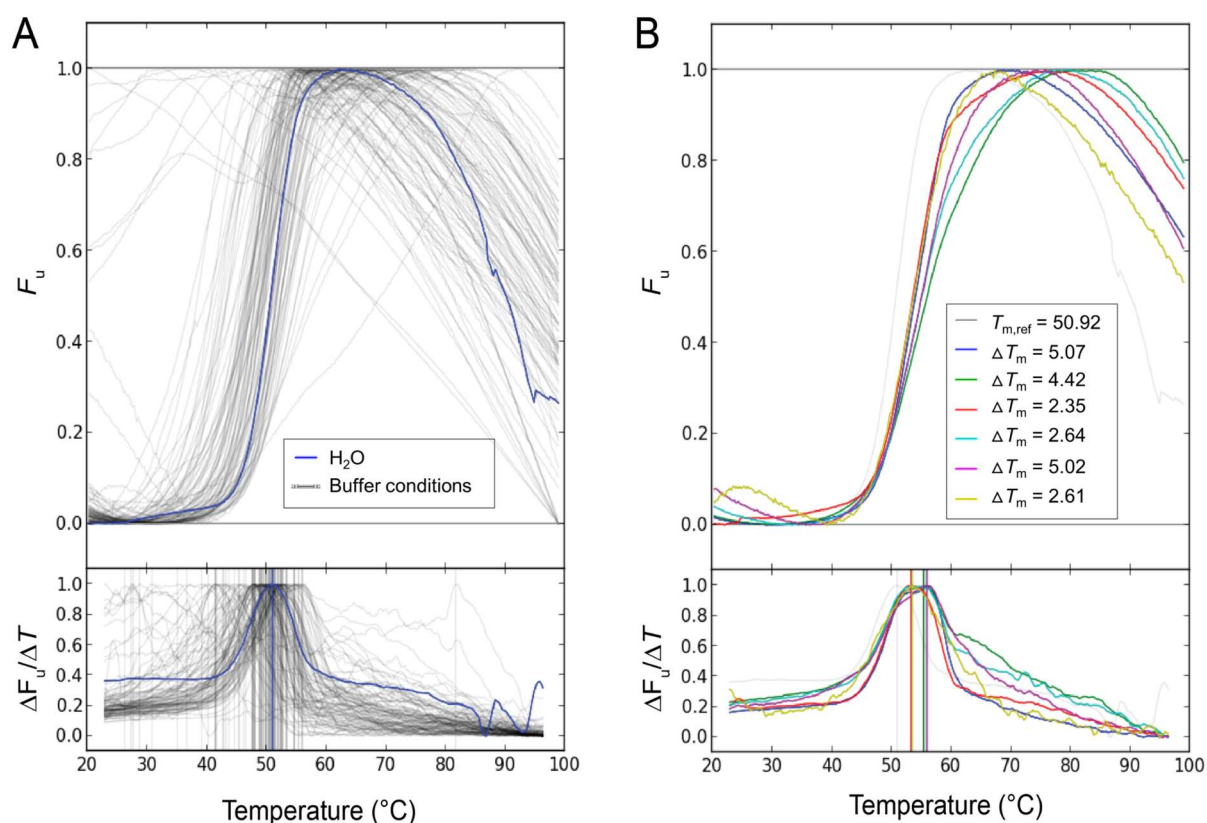


Figure 4.4: Effect of buffer conditions on TH thermal stability showing fraction of unfolded protein (F_u) on increasing temperature for TH in pure water (blue) and the other 95 buffer conditions (grey) (A). Stabilizing buffer conditions (B) are obtained at 0.03 M (red), 0.06 M (cyan), 0.12 M (blue), 0.15 M (pink) Tris-HCl and at 0.15 M NaCl with 0.06 M Tris-HCl (yellow) compared to $T_{m,ref}$. Lower panels show the first derivative and vertical lines denote the T_m . The fluorescence signal is scaled to 0-1.

4.1.3.2 NaCl concentrations

The stability of TH was further tested in 20 mM Hepes pH 7 at different NaCl concentrations as described in section 3.2.4.2. Although the highest stabilization was obtained with 20 mM Hepes pH 7 and 400 mM NaCl, which represents a high ionic strength, we decided to continue using 200 mM NaCl for screening purposes. The 400 mM NaCl buffer can be used in future experiments where a higher stability of TH is needed, e.g. for crystallization.

4.2 Finding potential pharmacological chaperones for TH

In this work, we have used TH-wt to screen for compounds and validate them further. However, we have also purified the TH-R202H mutant that might be a target for the future chaperone therapy. Some experiments have therefore been performed also on this TH enzyme and the preliminary results from these are shown in section 4.7.

4.2.1 Screening of the NOCE library

The graphs in Figure 4.5A represent the screening of TH in presence of each of the 344 compounds in the NOCE library. The melting curves of TH in presence of compounds at a final concentration of ~100 μ M and 5% DMSO are shown in grey and the control (TH without compound, but with 5% DMSO) is shown in blue. The T_m obtained for the DMSO control, i.e. $T_{m,ref}$, was $50 \pm 0.4^\circ\text{C}$. Seven hits from the NOCE library were selected for further examination as they provided stabilization of TH of $\geq 1.8^\circ\text{C}$ (Figure 4.5B). The 19 hits from the FDA library, identified previously by Dr Magnus Hole, were also included for further concentration-dependent binding analysis. Thus, the HTS of the FDA and NOCE libraries has led to identification of 26 primary hits that appear to bind TH in a stabilizing manner.

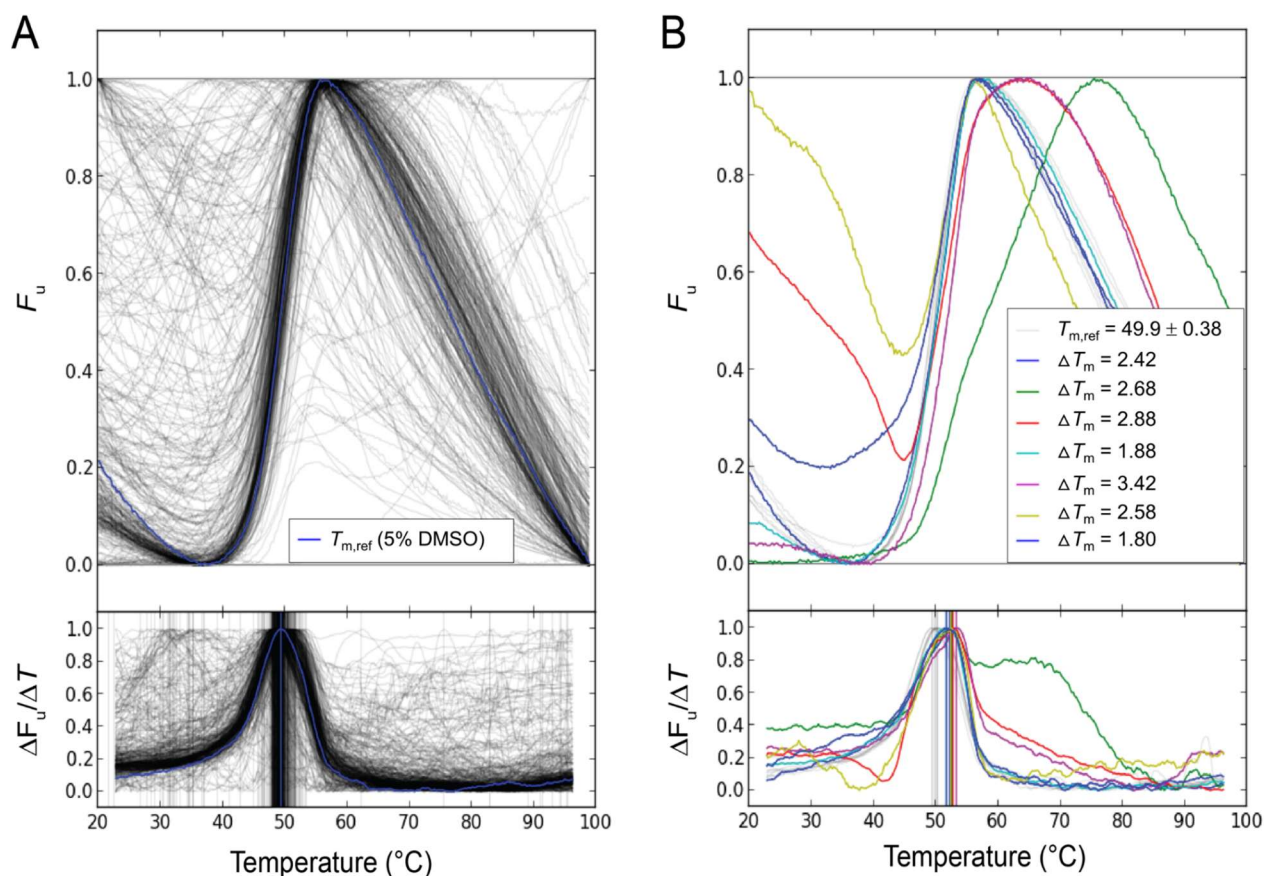


Figure 4.5: Screening of NOCE library. (A) The melting curves of TH represented as fraction of unfolded protein (F_u) upon increasing temperature. TH without compound is shown in blue and in the presence of each of the 344 compounds in grey. (B) Compounds stabilizing TH $\geq 1.8^\circ\text{C}$ were selected as primary hits. The lower panels show the first derivative and vertical lines denote the T_m . The fluorescence signal is scaled to 0-1.

4.2.2 Validation of primary hits

4.2.2.1 First validation

To exclude false positives among the 26 primary hits, a concentration-dependent binding assay was performed in two stages. In the first validation, we obtained 8 hit compounds that provided stabilization of TH. The hit compounds selected showed that the effect decreased with lower compound concentration as shown in Figure 4.6, and this indicates that the compounds are indeed binding and stabilizing the enzyme. These compounds are named 1-8 and the remaining 18 compounds that did not show this trend were excluded from further analysis (not shown).

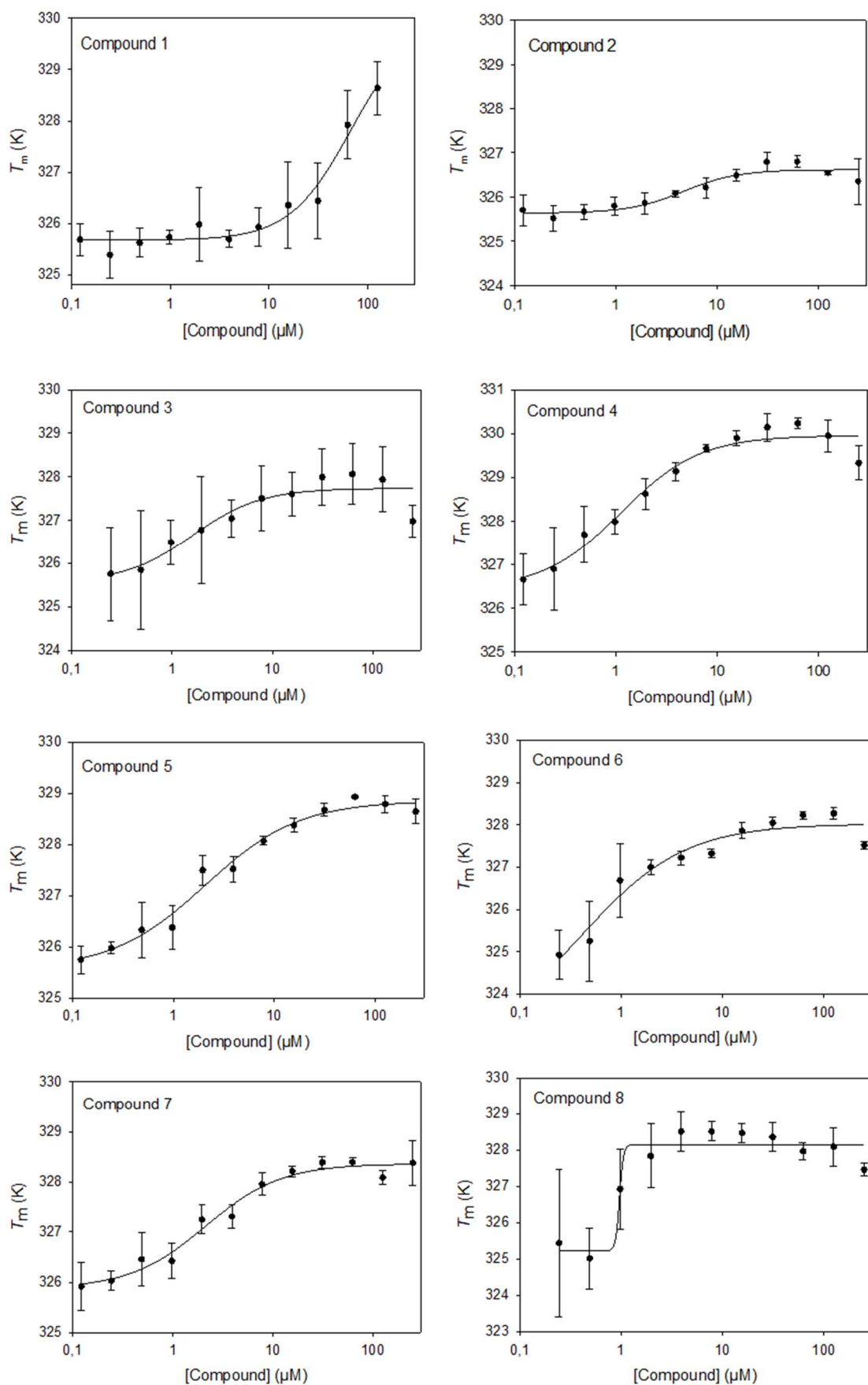


Figure 4.6: The concentration-dependent effect of compounds 1-8 on the T_m of TH. The four-parameter logistic nonlinear regression equation in SigmaPlot was used for curve fittings.

4.2.2.2 Second validation

The second validation was performed as the first, but with more concentrations. The compounds that give a sigmoidal shape when plotting the T_m of TH versus compound concentration are shown in Figure 4.7. Compound 1, 3, 6 and 8 did not show a good binding curve with the increasing number of concentrations and were therefore excluded. However, compound 8 is identified as DA which is known as a natural feedback inhibitor of TH. DA has a stabilizing effect on TH only at low concentrations and it does not display a concentration-dependent curve in the concentration range that we are using (not shown).

The four-parameter logistic nonlinear regression equation was used for curve fitting in SigmaPlot to obtain EC_{50} . From the fittings shown in Figure 4.7 the EC_{50} -values obtained showed the following order with respect to apparent binding affinity: compound 4 > compound 2 > compound 5 > compound 7. Values are shown in Table 4-1.

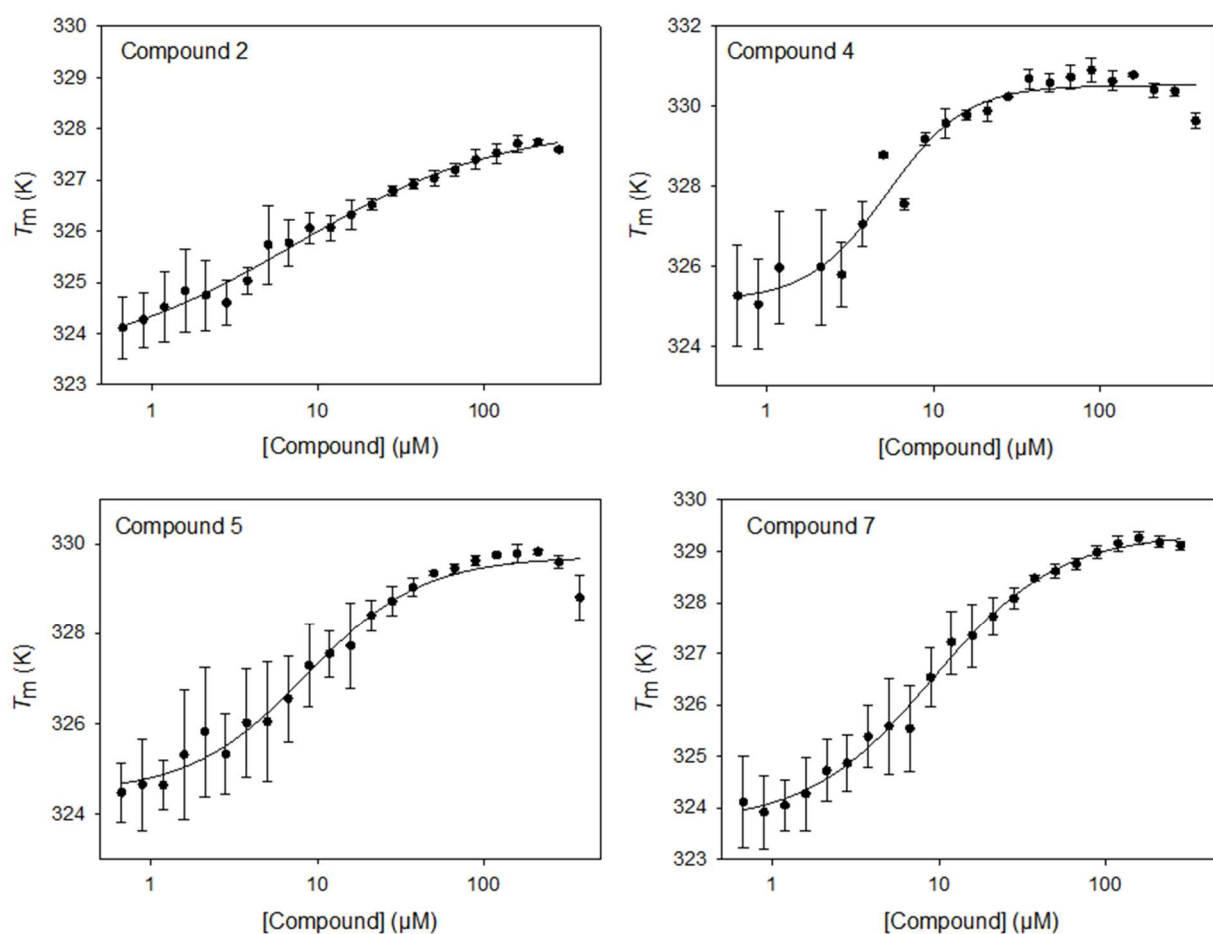
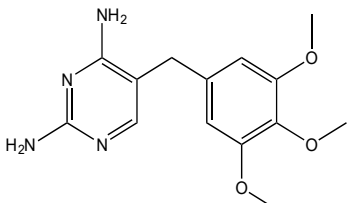
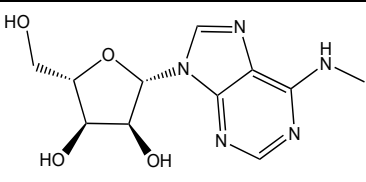
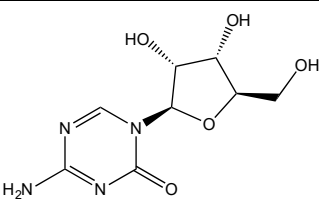
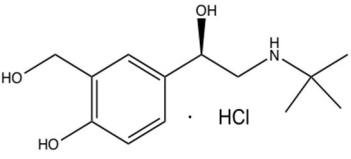
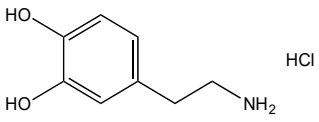


Figure 4.7: The concentration-dependent stabilization of compounds 2, 4, 5 and 7 on TH. To determine EC_{50} values, the points were fitted using four-parameter logistic nonlinear regression equation in SigmaPlot.

Thus, the hit compounds with pharmacological chaperone potential for TH are considered as follows: Trimethoprim (compound 2), N6-methyladenosine (compound 4), Azacytidine-5 (compound 5) and Levalbuterol-HCl (compound 7). We also decided to include DA in further studies (Table 4-1).

Table 4-1: The compound name, 2D-structure and kinetic parameters are shown for the selected hit compounds.

*From initial screening (~100 μM).

Compound no.	Name	Structure	dT_m^*	EC_{50} (μM)	K_d (μM)
2	Trimethoprim		2.7	7.3 ± 2.6	$0.51 \pm 1.76 \times 10^{-7}$
4	N6-methyladenosine		1.9	5.3 ± 0.6	-
5	Azacytidine-5		1.3	8.6 ± 1.5	-
7	Levalbuterol-HCl		1.7	9.2 ± 1.1	$3.38 \pm 2.52 \times 10^{-7}$
8	Dopamine HCl		2.1	1.0 ± 0.1	-

4.3 Evaluating the effect of hit compounds on TH activity

4.3.1 Testing inhibitory effect on TH

To exclude hit compounds with inhibitory effect on TH activity, an enzymatic activity assay in presence of each hit compound at 100 μM was performed. The results showed that Levalbuterol-HCl and Azacytidine-5 had no effect on TH-activity while Trimethoprim increased the activity by $\sim 20\%$ (Figure 4.8A). N6-methyladenosine causes a $\sim 12\%$ decrease in TH activity, but the DA, identified as a hit in the HTS and a known feedback inhibitor of TH, almost abolishes TH activity ($\sim 97\%$ reduction at 100 μM) (Figure 4.8A). The inhibitory potential of both inhibitors was analyzed by performing the activity assay at a range of compound concentrations, which also provides the IC_{50} , and by this method the inhibitory effect of N6-methyladenosine was actually determined to be very low. For DA, the IC_{50} was determined to be 1 μM (Figure 4.8B).

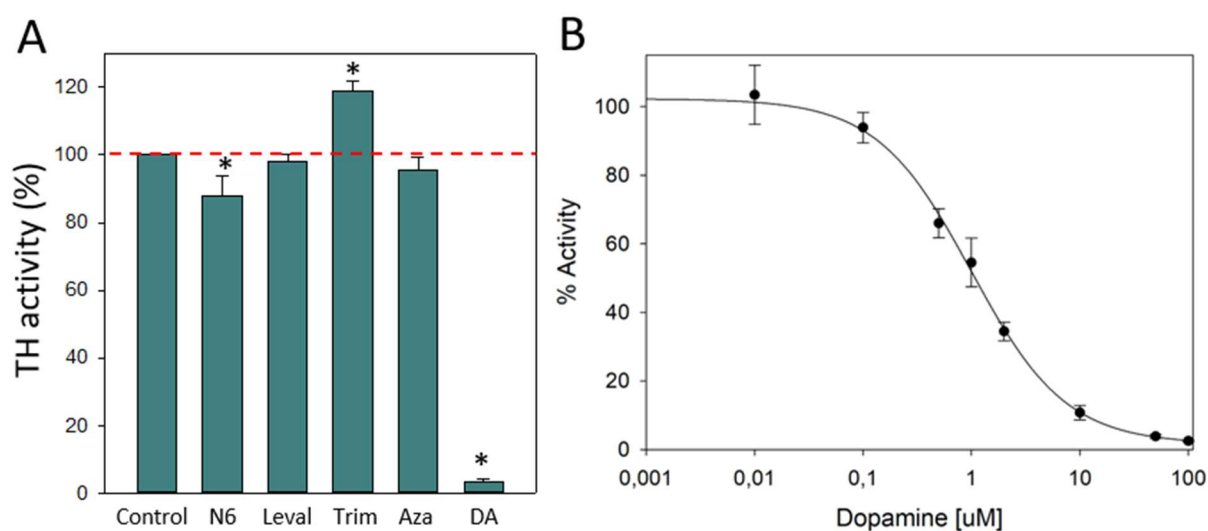


Figure 4.8: (A) The effect of the hit compounds on the activity of TH. The red line marks the activity in absence of compound. The full compound names are N6-methyladenosine (N6), Levalbuterol-HCl (Leval), Trimethoprim (Trim), Azacytidine-5 (Aza), and dopamine (DA). (B) IC_{50} curve for DA showing strong inhibition of TH at high concentrations. Determination of IC_{50} value of DA was done using the four-parameter logistic nonlinear regression equation in SigmaPlot. * $p < 0.05$ compared with the control without compound, as calculated by t-test analysis is considered as significant difference.

4.4 Protection of TH towards limited proteolysis by trypsin

We performed the proteolysis according to Hole *et al.* and also obtained fragments migrating in the SDS-PAGE gel according to molecular weights of 60 kDa (full-length), 57 kDa and 52-54 kDa (Hole *et al.*, 2015). The rate of this cleavage of TH is decreased through binding and stabilization by DA (see section 4.7 about the R202H mutant) and the ability of the hit compounds to also confer protection is a good test to include in the process of finding a pharmacological chaperone.

4.4.1 Limited proteolysis with hit compounds

After optimizing the experiment according to different TH:trypsin ratio and reaction time (not shown), conditions of 200:1 (TH:trypsin) and 60 s were applied to the final test and the results are shown in Figure 4.9. The results from the effect of proteolysis of TH by the four compounds are presented as means of three parallels and given as percentages of the control (no trypsin), which was set to 100% (Figure 4.9A).

Contrary to the protection towards TH proteolysis shown by DA (Hole *et al.*, 2015), TH is proteolyzed to the same extent both without and with the four hit compounds. In fact, for all the compounds except Levalbuterol-HCl, the proteolysis of the N-terminal was rather slightly accelerated (Figure 4.9).

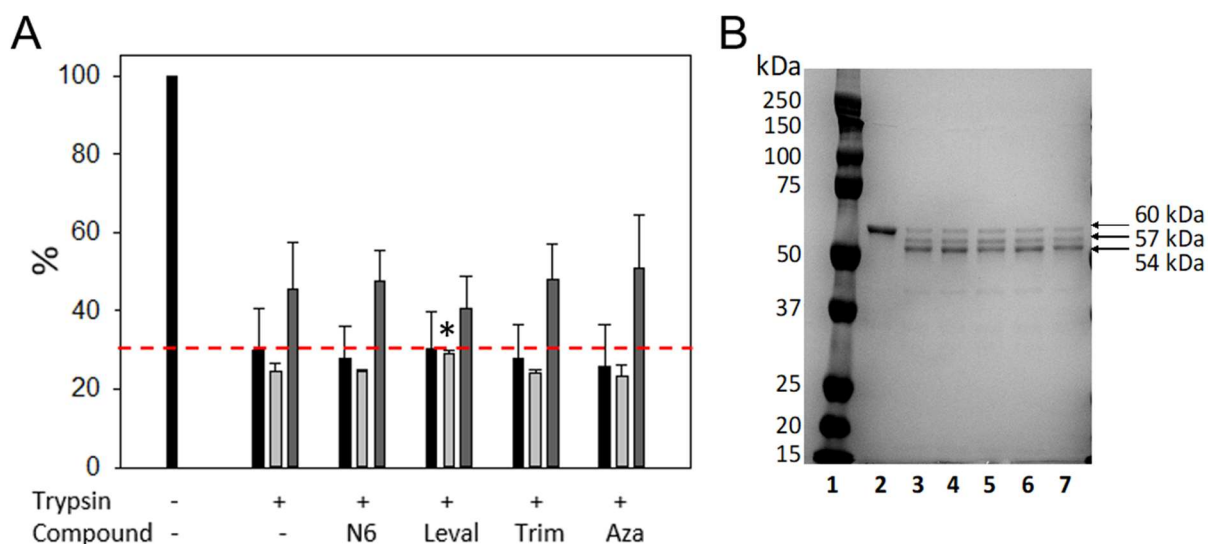


Figure 4.9: The effect of compounds on limited proteolysis of TH. (A) Values from triplicate measurements show percent remaining full-length TH (60 kDa band) (black) and emergence of the characteristic bands at 57 (light grey) and 54 kDa (dark grey). (B) The SDS-gel shown is from one of three measurements. Lane 1: Precision marker; lane 2: uncut full-length protein; lane 3: N6-methyladenosine(N6); lane 4: Levalbuterol-HCl (Leval); lane 5: Trimethoprim (Trim); lane 6: Azacytidine-5 (Aza). * $p < 0.05$ compared with the control with trypsin without compound, as calculated by t-test analysis.

4.5 Determination of binding affinities

4.5.1 Determination of K_d by ITC

The first set of ITC experiments were performed to determine the K_d -value for the binding of the compounds to TH, which is a more adequate measure of affinity than the EC_{50} obtained from concentration dependent DSF (see above). At 30 μ M protein and 300 μ M compound, the raw data plots indicated binding for only two of the four hits; Trimethoprim and Levalbuterol-HCl (Figure 4.10). The thermogram for Levalbuterol-HCl (Figure 4.10D) shows that the first peak represents a very high heat pulse while it already at the second injection is much smaller. This indicates that the protein has reached the point of saturation too rapidly for analysis. While the raw thermogram for Trimethoprim could be analyzed at this concentration (Figure 4.11A), the titration was carried out a second time with increased protein concentration (90 μ M) for Levalbuterol-HCl to provide more available proteins for ligands to bind (Figure 4.11B).

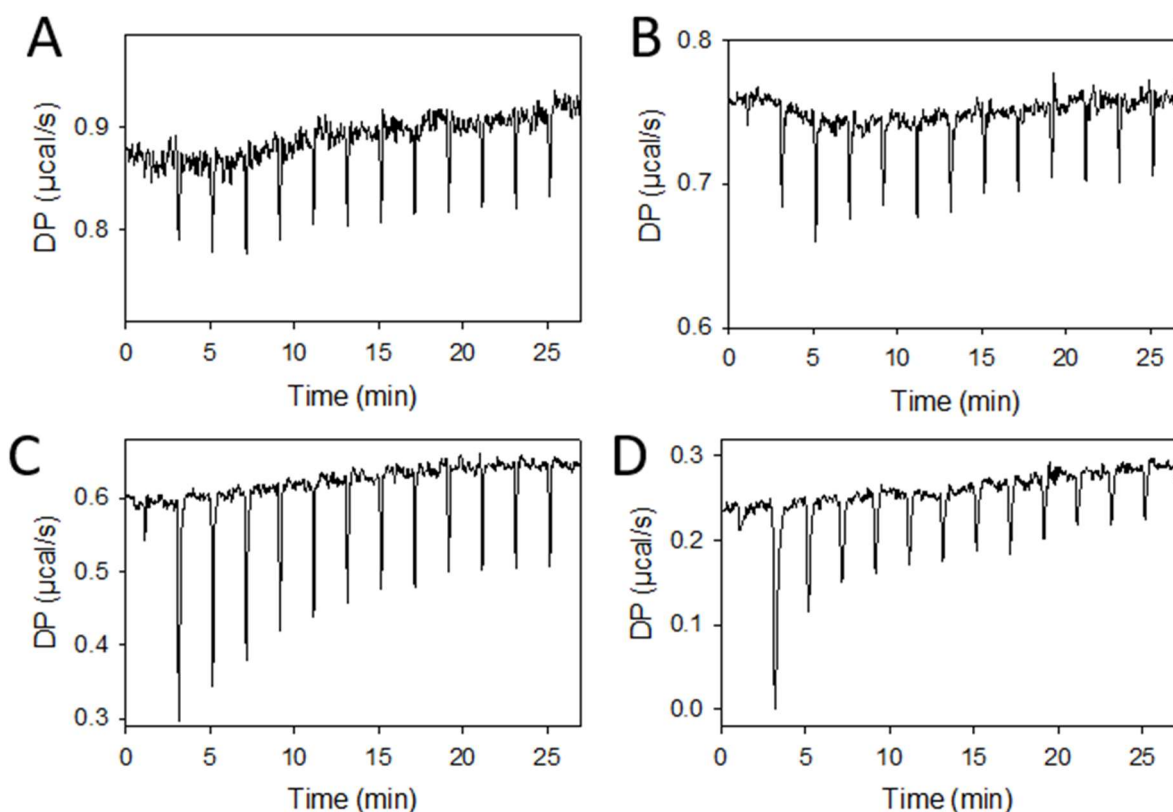


Figure 4.10: Raw data from ITC binding experiment. Titration of 30 μM TH with 300 μM (A) N6-methyladenosine, (B) Azacytidine-5, (C) Trimethoprim or (D) Levalbuterol-HCl at 25 $^{\circ}\text{C}$.

The data were kindly analyzed by Peter Gimeson (Malvern Panalyticals) using the Malvern PEAQ software. The area under the heat pulses shown as peaks in the thermograms for both Trimethoprim and Levalbuterol-HCl were integrated and a single set of sites model was applied as shown in Figure 4.11. This gives K_d -values of $0.51 \pm 1.76 \times 10^{-7} \mu\text{M}$ and $3.38 \pm 2.52 \times 10^{-7} \mu\text{M}$ for Trimethoprim and Levalbuterol-HCl, respectively. These values are much lower than the EC_{50} values obtained with concentration-dependent DSF (Table 4-1), but both parameters show that Trimethoprim displays highest affinity for TH. Applying the model also gives a value for the reaction stoichiometry (n) and therefore the number of binding sites per TH subunit. The values obtained were $0.24 \pm 3.7 \times 10^{-4}$ for Trimethoprim and $0.45 \pm 1.5 \times 10^{-2}$ for Levalbuterol-HCl. These values are very low, but this could be due to overestimation of the concentration of actively binding TH. If e.g. iron is needed for the binding, only the TH subunits with iron in the correct state can bind. Furthermore, another explanation for $n \leq 0.5$ per TH subunit would be a binding of the compounds to intersubunit regions, with 1 compound per dimer and thus 0.5 per subunit (see next section).

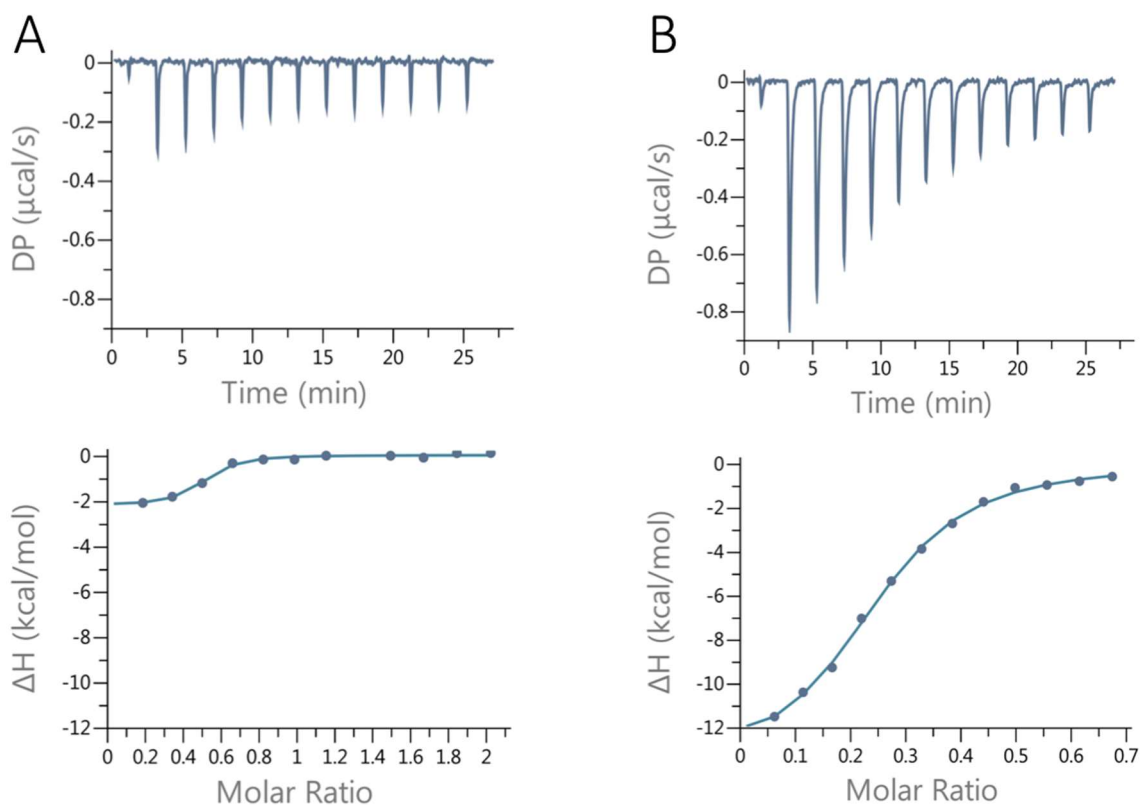


Figure 4.11: The binding of Trimethoprim and Levalbuterol-HCl to TH studied by ITC. (A) 30 μM TH was titrated with 300 μM Trimethoprim and (B) 90 μM TH was titrated with 300 μM of Levalbuterol-HCl. The upper panels show the thermograms for binding of the compounds to TH. The lower panels show the binding curve where each point represents the integrated heat pulses of each corresponding peak in the thermogram fitted to a single-set-of-sites

4.6 Molecular docking

Lastly, molecular docking was performed for all four hit compounds. Figure 4.12 shows the binding of the compounds into the active site of the catalytic domain of TH. We see that two of five compounds (2 and 7) appear to bind in the substrate-analogue (thienylalanine) binding pocket (Figure 4.12B, E), suggesting a possible binding mechanism of competition between the compound and substrate. Thienylalanine (THA) is used for visualization as it is thought to bind and occupy TH in a similar manner as PAH (Teigen et al., 2007). Docking of compounds to TH predicts the binding affinity by utilizing the scoring function, gscore, as shown in Table 4-2. As expected, DA obtained the highest negative gscore, indicating a strong binding. N6-methyladenosine seems to mainly occupy the cofactor binding site which might explain the observed effect it has on TH-activity. Overall, the gscore predicts that the strongest and weakest binding to TH in the active site are Azacytidine and N6-methyladenosine, respectively (DA excluded).

The program Fpocket (<http://fpocket.sourceforge.net/>) identified an intradimeric - possibly allosteric - site in TH (Figure 4.13). Docking to this binding site, at the interphase between the monomers in both TH dimers (2 binding sites per tetramer), was also performed as seen in Figure 4.13 (Le Guilloux et al., 2009). Contrary to the gscore obtained for the hit compounds when docking to the active site, except for Trimethoprim, the obtained gscores when docking to the allosteric binding site of TH are more negative, i.e. indicating higher affinity. The gscore and the corresponding approx. K_d -values for the hit compounds are summarized in Table 4-2.

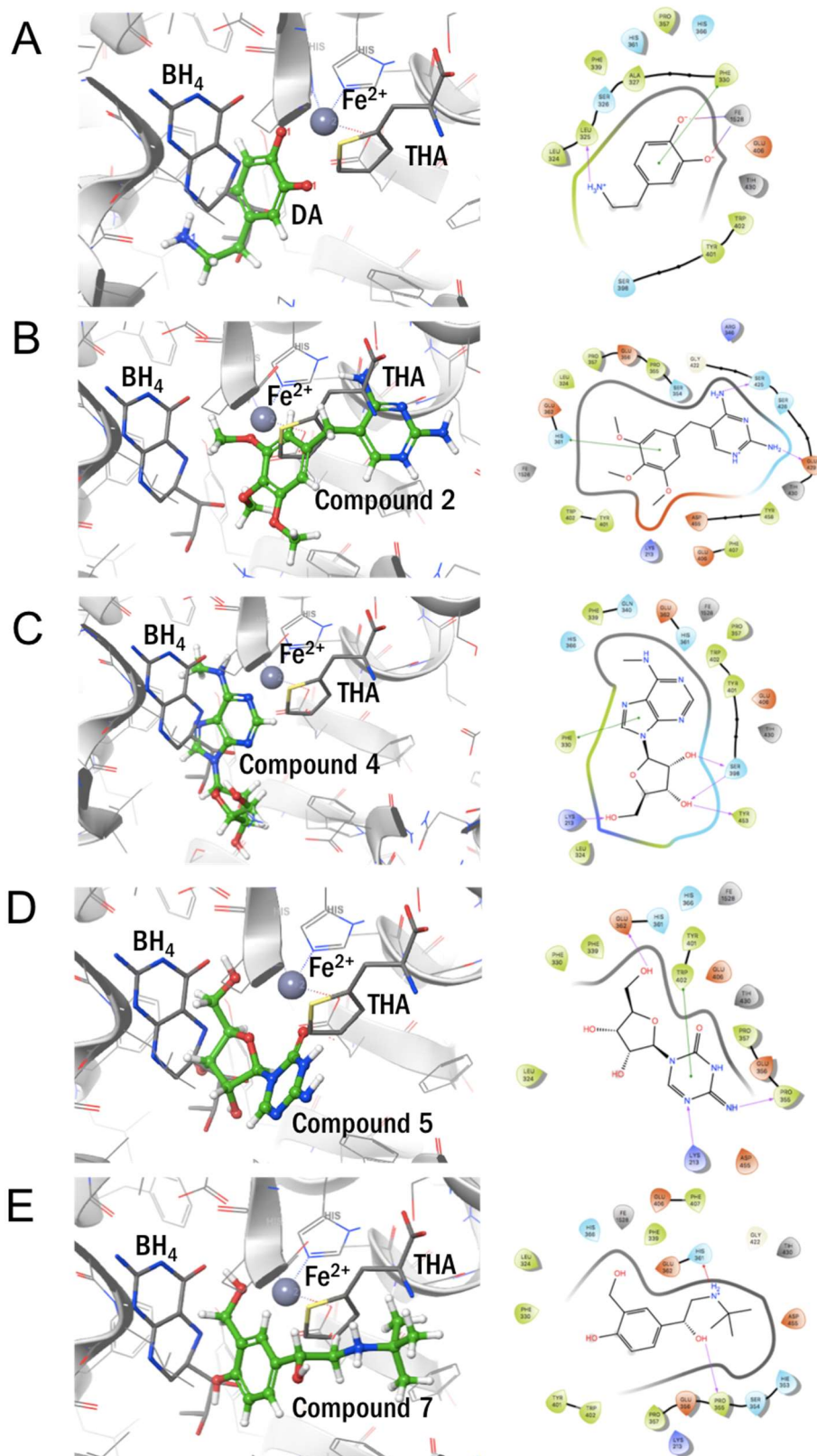


Figure 4.12: Molecular docking models. Binding of compounds in the active site of TH, here shown with the iron as a grey sphere (left). Compounds (green sticks) shown together with BH₄ and thienylalanine (THA). Both cofactor and THA are displayed in grey. The complexes composed of TH (PDB ID: 2XSN) and compounds are shown in 2D representations showing interactions between the ligand and residues within the active site (right). Purple denotes H-bonding, red denotes Pi-cation interactions, green denotes Pi-Pi stacking and blue/pink indicates salt bridges. (A) Dopamine, (B) Trimethoprim, (C) N₆-methyladenosine, (D) Azacytidine-5, (E) Levalbuterol-HCl.

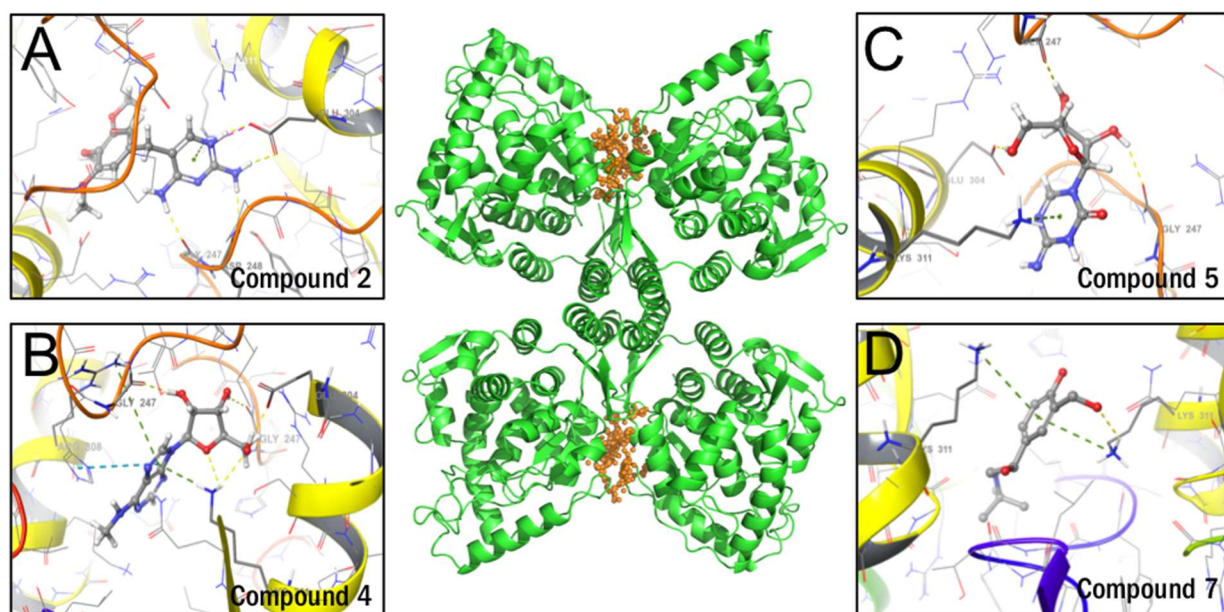


Figure 4.13: Docking of hit compounds to the putative allosteric site identified by Fpocket (colored in orange) at the interphase between the monomers of the tetrameric structure of TH (shown in green). Each compound is shown individually in the allosteric binding site (A) Trimethoprim, (B) N6-methyladenosine, (C) Azacytidine-5 and (D) Levalbuterol-HCl.

Table 4-2: Hit compounds from molecular docking represented with compound numbers, name, 2D structure and Glide score (gscore).

Compound no.	Name	gscore ¹ (kcal/mol)	gscore ² (kcal/mol)	K_d^2 (μ M)
2	Trimethoprim	- 5.2	- 5.1	182.8
4	N6-methyladenosine	- 4.9	- 5.9	50.3
5	Azacytidine-5	- 5.5	- 6.2	29.1
7	Levalbuterol-HCl	- 5.3	- 6.2	27.3
8	Dopamine-HCl	- 6.4	- 6.8	10.6

¹Docking to the active site

² Docking to the allosteric binding site

4.7 The mutant TH-R202H

This THD-associated mutant has been studied earlier showing that the TH-R202H has reduced stability (Calvo et al., 2010) and is not stabilized by DA-binding (Korner et al., 2015). It is common to purify low amounts of unstable proteins, but the purification process proceeded in this work shows otherwise. Before studying the effect of the hit compounds identified using TH-wt, we performed some experiments to verify that our purified TH-R202H is behaving as previously described (Calvo et al., 2010; Korner et al., 2015).

4.7.1 Testing the effect of DA on TH-R202H mutant

4.7.1.1 Stabilizing effect of DA on TH-R202H

By using DSF, we can see that the TH-R202H mutant purified in this work displays higher T_m -values than previously reported (Calvo et al., 2010; Korner et al., 2015), i.e. $50.9 \pm 0.17^\circ\text{C}$. This is almost as stable as TH-wt at $51.5 \pm 0.36^\circ\text{C}$ (Grey lines in Figure 4.14A and B). However, the results clearly show that DA stabilizes the mutant much less than the increase of 3-4°C for TH-wt (Figure 4.14A and B and Figure 4.15). Thus, as earlier reported by Korner *et al.*, the mutant is indeed much less stabilized by DA than TH-wt (Korner et al., 2015). As seen in Figure 4.15 the stability of TH (both wt and R202H) decreases with increasing concentration of DA.

Interestingly, the first derivative graphs of TH-wt – where the T_m values are easily observed – show one peak in the absence of DA and two peaks in the presence of DA (Figure 4.14A). Two unfolding peaks have shown to be characteristic for PAH as the RD melts before the CD upon increasing temperature (Thorolfsson et al., 2002). Moreover, the TH-R202H mutant shows three, or at least two, unfolding peaks even in the absence of DA (Figure 4.14B), suggesting that the mutation somehow changes the structure possibly making the OD, RD and CD of the mutant unfold under different temperatures. The different peaks are less prominent in the presence of DA, which suggest that DA is still stabilizing the mutant to some extent.

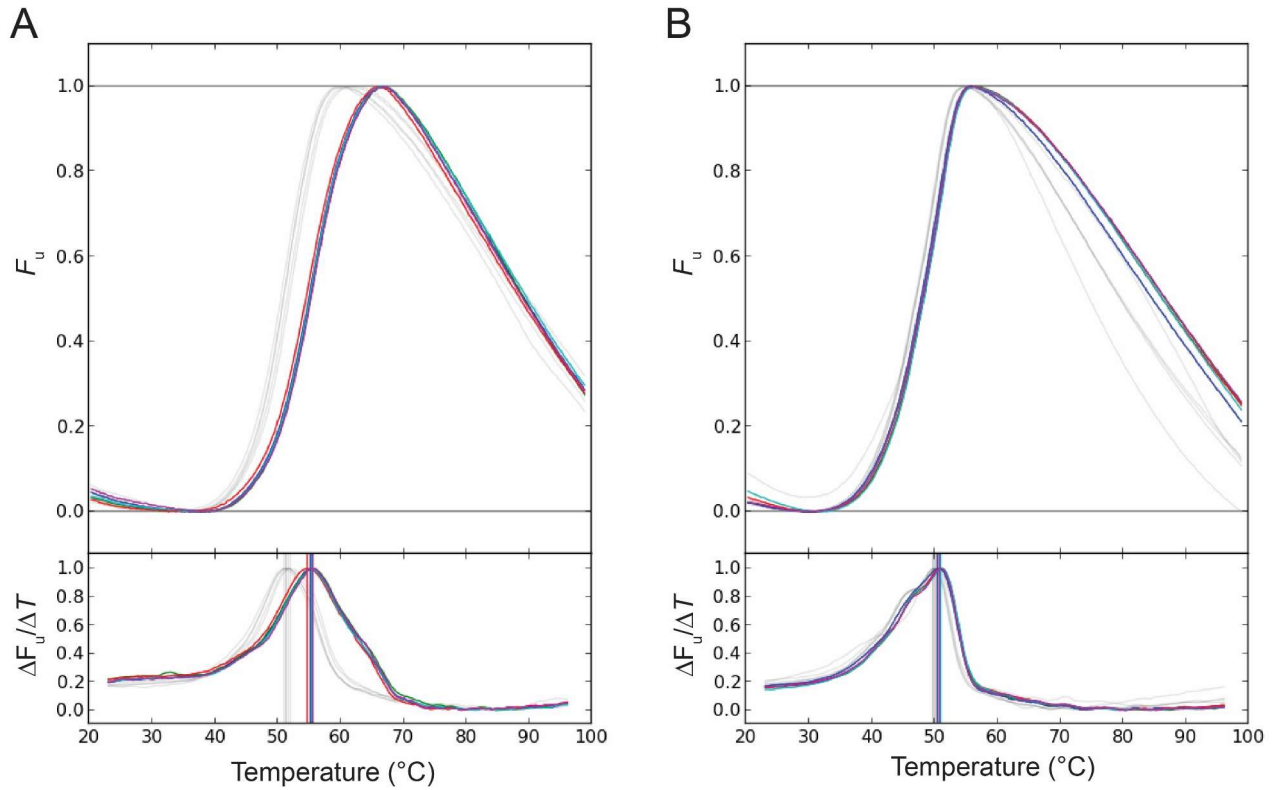


Figure 4.14: Stabilization by stoichiometric amounts of DA. The melting curves are represented as fraction of unfolded protein (F_u) upon increasing temperature. (A) TH-wt without DA ($T_m 51.5 \pm 0.36^{\circ}\text{C}$, grey lines) and with 1X DA ($55.3 \pm 0.3^{\circ}\text{C}$, colored lines) and (B) TH-R202H without DA ($T_m 50.9 \pm 0.17^{\circ}\text{C}$, grey lines) and with 1X DA ($52.4 \pm 0.09^{\circ}\text{C}$, colored lines). The lower panels show the first derivative and vertical lines denote the T_m . In both panels the fluorescence signal is scaled to 0-1.

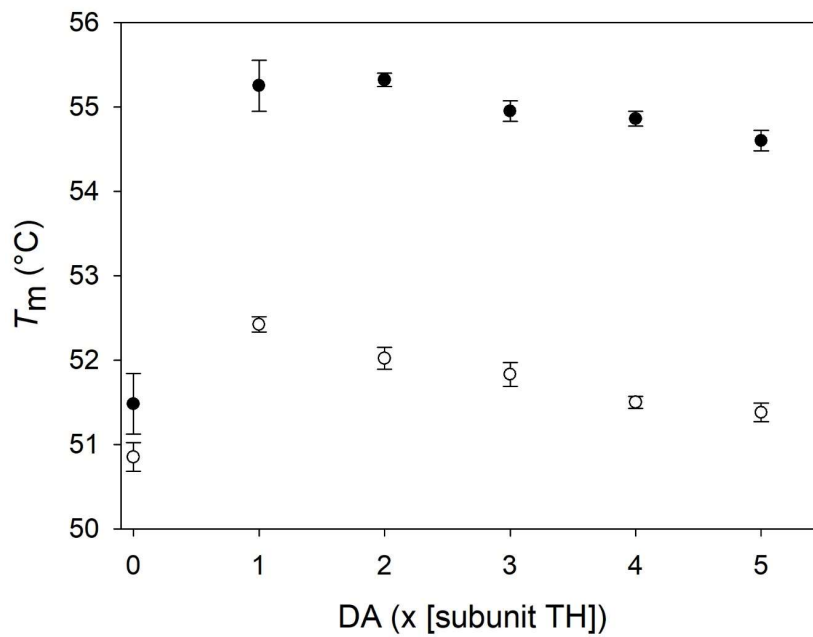


Figure 4.15: The effect of DA on TH stability. The T_m values of unfolding for TH-wt (black circles) and TH-R202H (white circles) in presence of increasing concentration of DA.

4.7.1.2 Protective effect of DA on TH-wt and TH-R202H mutant

Limited proteolysis was performed with DA on TH-R202H using TH-wt as a control and the results are shown in Figure 4.16. The density of each band on the gel was measured and displayed as a bar plot. The results obtained show that the TH-R202H mutant is in fact less prone to trypsinization than TH-wt, but it is proteolyzed to the same extent both without and with DA. The protection of TH-wt proteolysis by DA is in agreement with results from earlier studies (Hole et al., 2015; McCulloch & Fitzpatrick, 1999), likewise for the less protection by DA for the TH-R202H mutant (Korner et al., 2015).

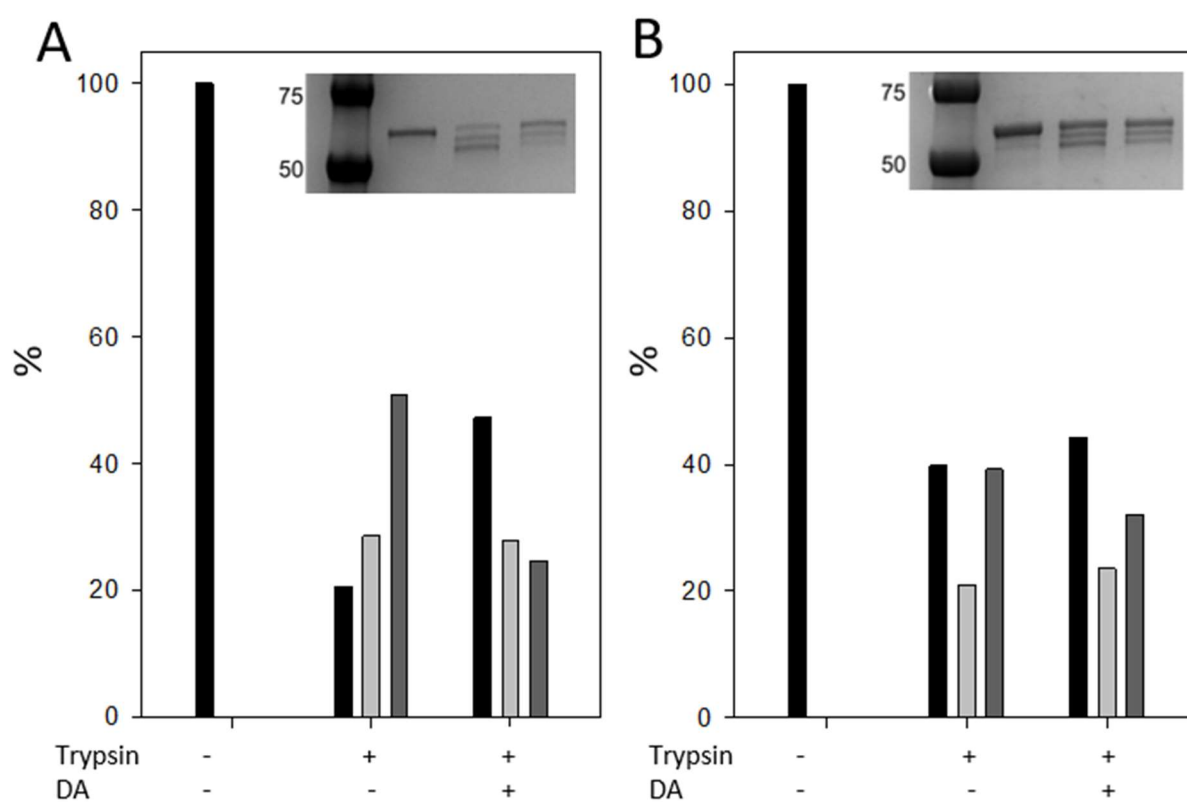


Figure 4.16: Trypsinization of (A) TH-wt and (B) TH-R202H, and effect of DA. The figures show the measured band intensities from the SDS-PAGE gels (representative gels shown in the insets). In the gels, lane 1: Precision marker; lane 2: uncut full-length protein; lane 3: with trypsin; lane 4: with trypsin and DA. The experiment was performed once to confirm previously published data (Korner et al., 2015).

4.7.2 Testing effect of hit compounds on R202H mutant

4.7.2.1 Determination of EC_{50} with hit compounds using DSF

Figure 4.17 shows the effect of hit compounds on the mutant. Here, Trimethoprim shows no effect on the thermal stability on TH-R202H although it stabilizes TH-wt. Among the primary hits, N6-methyladenosine shows less effect on the stability of the mutant, compared with TH-wt. Both Levalbuterol-HCl and Azacytidine-5 cause a dose-dependent stabilization of the R202H-mutant, but to a lesser extent than TH-wt.

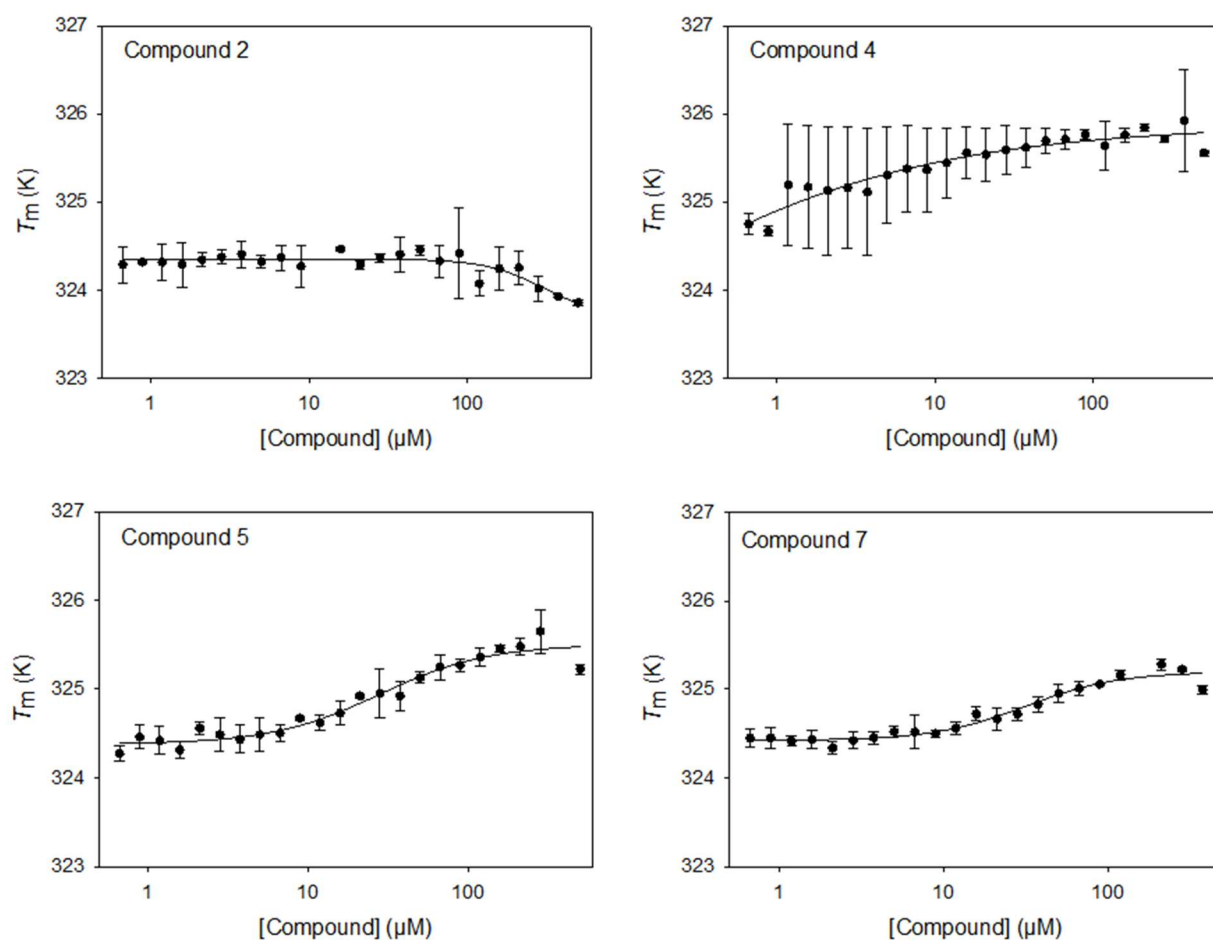


Figure 4.17: Concentration-dependent curves showing the effect of compounds 2, 4, 5 and 7 on TH-R202H. The change in temperature is plotted against compound concentration representing the mean \pm SD. The data were fitted to the four-parameter logistic nonlinear regression equation in SigmaPlot.

4.7.2.2 Limited proteolysis with hit compounds

Figure 4.18 shows the results from protection from proteolysis of TH-R202H by the four hit compounds which are presented as means of three parallels in the bar plot (Figure 4.18A) and given as percentages of the control (TH-R202H without trypsin, set to 100%). A representative gel is shown in Figure 4.18B. Similar to what has been shown for TH-wt, the hit compounds did not protect TH-R202H from limited proteolysis by trypsin, **except for Levalbuterol-HCl** which shows a significant protection (p -value <0.1). In fact, the other compounds appear to slightly accelerate trypsinization on the N-terminal, however without significant difference.

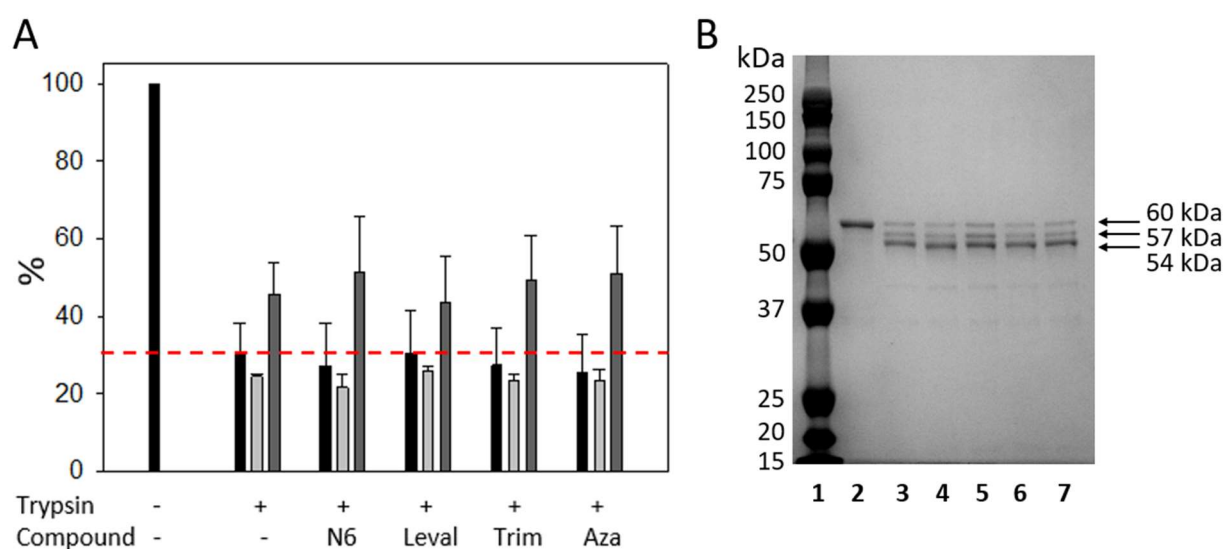


Figure 4.18: The effect of compounds on the limited proteolysis of TH-R202H. (A) Values from triplicate measurements show percent remaining of full-length TH (60 kDa band) (black) and the truncated forms at 57 kDa (light grey) and 54 kDa (dark grey). (B) The SDS-gel shown, are from one of three measurements. Lane 1: Precision marker; lane 2: uncut full-length protein; lane 3: N6-methyladenosine(N6); lane 4: Levalbuterol-HCl (Leval); lane 5: Trimethoprim (Trim); lane 6: Azacytidine-5 (Aza).

5 Discussion

The lack of an effective treatment of THD, especially for the most severe form (Type B), has prompted the investigation on pharmacological chaperones as an alternative therapy for this disorder. Although L-DOPA has shown to improve the symptoms of THD, there are side effects and insufficient response associated with L-DOPA treatment. In this work, we have focused on finding compounds with pharmacological chaperone potential for TH including the most common misfolding mutation in THD, the TH-R202H mutant. Here follows a discussion of the results obtained.

Effort to make an optimized TH did not succeed

Just prior to this masters project, an attempt to create an improved version of the published His-MBP-TH fusion protein (Bezem et al., 2016) was made with the aim to remove some extra amino acids at the N-terminus by site-directed-mutagenesis. The extra amino acids are removed as they are remnants after expression of recombinant fusion proteins. This required the amino acid sequence around the TEV-protease cleavage site (ENLYFQ/G) to be reduced by 3 amino acids (GAM), and thus the linker between the MBP and TH became shorter (Figure 3.1). The expression and purification of the published and *optimized* His-MBP-TH is identical, but this change has surprisingly shown to influence the access to the TEV protease cutting site between His-MBP and TH so much that the cutting is completely abolished for this *optimized* His-MBP-TH. Although recombinant fusion proteins offer many advantages, this result clearly shows that there are also drawbacks. In this specific case 3 extra amino acids at the N-terminus could not be avoided. Luckily, for this project, where this region is not the focus of the study, these residues are not expected to influence the results, but for other experiments having a native N-terminus can be important.

Five primary hit compounds identified on TH

The screening and concentration-dependent binding assay identified compounds that increased the thermal stability of TH. In this DSF-based high throughput method used to determine conditions and identify compounds that affect the protein stability one must accept the drawback of potentially missing out some compounds that might have a stabilizing effect on the enzyme. Some reasons are that parallel samples are not customarily performed, the solubility of each compound in the chosen buffer is not tested and because one cannot check

each melting curve for artefacts. However, this is a known drawback of HTS that is accepted because an efficient method is indeed needed when screening large compound libraries. Starting out with 1624 compounds in the screening of the FDA-approved and NOCE libraries, resulted in five validated hit compounds Trimethoprim, N6-methyladenosine, Azacytidine-5 and Levalbuterol-HCl. In addition to these potential pharmacological chaperones, dopamine-HCl, which is present in the FDA library, was identified as a hit in the initial screening. Identifying DA, the natural feedback inhibitor of TH, as a binder in the screening was reassuring and since the TH-DA interaction is well characterized we decided to include it as a negative control in the following steps.

The hit compounds most probably bind outside the active site

In the validation steps using DSF, the four hit compounds displayed a characteristic sigmoidal curve with EC₅₀-values between 4 and 10 μM. These values were obtained by using Logistic nonlinear regression four-parameter function in SigmaPlot. The EC₅₀-value can be viewed as an approximation of the K_d value, but with an absolute requirement of very good data. Our experiments unfortunately had high experimental errors especially at low compound concentrations and thus we employed ITC, a method that can determine the accurate K_d -value for binding and does not require a dye. The thermograms for both N6-methyladenosine and Azacytidine-5 did not show any binding to TH probably due to the chosen protein and compound concentration for these initial experiments. The chosen protein concentration in this experiment (30 μM) is an appropriate start concentration when the K_d is unknown, but more ITC-experiments at higher protein concentrations must be performed to properly measure the K_d for these two hits.

The thermograms for Trimethoprim and Levalbuterol-HCl showed binding to TH with good concentration dependent data to provide a K_d value of $0.51 \pm 1.76 \times 10^{-7}$ μM and $3.38 \pm 2.52 \times 10^{-7}$, respectively. These values are much lower than the approximate K_d -values obtained with concentration-dependent DSF, and the low value indicates a strong binding affinity towards the protein. Based on these results, Levalbuterol-HCl and Trimethoprim are the only compounds that might have a stabilizing effect for TH. Applying the single set of sites-model also gave a value for the reaction stoichiometry (n) and therefore the number of binding sites per TH subunit, which were $0.24 \pm 3.7 \times 10^{-4}$ for Trimethoprim and $0.45 \pm 1.5 \times 10^{-2}$ for Levalbuterol-HCl. For compounds binding to the active site of TH, the n-value is expected to be 1, and a low n-value suggests that not all TH is binding the compound or, more probably, that the compounds

bind at intermonomer sites (e.g. $n=1$ per dimer). The docking results showed that all four hit compounds should be able to bind in the active site, although with less affinity than DA (gscore of -6.4 kcal/mol) that is well known to bind directly to the active site iron (Andersson et al., 1988). However, they also dock to the interphase between the monomers in each of the dimers in the tetrameric structure of TH. In fact, to this allosteric binding pocket they appear to bind better (a more negative gscore) than to the active site.

Since the n -values of both compounds are closer to 0.5, this supports the latter docking result, which would explain $n=1$ per TH dimer (2 per tetrameric unit). Another result supporting that the compounds bind outside the active site is from the TH activity assay in presence of the hit compounds. The results showed that none of the four hit compounds affected the enzyme activity in an inhibitory manner and thus are unlikely to compete with the natural ligands for binding to the active site. The feedback inhibitor DA was included in the assay and almost abolished TH activity as expected ($\sim 97\%$ reduction). Indeed, when the hit compounds and DA were docked to the active site of TH, a better gscore was obtained for DA than the four hit compounds. Thus, all the results obtained so far are supporting that the compounds bind in other binding pockets than the active site.

The binding of FDA-approved hit compounds on TH might explain their side effects

The four hit compounds that have shown to bind and stabilize TH in this work are identified from the off- patent FDA-approved drug library, where 95% drugs have been licensed by the US Food and Drug Administration for medical use. To date, the drugs are used to treat different disorders and conditions. Trimethoprim is an antibiotic used for treatment of infections, especially urinary tract infections but also used in combination with other drugs to treat pneumonia and diarrhea. Levalbuterol-HCl, also known under the market name Xopenex[®], is a short-acting beta agonist (SABA) used in asthma treatment and chronic obstructive pulmonary disease (COPD). Azacytidine-5 (Vidaza[®]) is an antineoplastic drug used in cancer treatment and has been licensed for use in all subtypes of myelodysplastic syndromes (MDS) and/or myeloid leukemia after intensive chemotherapy (Raj et al., 2006). To our knowledge there is no reports on N6-methyladenosine as a drug. N6-methyladenosine is a modified mRNA where the adenosine base at the nitrogen 6-position is methylated and this modification of the human mRNA molecules has been shown to play a critical role in various cancer development

(Niu et al., 2018). It will be interesting to see if TH-related side effects are seen when and if the molecule comes into the market as a potential drug.

Interestingly, common side effects using Trimethoprim are nausea, vomiting, diarrhea, itching and rash. Vomiting and nausea are often connected to stimulation of the dopamine D₂-receptor which is located in the chemoreceptor trigger zone (CTZ) in the brain. The stimulation of the D₂-receptor causing these side effects can potentially be explained by the strong binding affinity (a low K_d) and the increasing effect that Trimethoprim had on TH activity leading to higher levels of DA. In fact, it has been addressed elsewhere that Trimethoprim affect the catecholamine synthesis pathway, resulting with an increased level of neurotransmitters (Sakai et al., 1995). The study suggests that Trimethoprim, an inhibitor of dihydrofolate reductase (DHFR), also act on the CNS enzyme dihydropteridine reductase (DHPR) in the recycling synthesis of BH₄. Inhibition of both enzymes is thought to decrease the regeneration of BH₄, which in turn should result in a feedback stimulation to the synthesis of BH₄ from guanosine triphosphate (GTP). This indeed suggest that Trimethoprim might have several acting mechanisms within the catecholamine synthesis pathway leading to an increase level of neurotransmitters.

Moreover, one of many common side effects reported for Levalbuterol-HCl is shaking. Despite the fact that the activity measurements did not proof inhibition, it seems that this compound might alter DA synthesis leading to a reduced amount of DA which is associated with shaking and tremor, a Parkinson-like side effect. Insomnia has also been reported as a side effect and it is well known that the sleep onset is associated with changes in levels of circulating catecholamines (Irwin et al., 1999). Additionally, the inhibition of the biosynthesis of catecholamines has been shown to induce a temporary hypersomnia increasing both paradoxical sleep and slow wave sleep. Other side effects mentioned in the product info of the drug includes anxiety, nervousness, dizziness and nausea. In fact, this is supported by a study showing that treatment with a TH-inhibitor, alpha-methyl-p-tyrosine (AMPT), has shown to cause similar side effects such as pathological anxiety, decreased calmness, increased depression, sleepiness, tension and anger (McCann et al., 1995).

Chemotherapy-induced nausea and vomiting is a common side effect of many cancer treatment and this side effect is mentioned in the product info of Azacytidine-5 (Vidaza[®]) among other side effects such as tiredness, insomnia, anxiety and dizziness. The adverse reaction is often

associated with levels of neurotransmitters, which can possibly explain the side effects using Azacytidine-5 as discussed above for Levalbuterol-HCl.

The TH-R202H mutant is stable, but is not properly regulated by DA

There are studies that have been conducted on the THD-associated mutant showing that the TH-R202H has reduced stability (Calvo et al., 2010) and is not able to bind DA (Korner et al., 2015). In this work, our purified mutant has shown to behave differently. The purification yielded a good amount of TH-R202H, which is unexpected if the protein is unstable. When removing the fusion partner from TH-R202H, the protein still remained stable to an extent reflected by the percentage yield of 24% compared to the wild-type of 34%. This is supported by the results obtained from the DSF-based HTS showing that the mutant displays a much higher T_m -value than previously reported (Calvo et al., 2010), i.e. $50.9 \pm 0.17^\circ\text{C}$ which is very close to the stability of TH-wt at $51.5 \pm 0.36^\circ\text{C}$.

In agreement with earlier results reported by Korner *et al.* (Korner et al., 2015), the TH-R202H mutant is stable, but is not properly regulated by DA. The results clearly show that DA stabilizes the mutant much less than TH-wt (1-2°C vs. 3-4°C) indicating that the mutant does bind to DA but is not able to be stabilized to the same extent as TH-wt. This is in fact also supported by the results obtained for limited proteolysis by trypsin showing that DA does not protect TH-R202H against trypsinization. This suggest further that the mutation of arginine (R) to a histidine (H) in position 202 somehow changes the tetrameric structure and that the mutant has conformational defects that appears to change the interactions between domains. This is supported by the DSF profiles with more disengaged domain transitions in forms of different unfolding peaks. Other mutations decrease more the stability and increase the mobility, therefore increasing the proteolysis, but for the TH-R202H mutant it seems that we have a discrete conformational change. This explains the different concentration-dependent binding profiles obtained for TH-wt and TH-R202H with each hit compound. E.g. Trimethoprim showed no effect on the thermal stability of TH-R202H, contrary to TH-wt.

One of four hit compounds can be considered a possible candidate for pharmacological chaperone therapy for TH

In the beginning of this work, four compounds were identified as hits based on the concentration-dependent binding DSF profiles. So far, only one of these four hit compounds

show potential as a pharmacological chaperone. As mentioned earlier, Trimethoprim did not exert any effect on the thermal stability on TH-R202H. There are large standard deviations at lower concentration of N6-methyladenosine as seen in the DSF-profile and the protective effect of Azacytidine-5 towards proteolysis of the mutant is not significant. Although the inhibition of Levalbuterol-HCl in the activity assay is non-significant compared to the other compounds, it binds with high affinity (the low K_d -value obtained by ITC) and still show an effect on the thermal stability of TH. This is supported by the large negative gscore obtained by molecular docking at the allosteric binding pocket as the compound most probably bind outside the active site as discussed earlier. In fact, Levalbuterol-HCl is the only compound that shows significant ($p < 0.05$) protection towards proteolysis of the 57 kDa truncated form of TH-wt and a trend is also seen ($p < 0.1$) for the mutant. Altogether, the data from this work identifies Levalbuterol-HCl as a potential pharmacological chaperone that may increase the steady state levels of TH in cells and *in vivo*.

6 Conclusion

The main aim with this work was to find potential pharmacological chaperones that stabilize tyrosine hydroxylase (TH) and its disease-associated mutant, TH1-p.R202H. From the experimental screening and validation, we discovered four primary hit compounds. All four hit compounds point towards binding of allosteric binding pockets of TH rather than the active site and only one compound could be identified as a potential pharmacological chaperone. This work has also provided important information regarding side-effects of these FDA-approved drugs possibly caused by their ability to bind and stabilize TH. We have gained a better insight into the THD-associated mutant R202H, which so far appears to confer a discrete conformational change affecting the proper stabilization by DA, but the stability of the protein itself remains intact.

7 Future work

To obtain more knowledge about the four hit compounds as potential pharmacological chaperones, future work should include further validation assays to gain a deeper understanding of the stabilizing effect of the compounds on both TH and TH-R202H. This is essential for the compounds to be applied as potential drug candidates for THD treatment.

For one of the compounds the stabilizing effect shown in the DSF-profile on the TH-R202H mutant is not strictly significant, due to the large standard deviations obtained. The experiment should be repeated in order to validate our findings. Moreover, two of four hit compounds did not show any form for binding to TH using ITC, probably because of the chosen protein- and compound concentration. Thus, more ITC-experiments at higher protein concentrations must be performed to properly measure the K_d for these two hits. Their effects on the TH should also be tested and analyzed to explore their functionality and toxicology in cells and eventually in animal models. To be able to fully understand the binding of the compounds on the enzyme, the full-length crystal structure of TH should also be solved. This enable further docking possibilities with the hit compounds.

8 References

- Andersen, O. A., Flatmark, T., & Hough, E. (2002). Crystal structure of the ternary complex of the catalytic domain of human phenylalanine hydroxylase with tetrahydrobiopterin and 3-(2-thienyl)-L-alanine, and its implications for the mechanism of catalysis and substrate activation. *J Mol Biol*, *320*(5), 1095-1108.
- Andersson, K. K., Cox, D. D., Que, L., Jr., Flatmark, T., & Haavik, J. (1988). Resonance Raman studies on the blue-green-colored bovine adrenal tyrosine 3-monooxygenase (tyrosine hydroxylase). Evidence that the feedback inhibitors adrenaline and noradrenaline are coordinated to iron. *J Biol Chem*, *263*(35), 18621-18626.
- Arturo, E. C., Gupta, K., Heroux, A., Stith, L., Cross, P. J., Parker, E. J., . . . Jaffe, E. K. (2016). First structure of full-length mammalian phenylalanine hydroxylase reveals the architecture of an autoinhibited tetramer. *Proc Natl Acad Sci U S A*, *113*(9), 2394-2399. doi:10.1073/pnas.1516967113
- Axelrod, J., & Weinshilboum, R. (1972). Catecholamines. *N Engl J Med*, *287*(5), 237-242. doi:10.1056/NEJM197208032870508
- Bartholini, G., Burkard, W. P., & Pletscher, A. (1967). Increase of cerebral catecholamines caused by 3,4-dihydroxyphenylalanine after inhibition of peripheral decarboxylase. *Nature*, *215*(5103), 852-853.
- Bezem, M. T., Baumann, A., Skjaerven, L., Meyer, R., Kursula, P., Martinez, A., & Flydal, M. I. (2016). Stable preparations of tyrosine hydroxylase provide the solution structure of the full-length enzyme. *Sci Rep*, *6*, 30390. doi:10.1038/srep30390
- Bobrovskaya, L., Dunkley, P. R., & Dickson, P. W. (2004). Phosphorylation of Ser19 increases both Ser40 phosphorylation and enzyme activity of tyrosine hydroxylase in intact cells. *J Neurochem*, *90*(4), 857-864. doi:10.1111/j.1471-4159.2004.02550.x
- Brennecke, P., Rasina, D., Aubi, O., Herzog, K., Landskron, J., Cautain, B., . . . Gribbon, P. (2019). EU-OPENSREEN: A Novel Collaborative Approach to Facilitate Chemical Biology. *SLAS Discov*, *24*(3), 398-413. doi:10.1177/2472555218816276
- Calvo, A. C., Scherer, T., Pey, A. L., Ying, M., Winge, I., McKinney, J., . . . Martinez, A. (2010). Effect of pharmacological chaperones on brain tyrosine hydroxylase and tryptophan hydroxylase 2. *J Neurochem*, *114*(3), 853-863. doi:10.1111/j.1471-4159.2010.06821.x
- Campbell, D. G., Hardie, D. G., & Vulliet, P. R. (1986). Identification of four phosphorylation sites in the N-terminal region of tyrosine hydroxylase. *J Biol Chem*, *261*(23), 10489-10492.
- Chipman, D. M., & Shaanan, B. (2001). The ACT domain family. *Curr Opin Struct Biol*, *11*(6), 694-700.
- Daubner, S. C., Le, T., & Wang, S. (2011). Tyrosine hydroxylase and regulation of dopamine synthesis. *Arch Biochem Biophys*, *508*(1), 1-12. doi:10.1016/j.abb.2010.12.017
- Di, L., Kerns, E. H., & Carter, G. T. (2009). Drug-like property concepts in pharmaceutical design. *Curr Pharm Des*, *15*(19), 2184-2194.
- Dobson, C. M. (2003). Protein folding and misfolding. *Nature*, *426*(6968), 884-890. doi:10.1038/nature02261
- Dunkley, P. R., Bobrovskaya, L., Graham, M. E., von Nagy-Felsobuki, E. I., & Dickson, P. W. (2004). Tyrosine hydroxylase phosphorylation: regulation and consequences. *J Neurochem*, *91*(5), 1025-1043. doi:10.1111/j.1471-4159.2004.02797.x
- Ellis, R. J. (1990). The molecular chaperone concept. *Semin Cell Biol*, *1*(1), 1-9.

- Erlandsen, H., Flatmark, T., Stevens, R. C., & Hough, E. (1998). Crystallographic analysis of the human phenylalanine hydroxylase catalytic domain with bound catechol inhibitors at 2.0 Å resolution. *Biochemistry*, *37*(45), 15638-15646. doi:10.1021/bi9815290
- Fitzpatrick, P. F. (1999). Tetrahydropterin-dependent amino acid hydroxylases. *Annu Rev Biochem*, *68*, 355-381. doi:10.1146/annurev.biochem.68.1.355
- Flatmark, T., Almas, B., Knappskog, P. M., Berge, S. V., Svebak, R. M., Chehin, R., . . . Martinez, A. (1999). Tyrosine hydroxylase binds tetrahydrobiopterin cofactor with negative cooperativity, as shown by kinetic analyses and surface plasmon resonance detection. *Eur J Biochem*, *262*(3), 840-849.
- Fossbakk, A., Kleppe, R., Knappskog, P. M., Martinez, A., & Haavik, J. (2014). Functional studies of tyrosine hydroxylase missense variants reveal distinct patterns of molecular defects in Dopa-responsive dystonia. *Hum Mutat*, *35*(7), 880-890. doi:10.1002/humu.22565
- Friesner, R. A., Banks, J. L., Murphy, R. B., Halgren, T. A., Klicic, J. J., Mainz, D. T., . . . Shenkin, P. S. (2004). Glide: a new approach for rapid, accurate docking and scoring. 1. Method and assessment of docking accuracy. *J Med Chem*, *47*(7), 1739-1749. doi:10.1021/jm0306430
- Fujisawa, H., & Okuno, S. (2005). Regulatory mechanism of tyrosine hydroxylase activity. *Biochem Biophys Res Commun*, *338*(1), 271-276. doi:10.1016/j.bbrc.2005.07.183
- Goodwill, K. E., Sabatier, C., Marks, C., Raag, R., Fitzpatrick, P. F., & Stevens, R. C. (1997). Crystal structure of tyrosine hydroxylase at 2.3 Å and its implications for inherited neurodegenerative diseases. *Nat Struct Biol*, *4*(7), 578-585.
- Goodwill, K. E., Sabatier, C., & Stevens, R. C. (1998). Crystal structure of tyrosine hydroxylase with bound cofactor analogue and iron at 2.3 Å resolution: self-hydroxylation of Phe300 and the pterin-binding site. *Biochemistry*, *37*(39), 13437-13445. doi:10.1021/bi981462g
- Gordon, S. L., Quinsey, N. S., Dunkley, P. R., & Dickson, P. W. (2008). Tyrosine hydroxylase activity is regulated by two distinct dopamine-binding sites. *J Neurochem*, *106*(4), 1614-1623. doi:10.1111/j.1471-4159.2008.05509.x
- Grant, G. A. (2006). The ACT domain: a small molecule binding domain and its role as a common regulatory element. *J Biol Chem*, *281*(45), 33825-33829. doi:10.1074/jbc.R600024200
- Gregersen, N., Bross, P., Vang, S., & Christensen, J. H. (2006). Protein misfolding and human disease. *Annu Rev Genomics Hum Genet*, *7*, 103-124. doi:10.1146/annurev.genom.7.080505.115737
- Hartl, F. U., Bracher, A., & Hayer-Hartl, M. (2011). Molecular chaperones in protein folding and proteostasis. *Nature*, *475*(7356), 324-332. doi:10.1038/nature10317
- Hartl, F. U., & Hayer-Hartl, M. (2002). Molecular chaperones in the cytosol: from nascent chain to folded protein. *Science*, *295*(5561), 1852-1858. doi:10.1126/science.1068408
- Hastings, T. G., & Zigmond, M. J. (1994). Identification of catechol-protein conjugates in neostriatal slices incubated with [³H]dopamine: impact of ascorbic acid and glutathione. *J Neurochem*, *63*(3), 1126-1132.
- Haycock, J. W. (1993). Multiple signaling pathways in bovine chromaffin cells regulate tyrosine hydroxylase phosphorylation at Ser19, Ser31, and Ser40. *Neurochem Res*, *18*(1), 15-26.
- Haycock, J. W. (2002). Species differences in the expression of multiple tyrosine hydroxylase protein isoforms. *J Neurochem*, *81*(5), 947-953.

- Hoffmann, G. F., Assmann, B., Brautigam, C., Dionisi-Vici, C., Haussler, M., de Klerk, J. B., . . . Wevers, R. A. (2003). Tyrosine hydroxylase deficiency causes progressive encephalopathy and dopa-nonresponsive dystonia. *Ann Neurol*, *54 Suppl 6*, S56-65. doi:10.1002/ana.10632
- Hole, M., Jorge-Finnigan, A., Underhaug, J., Teigen, K., & Martinez, A. (2016). Pharmacological Chaperones that Protect Tetrahydrobiopterin Dependent Aromatic Amino Acid Hydroxylases Through Different Mechanisms. *Curr Drug Targets*, *17*(13), 1515-1526.
- Hole, M., Underhaug, J., Diez, H., Ying, M., Rohr, A. K., Jorge-Finnigan, A., . . . Martinez, A. (2015). Discovery of compounds that protect tyrosine hydroxylase activity through different mechanisms. *Biochim Biophys Acta*, *1854*(9), 1078-1089. doi:10.1016/j.bbapap.2015.04.030
- Hong, P., Koza, S., & Bouvier, E. S. (2012). Size-Exclusion Chromatography for the Analysis of Protein Biotherapeutics and their Aggregates. *J Liq Chromatogr Relat Technol*, *35*(20), 2923-2950. doi:10.1080/10826076.2012.743724
- Hung, Y. F., Valdau, O., Schunke, S., Stern, O., Koenig, B. W., Willbold, D., & Hoffmann, S. (2014). Recombinant production of the amino terminal cytoplasmic region of dengue virus non-structural protein 4A for structural studies. *PLoS One*, *9*(1), e86482. doi:10.1371/journal.pone.0086482
- Haavik, J., & Flatmark, T. (1980). Rapid and sensitive assay of tyrosine 3-monoxygenase activity by high-performance liquid chromatography using the native fluorescence of DOPA. *J Chromatogr*, *198*(4), 511-515.
- Haavik, J., Le Bourdelles, B., Martinez, A., Flatmark, T., & Mallet, J. (1991). Recombinant human tyrosine hydroxylase isozymes. Reconstitution with iron and inhibitory effect of other metal ions. *Eur J Biochem*, *199*(2), 371-378.
- Haavik, J., & Toska, K. (1998). Tyrosine hydroxylase and Parkinson's disease. *Mol Neurobiol*, *16*(3), 285-309. doi:10.1007/BF02741387
- Irwin, M., Thompson, J., Miller, C., Gillin, J. C., & Ziegler, M. (1999). Effects of sleep and sleep deprivation on catecholamine and interleukin-2 levels in humans: clinical implications. *J Clin Endocrinol Metab*, *84*(6), 1979-1985. doi:10.1210/jcem.84.6.5788
- Jorge-Finnigan, A., Kleppe, R., Jung-Kc, K., Ying, M., Marie, M., Rios-Mondragon, I., . . . Martinez, A. (2017). Phosphorylation at serine 31 targets tyrosine hydroxylase to vesicles for transport along microtubules. *J Biol Chem*, *292*(34), 14092-14107. doi:10.1074/jbc.M116.762344
- Kageyama, T., Nakamura, M., Matsuo, A., Yamasaki, Y., Takakura, Y., Hashida, M., . . . Shimohama, S. (2000). The 4F2hc/LAT1 complex transports L-DOPA across the blood-brain barrier. *Brain Res*, *879*(1-2), 115-121.
- Kaneda, N., Kobayashi, K., Ichinose, H., Kishi, F., Nakazawa, A., Kurosawa, Y., . . . Nagatsu, T. (1987). Isolation of a novel cDNA clone for human tyrosine hydroxylase: alternative RNA splicing produces four kinds of mRNA from a single gene. *Biochem Biophys Res Commun*, *146*(3), 971-975.
- Kleppe, R., Toska, K., & Haavik, J. (2001). Interaction of phosphorylated tyrosine hydroxylase with 14-3-3 proteins: evidence for a phosphoserine 40-dependent association. *J Neurochem*, *77*(4), 1097-1107.
- Kobayashi, K. (2001). Role of catecholamine signaling in brain and nervous system functions: new insights from mouse molecular genetic study. *J Investig Dermatol Symp Proc*, *6*(1), 115-121. doi:10.1046/j.0022-202x.2001.00011.x

- Korner, G., Noain, D., Ying, M., Hole, M., Flydal, M. I., Scherer, T., . . . Thony, B. (2015). Brain catecholamine depletion and motor impairment in a Th knock-in mouse with type B tyrosine hydroxylase deficiency. *Brain*, *138*(Pt 10), 2948-2963. doi:10.1093/brain/awv224
- Kumer, S. C., & Vrana, K. E. (1996). Intricate regulation of tyrosine hydroxylase activity and gene expression. *J Neurochem*, *67*(2), 443-462.
- Le Guilloux, V., Schmidtke, P., & Tuffery, P. (2009). Fpocket: an open source platform for ligand pocket detection. *BMC Bioinformatics*, *10*, 168. doi:10.1186/1471-2105-10-168
- Leavitt, S., & Freire, E. (2001). Direct measurement of protein binding energetics by isothermal titration calorimetry. *Curr Opin Struct Biol*, *11*(5), 560-566.
- Lewis, D. A., Melchitzky, D. S., & Haycock, J. W. (1993). Four isoforms of tyrosine hydroxylase are expressed in human brain. *Neuroscience*, *54*(2), 477-492.
- Lilienbaum, A. (2013). Relationship between the proteasomal system and autophagy. *Int J Biochem Mol Biol*, *4*(1), 1-26.
- Markham, A. (2016). Migalastat: First Global Approval. *Drugs*, *76*(11), 1147-1152. doi:10.1007/s40265-016-0607-y
- McCann, U. D., Thorne, D., Hall, M., Popp, K., Avery, W., Sing, H., . . . Belenky, G. (1995). The effects of L-dihydroxyphenylalanine on alertness and mood in alpha-methyl-para-tyrosine-treated healthy humans. Further evidence for the role of catecholamines in arousal and anxiety. *Neuropsychopharmacology*, *13*(1), 41-52. doi:10.1016/0893-133X(94)00134-L
- McCulloch, R. I., & Fitzpatrick, P. F. (1999). Limited proteolysis of tyrosine hydroxylase identifies residues 33-50 as conformationally sensitive to phosphorylation state and dopamine binding. *Arch Biochem Biophys*, *367*(1), 143-145. doi:10.1006/abbi.1999.1259
- Meisburger, S. P., Taylor, A. B., Khan, C. A., Zhang, S., Fitzpatrick, P. F., & Ando, N. (2016). Domain Movements upon Activation of Phenylalanine Hydroxylase Characterized by Crystallography and Chromatography-Coupled Small-Angle X-ray Scattering. *J Am Chem Soc*, *138*(20), 6506-6516. doi:10.1021/jacs.6b01563
- Meng, X. Y., Zhang, H. X., Mezei, M., & Cui, M. (2011). Molecular docking: a powerful approach for structure-based drug discovery. *Curr Comput Aided Drug Des*, *7*(2), 146-157.
- Mizushima, N. (2007). Autophagy: process and function. *Genes Dev*, *21*(22), 2861-2873. doi:10.1101/gad.1599207
- Molinoff, P. B., & Axelrod, J. (1971). Biochemistry of catecholamines. *Annu Rev Biochem*, *40*, 465-500. doi:10.1146/annurev.bi.40.070171.002341
- Morris, G. M., & Lim-Wilby, M. (2008). Molecular docking. *Methods Mol Biol*, *443*, 365-382. doi:10.1007/978-1-59745-177-2_19
- Muchowski, P. J. (2002). Protein misfolding, amyloid formation, and neurodegeneration: a critical role for molecular chaperones? *Neuron*, *35*(1), 9-12.
- Nagatsu, T., Levitt, M., & Udenfriend, S. (1964). Tyrosine Hydroxylase. The Initial Step in Norepinephrine Biosynthesis. *J Biol Chem*, *239*, 2910-2917.
- Nagatsu, T., Nakashima, A., Ichinose, H., & Kobayashi, K. (2018). Human tyrosine hydroxylase in Parkinson's disease and in related disorders. *J Neural Transm (Vienna)*. doi:10.1007/s00702-018-1903-3
- Nandi, D., Tahiliani, P., Kumar, A., & Chandu, D. (2006). The ubiquitin-proteasome system. *J Biosci*, *31*(1), 137-155.

- Niesen, F. H., Berglund, H., & Vedadi, M. (2007). The use of differential scanning fluorimetry to detect ligand interactions that promote protein stability. *Nat Protoc*, 2(9), 2212-2221. doi:10.1038/nprot.2007.321
- Niu, Y., Wan, A., Lin, Z., Lu, X., & Wan, G. (2018). N (6)-Methyladenosine modification: a novel pharmacological target for anti-cancer drug development. *Acta Pharm Sin B*, 8(6), 833-843. doi:10.1016/j.apsb.2018.06.001
- O'Shea, E. K., Rutkowski, R., & Kim, P. S. (1989). Evidence that the leucine zipper is a coiled coil. *Science*, 243(4890), 538-542.
- Pons, R., Syrengelas, D., Youroukos, S., Orfanou, I., Dinopoulos, A., Cormand, B., . . . Artuch, R. (2013). Levodopa-induced dyskinesias in tyrosine hydroxylase deficiency. *Mov Disord*, 28(8), 1058-1063. doi:10.1002/mds.25382
- Quinsey, N. S., Luong, A. Q., & Dickson, P. W. (1998). Mutational analysis of substrate inhibition in tyrosine hydroxylase. *J Neurochem*, 71(5), 2132-2138.
- Raj, K., & Mufti, G. J. (2006). Azacytidine (Vidaza(R)) in the treatment of myelodysplastic syndromes. *Ther Clin Risk Manag*, 2(4), 377-388.
- Ramsey, A. J., & Fitzpatrick, P. F. (1998). Effects of phosphorylation of serine 40 of tyrosine hydroxylase on binding of catecholamines: evidence for a novel regulatory mechanism. *Biochemistry*, 37(25), 8980-8986. doi:10.1021/bi980582l
- Ringe, D., & Petsko, G. A. (2009). What are pharmacological chaperones and why are they interesting? *J Biol*, 8(9), 80. doi:10.1186/jbiol186
- Roberts, K. M., & Fitzpatrick, P. F. (2013). Mechanisms of tryptophan and tyrosine hydroxylase. *IUBMB Life*, 65(4), 350-357. doi:10.1002/iub.1144
- Rosano, G. L., & Ceccarelli, E. A. (2014). Recombinant protein expression in Escherichia coli: advances and challenges. *Front Microbiol*, 5, 172. doi:10.3389/fmicb.2014.00172
- Sakai, T., Matsuishi, T., Yamada, S., Komori, H., & Iwashita, H. (1995). Sulfamethoxazole-trimethoprim double-blind, placebo-controlled, crossover trial in Machado-Joseph disease: sulfamethoxazole-trimethoprim increases cerebrospinal fluid level of biopterin. *J Neural Transm Gen Sect*, 102(2), 159-172.
- Sebaugh, J. L. (2011). Guidelines for accurate EC50/IC50 estimation. *Pharm Stat*, 10(2), 128-134. doi:10.1002/pst.426
- Senisterra, G. A., & Finerty, P. J., Jr. (2009). High throughput methods of assessing protein stability and aggregation. *Mol Biosyst*, 5(3), 217-223. doi:10.1039/b814377c
- Siltberg-Liberles, J., Steen, I. H., Svebak, R. M., & Martinez, A. (2008). The phylogeny of the aromatic amino acid hydroxylases revisited by characterizing phenylalanine hydroxylase from Dictyostelium discoideum. *Gene*, 427(1-2), 86-92. doi:10.1016/j.gene.2008.09.005
- Stokes, A. H., Hastings, T. G., & Vrana, K. E. (1999). Cytotoxic and genotoxic potential of dopamine. *J Neurosci Res*, 55(6), 659-665. doi:10.1002/(SICI)1097-4547(19990315)55:6<659::AID-JNR1>3.0.CO;2-C
- Szigetvari, P. D., Muruganandam, G., Kallio, J. P., Hallin, E. I., Fossbakk, A., Loris, R., . . . Haavik, J. (2019). The quaternary structure of human tyrosine hydroxylase: effects of dystonia-associated missense variants on oligomeric state and enzyme activity. *J Neurochem*, 148(2), 291-306. doi:10.1111/jnc.14624
- Teigen, K., McKinney, J. A., Haavik, J., & Martinez, A. (2007). Selectivity and affinity determinants for ligand binding to the aromatic amino acid hydroxylases. *Curr Med Chem*, 14(4), 455-467.

- Tekin, I., Roskoski, R., Jr., Carkaci-Salli, N., & Vrana, K. E. (2014). Complex molecular regulation of tyrosine hydroxylase. *J Neural Transm (Vienna)*, *121*(12), 1451-1481. doi:10.1007/s00702-014-1238-7
- Terpe, K. (2003). Overview of tag protein fusions: from molecular and biochemical fundamentals to commercial systems. *Appl Microbiol Biotechnol*, *60*(5), 523-533. doi:10.1007/s00253-002-1158-6
- Thorolfsson, M., Ibarra-Molero, B., Fojan, P., Petersen, S. B., Sanchez-Ruiz, J. M., & Martinez, A. (2002). L-phenylalanine binding and domain organization in human phenylalanine hydroxylase: a differential scanning calorimetry study. *Biochemistry*, *41*(24), 7573-7585.
- Urh, M., Simpson, D., & Zhao, K. (2009). Affinity chromatography: general methods. *Methods Enzymol*, *463*, 417-438. doi:10.1016/S0076-6879(09)63026-3
- van den Berg, S., Lofdahl, P. A., Hard, T., & Berglund, H. (2006). Improved solubility of TEV protease by directed evolution. *J Biotechnol*, *121*(3), 291-298. doi:10.1016/j.jbiotec.2005.08.006
- van den Heuvel, L. P., Luiten, B., Smeitink, J. A., de Rijk-van Andel, J. F., Hyland, K., Steenbergen-Spanjers, G. C., . . . Wevers, R. A. (1998). A common point mutation in the tyrosine hydroxylase gene in autosomal recessive L-DOPA-responsive dystonia in the Dutch population. *Hum Genet*, *102*(6), 644-646.
- Waugh, D. S. (2016). The remarkable solubility-enhancing power of Escherichia coli maltose-binding protein. *Postepy Biochem*, *62*(3), 377-382.
- Willemsen, M. A., Verbeek, M. M., Kamsteeg, E. J., de Rijk-van Andel, J. F., Aeby, A., Blau, N., . . . Wevers, R. A. (2010). Tyrosine hydroxylase deficiency: a treatable disorder of brain catecholamine biosynthesis. *Brain*, *133*(Pt 6), 1810-1822. doi:10.1093/brain/awq087
- Wiseman, T., Williston, S., Brandts, J. F., & Lin, L. N. (1989). Rapid measurement of binding constants and heats of binding using a new titration calorimeter. *Anal Biochem*, *179*(1), 131-137.
- Zhang, S., Huang, T., Ilangovan, U., Hinck, A. P., & Fitzpatrick, P. F. (2014). The solution structure of the regulatory domain of tyrosine hydroxylase. *J Mol Biol*, *426*(7), 1483-1497. doi:10.1016/j.jmb.2013.12.015
- Zhao, X., Li, G., & Liang, S. (2013). Several affinity tags commonly used in chromatographic purification. *J Anal Methods Chem*, *2013*, 581093. doi:10.1155/2013/581093
- Zhu, Y., Zhang, J., & Zeng, Y. (2012). Overview of tyrosine hydroxylase in Parkinson's disease. *CNS Neurol Disord Drug Targets*, *11*(4), 350-358.

9 Appendix

Layout of the RUBIC Buffer Screen

Figure 2:- Layout of the RUBIC Buffer Screen

	1	2	3	4	5	6	7	8	9	10	11	12
A	Water	100mM Citric Acid	100mM NaAcetate	100mM Citric Acid	100mM MES	100mM KPhosphate (monobasic)	100mM Citric Acid	100mM Bis-Tris	100mM Mes	100mM Na2Phosphate (dibasic)	100mM KPhosphate (monobasic)	100mM HEPES
		pH 4.0	pH 4.5	pH 5.0	pH 6.0	pH 6.0	pH 6.0	pH 6.5	pH 6.5	pH 7.0	pH 7.0	pH 7.0
B	100mM MOPS	100mM AmVAcetate	100mM Tris-HCl	100mM Na2Phosphate (dibasic)	100mM Imidazole	100mM HEPES	100mM Tris-HCl	100mM Tricine	100mM Bicine	100mM Bicine	100mM Tris-HCl	100mM CHES
		pH 7.0	pH 7.5	pH 7.5	pH 7.5	pH 8.0	pH 8.0	pH 8.0	pH 8.0	pH 8.5	pH 8.5	pH 9.0
C	Water	100mM Citric Acid	100mM NaAcetate	100mM Citric Acid	100mM MES	100mM KPhosphate	100mM Citric Acid	100mM Bis-Tris	100mM Mes	100mM Na2Phosphate	100mM KPhosphate	100mM HEPES
		250mM NaCl	250mM NaCl	250mM NaCl	250mM NaCl	250mM NaCl	250mM NaCl	250mM NaCl	250mM NaCl	250mM NaCl	250mM NaCl	250mM NaCl
		pH 4.0	pH 4.5	pH 5.0	pH 6.0	pH 6.0	pH 6.0	pH 6.5	pH 6.5	pH 7.0	pH 7.0	pH 7.0
D	100mM MOPS	100mM AmVAcetate	100mM Tris-HCl	100mM Na2Phosphate	100mM Imidazol	100mM HEPES	100mM Tris-HCl	100mM Tricine	100mM Bicine	100mM Bicine	100mM Tris-HCl	100mM CHES
		250mM NaCl	250mM NaCl	250mM NaCl	250mM NaCl	250mM NaCl	250mM NaCl	250mM NaCl	250mM NaCl	250mM NaCl	250mM NaCl	250mM NaCl
		pH 7.0	pH 7.5	pH 7.5	pH 7.5	pH 8.0	pH 8.0	pH 8.0	pH 8.0	pH 8.5	pH 8.5	pH 9.0
E	100mM SPG	100mM SPG	100mM SPG	100mM SPG	100mM SPG	100mM SPG	100mM SPG	100mM SPG	100mM SPG	100mM SPG	100mM SPG	100mM SPG
		pH 4.0	pH 4.5	pH 5.0	pH 6.0	pH 6.5	pH 7.0	pH 7.5	pH 8.0	pH 8.5	pH 9.0	pH 10.0
F	20mM HEPES	50mM HEPES	125mM HEPES	250mM HEPES	20mM Na2Phosphate (dibasic)	50mM Na2Phosphate (dibasic)	125mM Na2Phosphate (dibasic)	250mM Na2Phosphate (dibasic)	25mM Tris-HCl	50mM Tris-HCl	125mM Tris-HCl	250mM Tris-HCl
		pH 7.5	pH 7.5	pH 7.5	pH 7.5	pH 7.5	pH 7.5	pH 7.5	pH 8.0	pH 8.0	pH 8.0	pH 8.0
G	50mM HEPES	50mM HEPES	50mM HEPES	50mM HEPES	50mM HEPES	50mM HEPES	50mM Tris-HCl	50mM Tris-HCl	50mM Tris-HCl	50mM Tris-HCl	50mM Tris-HCl	50mM Tris-HCl
		50mM NaCl	250mM NaCl	50mM NaCl	750mM NaCl	1000mM NaCl	50mM NaCl	125mM NaCl	250mM NaCl	500mM NaCl	750mM NaCl	1000mM NaCl
		pH 7.5	pH 7.5	pH 7.5	pH 7.5	pH 8.0	pH 8.0	pH 8.0	pH 8.0	pH 8.0	pH 8.0	pH 8.0
H	50mM MES / Bis-Tris	50mM MES / Imidazole	50mM MOPS / PIPES	50mM MOPS / Bis-Tris propane	50mM MOPS / citric acid	50mM MOPS / HEPES-Na	0.1M Bicine / Troms base	50mM Imidazole	125mM Imidazole	250mM Imidazole	500mM Imidazole	500mM Imidazole
		pH 6.0	pH 6.5	pH 7.0	pH 7.5	pH 7.5	pH 8.5	pH 7.5	pH 7.5	pH 7.5	pH 7.5	pH 7.5

Concentrations shown are final concentration based on 25 µl assay (21 µl RUBIC Buffer Screen + 2 µl Protein sample + 2 µl SYPRO Orange dye diluted stock solution).